NON-COOPERATIVE DETECTION OF ULTRA WIDEBAND SIGNALS

THESIS

Brett D. Gronholz,

AFIT/GE/ENG/04-29

DEPARTMENT OF THE AIR FORCE

AIR UNIVERSITY

AIR FORCE INSTITUTE OF TECHNOLOGY

Wright-Patterson Air Force Base, Ohio

The views expressed in this thesis are those of the author and do not reflect the official policy or position of the United States Air Force, Department of Defense, or the United States Government.

AFIT/GE/ENG/04-29

NON-COOPERATIVE DETECTION OF ULTRA WIDEBAND SIGNALS

THESIS

Presented to the Faculty
Department of Electrical and Computer Engineering
Graduate School of Engineering and Management
Air Force Institute of Technology
Air University
Air Education and Training Command
In Partial Fulfillment of the Requirements for the
Degree of Master of Science in Electrical Engineering

Brett D. Gronholz, BSEE

December 2004

AFIT/GE/ENG/04-29

NON-COOPERATIVE DETECTION OF ULTRA WIDEBAND SIGNALS

Brett D. Gronholz, BSEE

Approved:

Michael A. Temple, Ph.D. Committee Chairman	6 Dec 04 Date
Maj Matthew E. Goda, Ph.D. Committee Member	6 DEC 04 Date
Robert F. Mills, Ph.D. Committee Member	6 DEC 2004 Date
Tom D. Niedzwiecki Committee Member	6 DEC 2004 Date

Table of Contents

List of Figures

Abstract

Ultra wideband (UWB) signals characteristically occupy a very large bandwidth resulting from extremely short duration pulses. Given an impulse-like UWB signal occurs so quickly and its energy is spread across such a large bandwidth, it is extremely difficult to detect without having prior knowledge of its existence.

This research develops and evaluates techniques for the non-cooperative (non-matched filter) detection of impulse-like UWB signals using channelized receiver architectures. Each technique considered is modeled and simulations conducted to characterize detection performance, the results of which are compared with the detection performance of three receivers: the matched filter receiver, which provides optimum detection performance in AWGN; the radiometer, or energy detector; and the multi-aperture cross correlation receiver. The input signal considered is a single UWB impulse in AWGN.

It is shown that a channelized receiver (with no downconversion) can provide approximately 2.5 dB improvement over the radiometer when performing detection using the temporal-temporal matrix (TTM). The TTM processing technique provides the best performance of all the proposed channelized receiver techniques. Although cross temporal matrix (CTM) detection performance exceeds that of the radiometer as well, it does not perform quite as well as TTM detection for all channel bandwidths. Two spectral-based techniques were considered as well with neither performing as well as the radiometer.

Detection with a downconverting channelized receiver is shown dependent on mixer phase value with performance variation generally minimized as the number of channels increases (channel bandwidth decreases). Although not always the case, there are combinations of signal-to-noise ratio and channel bandwidth whereby the downconverting channelized receiver performs better than the radiometer.

NON-COOPERATIVE DETECTION OF ULTRA WIDEBAND SIGNALS

1. Introduction

1.1 Introduction

The FCC's First Report and Order released in April 2002 made available the unlicensed spectrum between 3.1 and 10.6 GHz for ultra wideband (UWB) systems [1], an action which generated renewed interest in impulse signaling systems and research. Various people and groups have shown that operating an ultra wideband system in the vicinity of existing systems, including radars [2], narrowband military receivers [3], 802.11 wireless LANs [4–6], and GSM900, UMTS/WCDMA, and GPS [7], can have a detrimental effect on the performance of such systems. It would be beneficial to these systems to have the ability to detect the presence of a UWB signal and adjust operation characteristics to improve performance, if possible.

1.2 Problem Statement

Ultra wideband (UWB) signals characteristically occupy a very large bandwidth resulting from extremely short duration pulses. Given an impulse-like UWB signal occurs so quickly and its energy is spread across such a large bandwidth, it is extremely difficult to detect without having prior knowledge of its existence. This research focuses on developing techniques for the non-cooperative (non-matched filter) detection of impulse-like UWB signals using channelized receiver architectures.

1.3 Research Assumptions

The following assumptions were used throughout the research:

- The channel is modeled as being additive white Gaussian noise (AWGN).
- The impulse-like UWB signal is the only signal present in the RF environment.
- All RF filter spectral responses are centered at the UWB signal center frequency. The RF filter bandwidth is fixed when comparing results across receiver types and any signal-to-noise ratio (SNR) measurements are made at the output of the RF filter.
- All signals are received along a line-of-sight path from the transmitter. No multi-path signals are present.
- All signal detection is performed using test statistics generated under constant false alarm rate (CFAR) conditions, i.e., the detection threshold varies as a function of signal-to-noise ratio (SNR) such that a constant probability of false alarm of $P_{FA} = 10^{-2}$ is maintained.

1.4 Research Scope

Channelized receiver processing techniques were developed for the purpose of detecting impulse-like UWB signals. Each technique considered is modeled and simulations conducted to characterize detection performance, the results of which are compared with the detection performance of three receivers: the matched filter receiver, which provides optimum detection performance (highest probability of detection for a given signal-to-noise ratio) in AWGN; the radiometer, or energy detector; and the multi-aperture cross correlation receiver.

1.5 Research Approach

Initial research into impulse-like UWB signals provides analytic derivation of power spectral density expressions for signals employing various UWB modulations, including pulse position modulation (PPM), pulse amplitude modulation (PAM), biorthogonal pulse position modulation (BPPM), and a uniform pulse train (UPT)

as commonly used in radar applications (no random data modulation). The analytic results for each modulation type are then plotted to illustrate the characteristics of each spectrum.

A matched filter receiver model is developed next based on the correlator implementation of the matched filter. This receiver model assumes the shape and arrival time of the received UWB pulse are known a priori. Thus, the matched filter receiver provides optimum detection performance in AWGN and results for this model serve as an upper bound (best case) on achievable detection performance for the proposed channelized detection methods. Two non-cooperative receivers are also considered, including the radiometer and multi-aperture cross correlation receiver. Simulated detection results for these receivers serve as a baseline for detection performance using proposed channelized methods.

The research concludes with the development and detection performance characterization of a channelized receiver and downconverting channelized receiver model. Both the channelized and downconverting channelized receiver spectrally divide (channelize) the input signal into channels using bandpass filters. However, the downconverting channelized receiver also employs mixers and lowpass filters to independently downconvert each channelized signal to baseband. For both receivers, the final filtered signals are digitized in preparation for digital processing. The digital processor uses data from a finite length observation interval which is stored in matrices of dimension $M \times S$, where M is the number of receiver channels and S is the number of time samples spanning the interval. The detection performance of each processing technique is determined through simulation and subsequently compared with radiometric and matched filter results.

1.6 Materials and Equipment

The receiver architectures and detection techniques presented in this work were simulated using MATLAB® Version 7.0, developed by Mathworks, Inc. The

simulations were run on a 2.2 GHz Athlon XP personal computer and an AFIT mainframe UNIX based system.

1.7 Thesis Organization

Chapter 2 provides background information on the impulse-like ultra wideband signals, including different modulation types and their associated power spectral densities. The receiver architectures used for both cooperative and non-cooperative signal detection are introduced as well. Chapter 3 presents the methodology used for conducting the research, including a detailed discussion of how the four different data matrices (two time-based and two spectral-based) are generated from channelized receiver processing. The chapter concludes with a description of channelized receiver detection using each of these four matrices. Chapter 4 provides simulated detection results and analysis for both the cooperative and non-cooperative receivers considered. Chapter 5 presents conclusions drawn from the research and provides recommendations for possible future research. Additional supporting data is provided in the appendices: Appendix A contains simulated detection results for receiver channel bandwidths not included in Chapter 4; Appendix B contains processed matrix data and simulation results for an impulse-like UWB signal occurring at a different arrival time than what was used for results presented in Chapter 3 and Chapter 4; Appendix C contains the MATLAB® code used in the simulations.

2. Background

2.1 Introduction

This chapter introduces the characteristics of various ultra wideband (UWB) signals and the receivers that will be used for UWB signal detection. Section 2.2 describes various UWB modulations and associated power spectral densities. Section 2.3 describes matched filter detection, and Section 2.4 describes the non-cooperative detection receivers considered for this research, including the radiometer, the multi-aperture cross correlation receiver, and the channelized receiver. Section 2.5 summarizes the chapter.

2.2 Ultra Wideband Overview

Ultra wideband (UWB) systems transmit data over a very large bandwidth using extremely short duration pulses. The FCC's First Report and Order released in April 2002 [1] places emissions regulations on the effective isotropic radiated power (EIRP) of UWB devices to limit potential interference with narrowband systems utilizing the same spectrum. Specifically, the FCC specifies a maximum allowable UWB EIRP of 41.3 dBm in the 3.1 to 10.6 GHz band (measured at -10 dB points) for indoor and unrestricted handheld devices.

2.2.1 Ultra Wideband Definition. According to the FCC [1], a system is considered UWB if it has 1) a bandwidth greater than or equal to 500 MHz, or 2) a fractional bandwidth greater than 20%. Fractional bandwidth B_f is given by

$$B_f = 2\left(\frac{f_H - f_L}{f_H + f_L}\right) \tag{2.1}$$

where f_L and f_H are the lower and upper -10 dB bandwidth frequencies of a signal.

2.2.2 Ultra Wideband Communication Signaling. The analytic form that is often chosen to represent the transmitted UWB pulse is the Gaussian monocycle. Accounting for both transmit and receive antenna effects, the received UWB waveform is the second derivative of a Gaussian impulse and is given by

$$w(t) = \left[1 - 4\pi \left(\frac{t}{\tau_m}\right)^2\right] exp\left[-2\pi \left(\frac{t}{\tau_m}\right)^2\right] \tag{2.2}$$

where the impulse width parameter τ_m is approximately 0.4 times the pulse width T_w [8]. A single UWB pulse is plotted in Fig. 2.1 using $T_w = 0.4\ ns$.

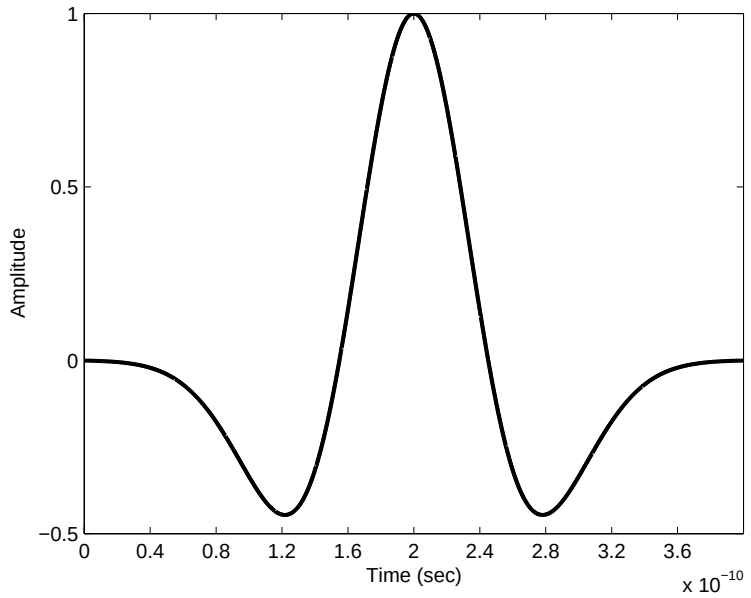

Figure 2.1 Received Gaussian Impulse Accounting for Transmit/Receive Antenna Effects

The general expression for a received UWB signal using an arbitrary modulation is

$$s(t) = \sum_{k=-\infty}^{\infty} A_k \cdot w\left(t - kT_s - B_k\Delta\right) \tag{2.3}$$

where A_k and B_k are specified according to modulation type, T_s is the symbol duration, and Δ is the relative position modulation offset. Four types of UWB signals are considered in this work by specifying various values for A_k and B_k in (2.3), including:

- Uniform Pulse Train (UPT): $A_k = B_k = 1$
- Pulse Position Modulation (PPM): $A_k = 1$ and $B_k = \pm 1$
- Pulse Amplitude Modulation (PAM): $A_k = \pm 1$ and $B_k = 1$
- Biorthogonal Pulse Position Modulation (BPPM): $A_k = \pm 1$ and $B_k = \pm 1$

As shown, the PPM and PAM signals are binary data modulated waveforms, i.e., either A_k or B_k has the $\pm$ sign variation for a given modulation type with one bit value determining the appropriate amplitude sign. The BPPM signal is a 4-ary data modulated waveform and thus both A_k and B_k terms have the $\pm$ sign variation with two bit values (one per term) determining the amplitude signs.

2.2.3 Ultra Wideband Power Spectral Density. The general analytic expression for the power spectral density (PSD) of an ultra wideband signal is derived using a method similar to those presented in [9–11]. To simplify the analysis, the signal at the receiver given in (2.3) will be described in terms of the modulation process and the pulse shape as $s(t) = m(t) * w(t)$, where $*$ is the convolution operation and $m(t)$, the modulation process, is given by:

$$m(t) = \sum_{k=-\infty}^{\infty} A_k \cdot \delta\left(t - kT_s - B_k\Delta\right) \tag{2.4}$$

The modulation process PSD is found by first calculating its autocorrelation function, $R_{mod}(\tau)$. It must be noted that $R_{mod}(\tau)$ is periodic in τ with T_s and the time-average autocorrelation function must be derived [10].

$$\hat{R}_{mod}(\tau) = \frac{1}{T_s}\int_0^{T_s} E\left[m\left(t\right) m\left(t+\tau\right)\right] dt \tag{2.5}$$

$$\hat{R}_{mod}(\tau) = \frac{1}{T_s}\int_0^{T_s} E\left[\sum_{k=-\infty}^{\infty} A_k \cdot \delta\left(t - kT_s - B_k\Delta\right) \cdot \sum_{l=-\infty}^{\infty} A_l \cdot \delta\left(t + \tau - lT_s - B_l\Delta\right)\right] dt \tag{2.6}$$

$$\hat{R}_{mod}(\tau) = \frac{1}{T_s}\sum_{l=-\infty}^{\infty} E\left[A_0 A_l\right] E\left[\delta\left(\tau - lT_s - \left(B_l - B_0\right)\Delta\right)\right] \tag{2.7}$$

The above expressions assume A_k and B_k are uncorrelated. The time-average autocorrelation is next split into two parts: $l = 0$ and $l \neq 0$.

$$\hat{R}_{mod}(\tau) = \frac{E\left[A_0^2\right]}{T_s}\delta(\tau) + \frac{1}{T_s}\sum_{l\neq 0} E\left[A_0 A_l\right] \cdot E\left[\delta\left(\tau - lT_s - \left(B_l - B_0\right)\Delta\right)\right] \tag{2.8}$$

The modulation process PSD, $S_{mod}(f)$, is then found by taking the Fourier transform of the time-average autocorrelation function in (2.8) .

$$S_{mod}(f) = \frac{E\left[A_0^2\right]}{T_s} + \frac{1}{T_s}\sum_{l=-\infty}^{\infty} E\left[A_0 A_l\right] \cdot E\left[e^{-j2\pi f(B_l - B_0)\Delta}\right] \cdot \left[\frac{1}{T_s}\delta\left(f - \frac{l}{T_s}\right) - 1\right] \tag{2.9}$$

Once the modulation process PSD has been found, the total UWB signal PSD is given by:

$$S_{UWB}(f) = S_{mod}(f)\left|W(f)\right|^2 \tag{2.10}$$

where $W(f)$ is the Fourier transform of the received UWB waveform, $w(t)$, given in (2.2). It can be shown that the Fourier transform of $w(t)$ is

$$W(f) = \frac{\pi\tau_m^3 f^2}{\sqrt{2}} \cdot exp\left(-\frac{\pi\tau_m^2 f^2}{2}\right) \tag{2.11}$$

2.2.3.1 PSD of Uniform Pulse Train.

A uniform train of UWB pulses is created using $A_k = 1$ and $B_k = 1$ in (2.3). Using these values, the analytic expression for the UPT power spectral density can be found by evaluating the expectations in (2.9) which are given by:

$$E\left[A_0^2\right] = E\left[A_0 A_l\right] = 1$$
$$E\left[e^{j2\pi f(B_l - B_0)\Delta}\right] = 1$$

The PSD for the modulation process then has the following analytic expression:

$$S_{UPT}(f) = \frac{1}{T_s^2} \sum_{l=-\infty}^{\infty} \delta\left(f - \frac{l}{T_s}\right) \tag{2.12}$$

and the total UPT power spectral density is found by substituting (2.12) into (2.10) for $S_{mod}(f)$.

2.2.3.2 PSD of Binary PPM Signal.

A binary pulse position modulated (PPM) UWB signal is created using $A_k = 1$ and allowing $B_k = \pm 1$ in (2.3). Using $P[B_k = 1] = P[B_k = -1] = 0.5$ and evaluating the expectations in (2.9) gives:

$$E\left[A_0^2\right] = E\left[A_0 A_l\right] = 1$$
$$E\left[e^{j2\pi f(B_l - B_0)\Delta}\right] = \frac{1}{2}\left[1 + cos\left(4\pi f \Delta\right)\right]$$

This yields a PSD for the modulation process given by

$$S_{PPM}(f) = \frac{1}{2T_s}\left[1 - cos\left(4\pi f\Delta\right)\right] + \frac{1}{2T_s^2}\left[1 + cos\left(4\pi f\Delta\right)\right] \sum_{l=-\infty}^{\infty} \delta\left(f - \frac{l}{T_s}\right) \tag{2.13}$$

The total PSD is found by substituting (2.13) into (2.10) for $S_{mod}(f)$.

2.2.3.3 PSD of Binary PAM Signal.

A binary pulse amplitude modulated (PAM) UWB signal is created by allowing $A_k = \pm 1$ and setting $B_k = 1$ in (2.3). Using $P[A_k = 1] = P[A_k = -1] = 0.5$, the expectations in (2.9) are given by:

$$\begin{aligned} E\left[A_0^2\right] &= 1 \\ E\left[A_0 A_l\right] &= 0, \quad \forall l \neq 0 \\ E\left[e^{j2\pi f(B_l - B_0)\Delta}\right] &= 1 \end{aligned}$$

This yields a PSD for the modulation process given by

$$S_{PAM}(f) = \frac{1}{T_s} \tag{2.14}$$

The total PSD is found by substituting (2.14) into (2.10) for $S_{mod}(f)$.

2.2.3.4 PSD of 4-Ary Biorthogonal PPM Signal.

A 4-ary biorthogonal pulse position modulated (BPPM) signal combines the characteristics of the binary PPM and PAM signals to create a 4-ary signaling scheme. A BPPM signal is created by allowing $A_k = \pm 1$ and $B_k = \pm 1$ in (2.3). Using $P[A_k = 1] = P[A_k = -1] = 0.5$ and $P[B_k = 1] = P[B_k = -1] = 0.5$, the analytic expression for the PSD can be found after evaluating the expectations in (2.9).

$$\begin{aligned} E\left[A_0^2\right] &= 1 \\ E\left[A_0 A_l\right] &= 0, \quad \forall l \neq 0 \\ E\left[e^{j2\pi f(B_l - B_0)\Delta}\right] &= \frac{1}{2}\left[1 + cos\left(4\pi f \Delta\right)\right] \end{aligned}$$

This yields a PSD for the modulation process given by

$$S_{BPPM}(f) = \frac{1}{T_s} \tag{2.15}$$

The total PSD is found by substituting (2.15) into (2.10) for $S_{mod}(f)$.

2.2.3.5 Comparison of UWB Signal PSDs. Analytic results derived above are shown plotted in Fig. 2.2 using parameter values of $T_w = 0.4\ ns$, $\Delta = T_w/2 = 0.2\ ns$, and $\tau_m = 0.4T_w = 0.16\ ns$. Both PPM and BPPM use a symbol duration of $T_s = 2T_w$ and PAM uses a symbol duration of $T_s = T_w$. The uniform pulse train uses a pulse repetition interval (PRI) of $T_s = 2T_w$.

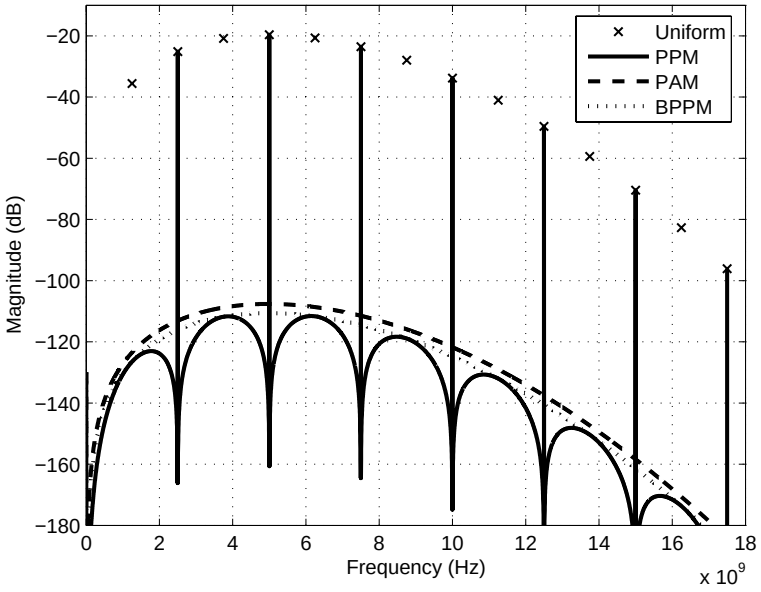

Figure 2.2 Analytic PSDs of Various UWB Waveforms

2.3 Cooperative Detection

2.3.1 Matched Filter Detection. A receiver can achieve optimum detection performance in additive white gaussian noise (AWGN) if the form and arrival time of the received UWB pulse are known. When these parameters are known, the correlator implementation of a matched filter (MF) receiver as shown in Fig. 2.3 [12] can be used to detect and estimate signal-of-interest (SOI) presence. In Fig. 2.3, $r(t)$ is the received signal comprised of a desired SOI component $s(t)$ and

an AWGN component $n(t)$. Although not functionally part of the MF process, RF filter W_{MF} has been incorporated for consistency with subsequent detectors to be considered. The detection process is completed by comparing the MF output test statistic Z with a threshold. If Z exceeds the threshold signal presence is declared.

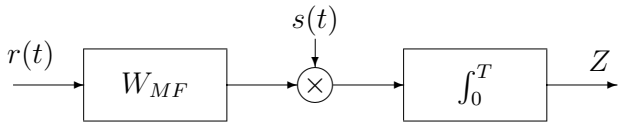

Figure 2.3 Matched Filter Detection Implemented with Correlation

2.4 Non-Cooperative Detection

Assuming signals in the environment are unknown, non-matched filter detection techniques must be employed. Non-matched filter detection is perhaps the most challenging detection approach that can be taken, and the problem is even more challenging when multiple signals exist simultaneously.

As with the matched filter detector described in the previous section, all non-cooperative detection techniques considered in this work generate a test statistic Z for threshold comparison. The test statistic output from each processing technique is compared with threshold Z_T which can be established using various detection criteria (e.g. Bayes, Neyman-Pearson, etc.) [13]. The SOI is declared "present" whenever Z exceeds Z_T. Assuming the SOI is *present* during test statistic generation, one of two conditions occurs, either 1) Z exceeds the threshold, valid detection occurs, and a probability of detection (P_D) can be computed, or 2) Z falls below the threshold, no detection occurs, and a probability of miss (P_M) can be computed. When the SOI is *not present* during processing, only channel noise is present and two additional conditions are possible, either 1) Z exceeds the threshold, in which case a false detection occurs and a probability of false alarm (P_{FA}) can be computed, or 2) Z falls below the threshold and no detection occurs as desired. The threshold can adapt to changing channel conditions such that a constant P_{FA} is maintained. This is known

as constant false alarm rate (CFAR) processing [14]. The following sections introduce three receiver structures that are considered for non-cooperative detection as part of this work, including the radiometer, multi-aperture cross correlation receiver, and channelized receiver.

2.4.1 Radiometric Detection. As shown in the radiometer block diagram of Fig. 2.4, a radiometer detects signal energy in bandwidth W_{RAD} Hz using a coherent processing time of T sec [15]. The resultant test statistic Z is compared to threshold value Z_T, if $Z > Z_T$ signal presence is declared (detection) and if $Z < Z_T$ detection does not occur.

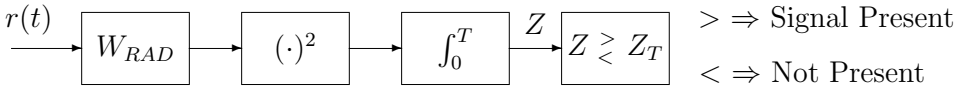

Figure 2.4 Radiometric Detection Using Bandwidth W_{RAD} and Coherent Integration Time T

2.4.2 Multi-Aperture Cross Correlation Receiver Detection. The multi-aperture cross correlation receiver in Fig. 2.5 intercepts a signal at two spatially separated antennas, filters the received signals, calculates the cross correlation (denoted by $\otimes$) for various relative arrival times, and compares the peak output response to a threshold set using Bayes, Neyman-Pearson, or other detection criteria. If the peak value exceeds the threshold, a signal is declared present. This implementation is an approximation of the correlator implementation of the matched filter receiver in Fig. 2.3 [16]. The major difference here is that instead of correlating a noisy received signal with a locally generated noise-free signal (as done with a reference signal in the matched filter receiver), two independently received noisy signals are cross correlated. In this case, the relative arrival time of the signals need not be calculated and/or estimated and time alignment (synchronization) with a locally generated reference is not required.

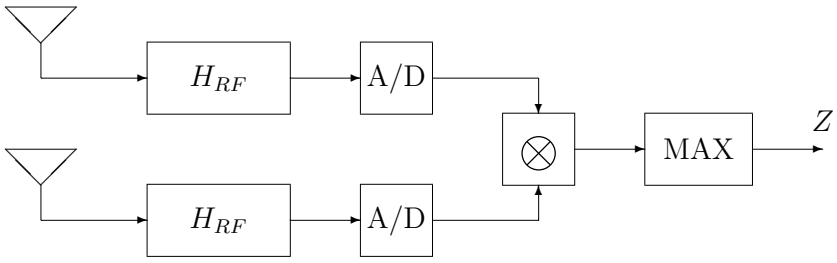

Figure 2.5 Multi-Aperture Cross-Correlation Receiver Detection

2.4.3 Channelized Receiver Detection. Channelized receiver techniques provide perhaps the best alternative to wideband radiometric detection, providing wide instantaneous bandwidth such that all signals present are simultaneously received without tuning the receiver to a specific signal [17]. Channelized receivers can be implemented using either analog or digital techniques. Regardless of the implementation, the fundamental channelized receiver consists of a bank of filters as shown in Fig. 2.6, the outputs of which are processed to arrive at some desired conclusion.

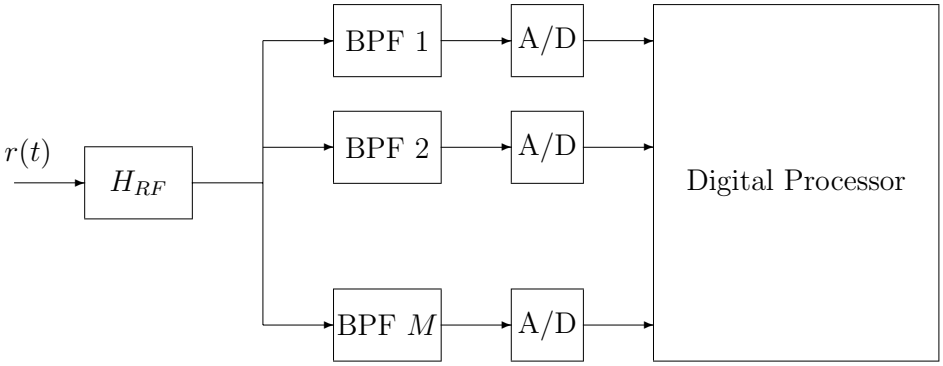

Figure 2.6 UWB Channelized Receiver

Unfortunately, implementing this receiver in digital hardware may not be practical since the UWB frequency range extends to frequencies higher than what current analog-to-digital converter technology supports (i.e. sampling at or above Nyquist is not feasible). One possible solution to this limitation is to use a downconverting channelized receiver as shown in Fig. 2.7, an approach which has been proposed

in [18]. As shown, the downconverting receiver uses M mixers operating at equally spaced frequencies $(f_1, f_2, ...f_M)$ and phase values $(\theta_1, \theta_2, ...\theta_M)$ which can be varied either dependently or independently as a function of implementation. The mixers are followed by a bank of M lowpass filters to decompose the received signal into M subbands. The downconverted outputs are then processed to arrive at some desired conclusion.

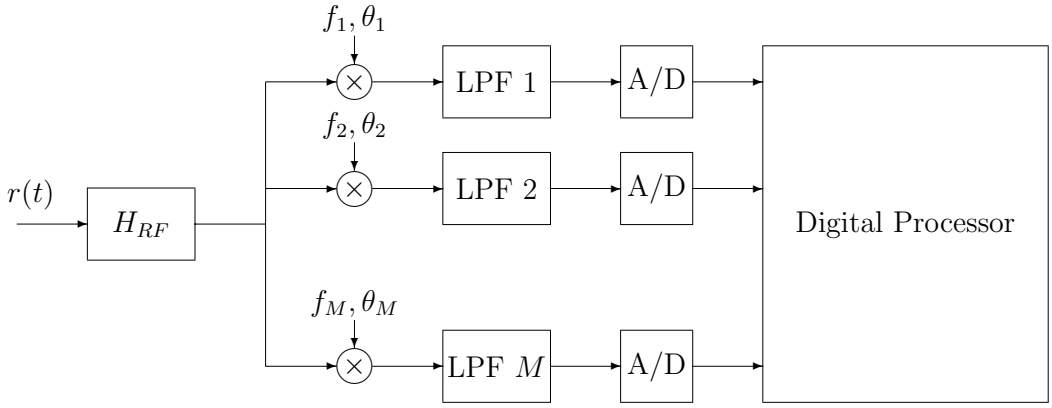

Figure 2.7 UWB Downconverting Channelized Receiver

2.5 Summary

This chapter introduced the characteristics of an ultra wideband signal, including the various modulation types and associated power spectral densities. The receiver structures used for detection in this work were also introduced, including the matched filter, radiometer, multi-aperture cross correlation receiver, and channelized receiver. Operations performed by the matched filter, radiometer, and multi-aperture cross correlation receiver are known, thus the detection performance of each can be readily analyzed through simulation. Basic channelized receiver structure and operation is also known. However, specific digital processing techniques for non-cooperative detection were unavailable. Therefore, several data processing techniques are introduced in Chapter 3 for signal detection.

3. Methodology

3.1 Introduction

This chapter introduces the channelized receiver processing methods developed to detect UWB signals. Fundamentally, the goal is to achieve the best possible detection performance, as bounded below by the radiometer and above by the matched filter. Each of the four processing techniques considered are presented in Section 3.2. The method used for determining probability of detection under fixed, constant false alarm rate conditions is presented in Section 3.3.

3.2 Channelized Receiver Processing

The channelized receiver outputs of Figs. 2.6 and 2.7 are used to form an $M \times S$ *Channelized Data Matrix* (CDM), where M is the number of channels and S is the number of time samples in the observation interval. This Channelized Data Matrix is processed using techniques introduced in the following sections with focus on achieving the best possible detection performance.

Parameters for generating data and figures presented in Chapters 3 and 4 are as follows:

- UWB Pulse Width – 0.4 ns
- Total Signal Duration (Observation Interval) – 5.2 ns
- Time Sample Spacing – 0.01 ns
- RF Filter Frequency Range (-4.0 dB Bandwidth) – 2.5 to 7.5 GHz
- Channel Bandwidth (-3.0 dB Bandwidth) – 250 MHz
- Number of Channels (M) – 20
- Downconversion Mixer Phase Values (at start of observation interval) – 0°

A plot of the received UWB signal based on these parameters is shown in Fig. 3.1. Additional data and figures for a received UWB signal time-offset from center are given in Appendix B.

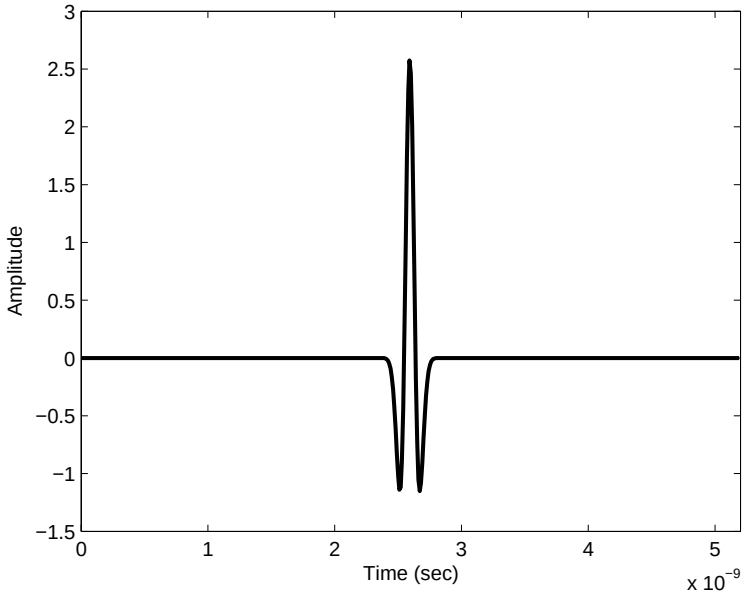

Figure 3.1 UWB Channelized Receiver Input Signal

3.2.1 Temporal-Temporal Matrix (TTM). The temporal-temporal matrix (TTM) is formed by performing an N-point inverse Fourier transform (IFFT) on each column (frequency samples) of the CDM and taking the absolute value of each element in the resultant matrix (to eliminate complex terms). Zero-padding is employed if there are more IFFT points than receiver channels ($N > M$) and truncation is employed if there are fewer IFFT points than receiver channels ($N < M$). The truncation is performed such that samples from lower frequency channels are maintained and samples from higher frequency channels are discarded as required. Representative TTMs for the received UWB pulse of Fig. 3.1 input to both the channelized receiver and the downconverting channelized receiver are shown in Fig. 3.2

and Fig. 3.3, respectively. These matrices were formed by processing the CDM columns using 64-point IFFTs.

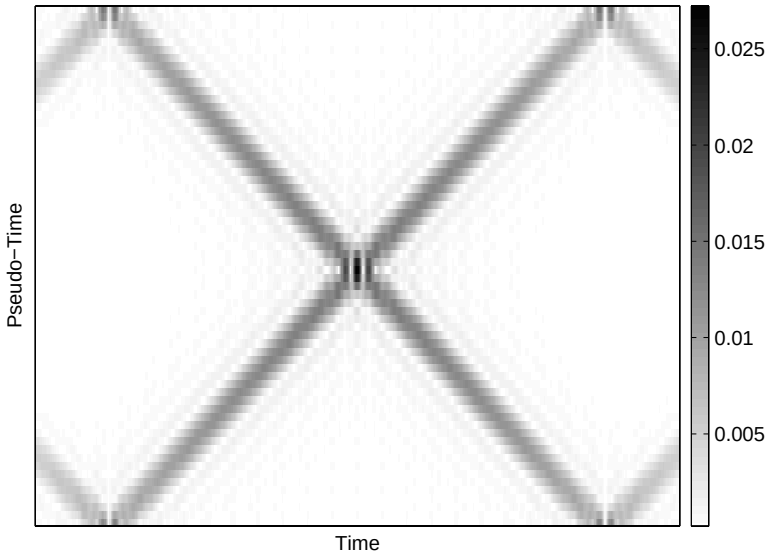

Figure 3.2 Temporal-Temporal Matrix (TTM) for Channelized Receiver Data, No Noise Present

3.2.2 Cross Temporal Matrix (CTM). The cross temporal matrix (CTM) is formed by calculating the absolute value of the correlation between all combinations of TTM columns. Individual CTM elements are given by

$$CTM(i,j) = \frac{1}{N_{ifft}} \left| \sum_{m=1}^{N_{ifft}} TTM^{*}(m,i) \cdot TTM(m,j) \right|, \;\; i = 1, ..., S, \; j = 1, ..., S \quad (3.1)$$

where N_{ifft} is the number of IFFT points used to form the TTM. The entire matrix can be constructed more efficiently using matrix operations per the following

$$CTM = \frac{1}{N_{ifft}} \left| TTM^{H} \cdot TTM \right| \quad (3.2)$$

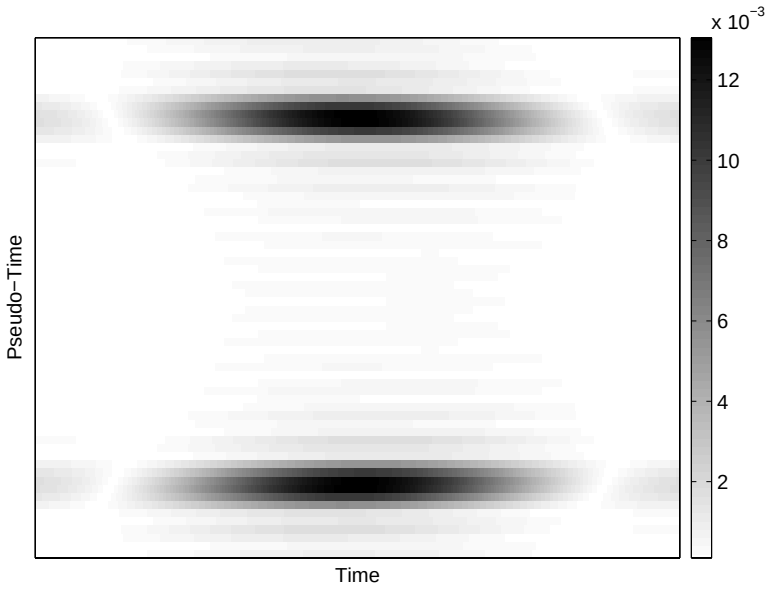

Figure 3.3 Temporal-Temporal Matrix (TTM) for Downconverting Channelized Receiver Data, No Noise Present

where $(\cdot)^H$ is the hermitian, or conjugate-transpose, operation. Representive CTMs for the received UWB pulse of Fig. 3.1 input to both the channelized receiver and the downconverting channelized receiver are shown in Fig. 3.4 and Fig. 3.5, respectively. These matrices were formed using the TTM matrices of Fig. 3.2 and Fig. 3.3.

3.2.3 Spectral-Spectral Matrix (SSM). The spectral-spectral matrix (SSM) is formed by performing an N-point Fourier transform (FFT) on each CDM row and taking the absolute value of each element in the matrix (to eliminate complex terms). The number of points in the FFT (N), must be greater than or equal to the number of samples in the observation interval (S) so that no time samples are truncated when performing the FFT. This ensures that time samples corresponding to a received UWB pulse are not inadvertantly discarded by the FFT operation. Zero-padding is employed if there are more FFT points than samples in the observation interval ($N > S$). Representative SSMs for the received UWB pulse of Fig. 3.1

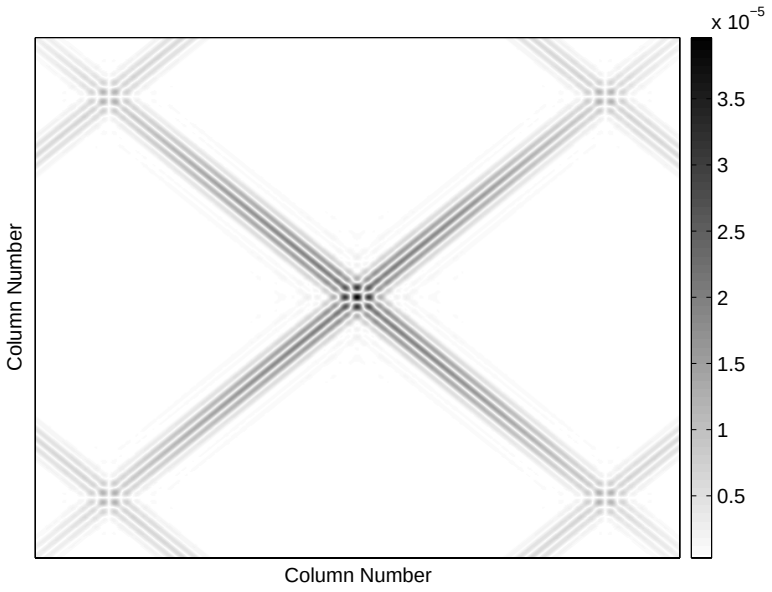

Figure 3.4 Cross Temporal Matrix (CTM) for Channelized Receiver Data, No Noise Present

input to both the channelized receiver and the downconverting channelized receiver are shown in Fig. 3.6 and Fig. 3.7, respectively. These matrices were formed by processing the CDM using 512-point FFTs.

3.2.4 Cross Spectral Matrix (CSM). The cross spectral matrix (CSM) is formed by calculating the absolute value of the correlation between all combinations of SSM columns. Individual CSM elements are given by

$$CSM(i,j) = \left| \frac{1}{M} \sum_{m=1}^{M} SSM^*(m,i) \cdot SSM(m,j) \right|, \quad i = 1, ..., N_{fft}, \;\; j = 1, ..., N_{fft} \tag{3.3}$$

where N_{fft} is the number of FFT points used to form the SSM. The entire CSM can be constructed more efficiently using matrix operations per the following

$$CSM = \frac{1}{M} \left| SSM^H \cdot SSM \right| \tag{3.4}$$

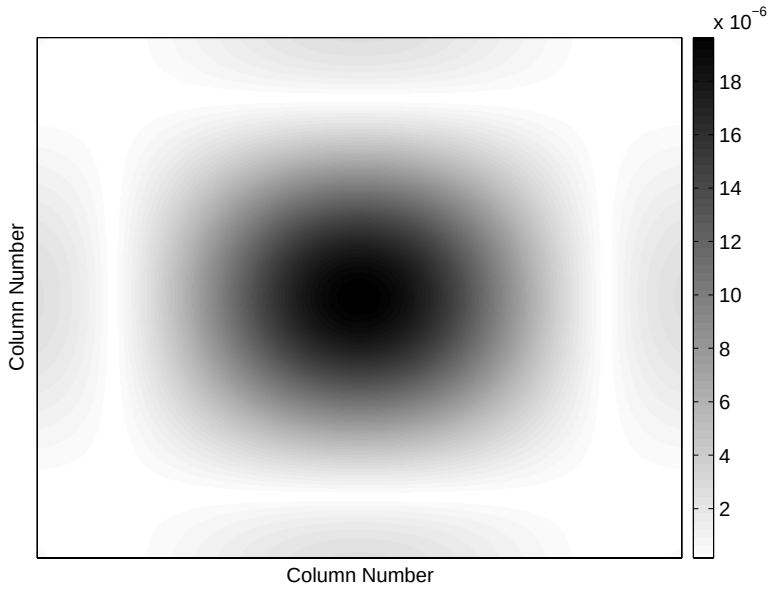

Figure 3.5 Cross Temporal Matrix (CTM) for Downconverting Channelized Receiver Data, No Noise Present

where $(\cdot)^H$ is the hermitian, or conjugate-transpose, operation. Representative CSMs for the received UWB pulse of Fig. 3.1 input to both the channelized receiver and the downconverting channelized receiver are shown in Fig. 3.8 and Fig. 3.9, respectively. These matrices were formed using the SSM matrices of Fig. 3.6 and Fig. 3.7.

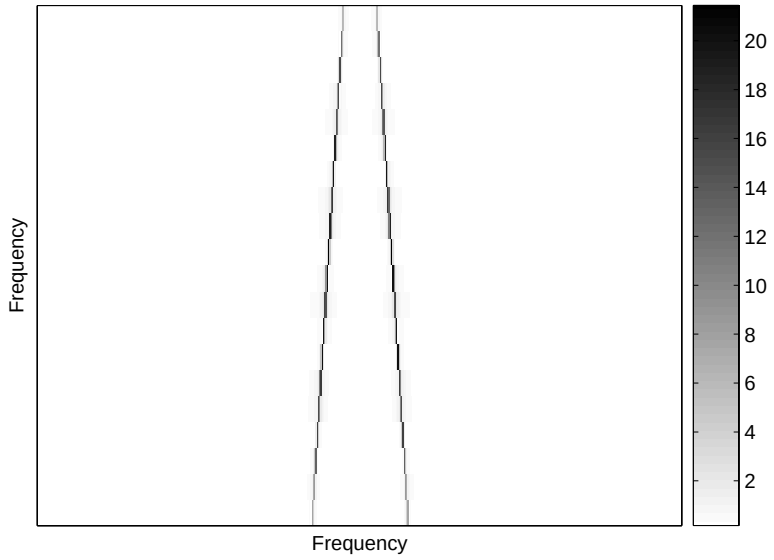

Figure 3.6 Spectral-Spectral Matrix (SSM) for Channelized Receiver Data, No Noise Present

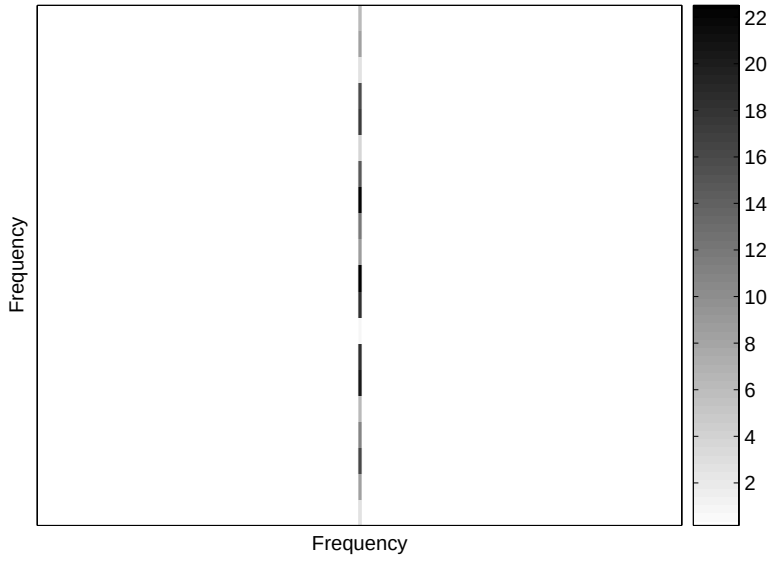

Figure 3.7 Spectral-Spectral Matrix for Downconverting Channelized Receiver Data, No Noise Present

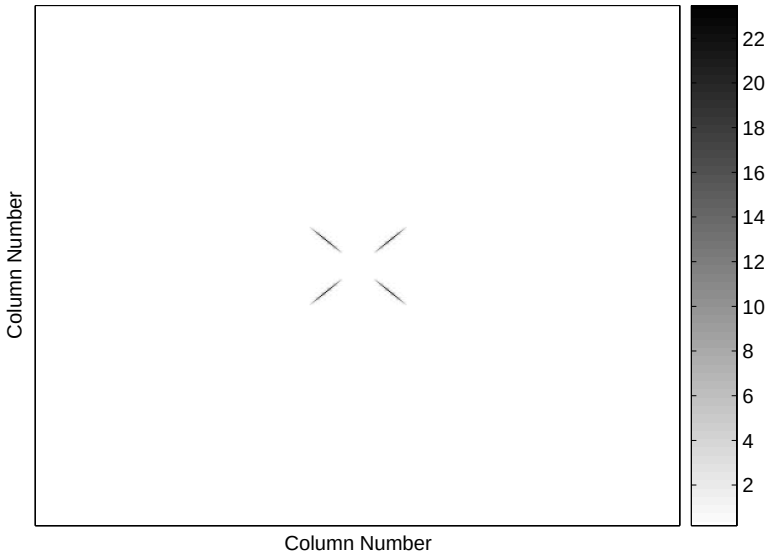

Figure 3.8 Cross Spectral Matrix (CSM) for Channelized Receiver Data, No Noise Present

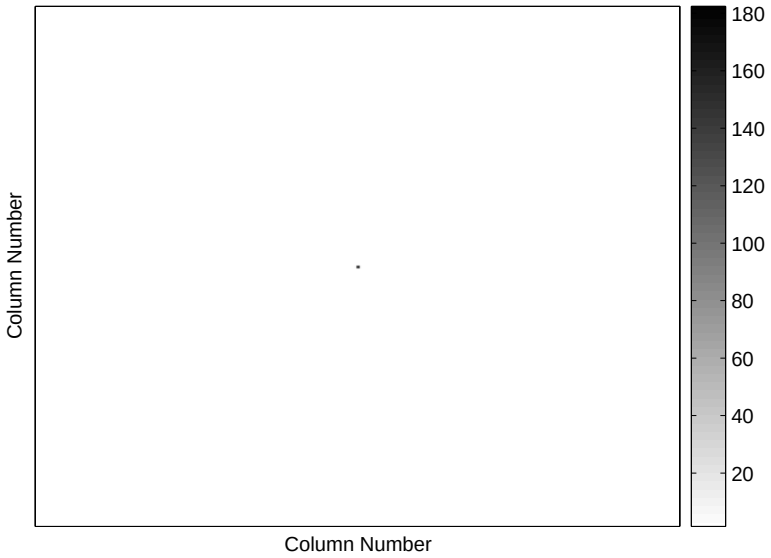

Figure 3.9 Cross Spectral Matrix (CSM) for Downconverting Channelized Receiver Data, No Noise Present

3.3 Channelized Receiver Detection

Two-dimensional threshold detection is performed on each of the processed matrices (TTM, CTM, SSM, CSM) described above to determine probability of detection (P_D) for that particular processing method. Note that for both the TTM and SSM cases, only *linear transformation* (IFFT and FFT, respectively) of the channelized data matrix occurs and there is no anticipated processing gain (improvement) in terms of enhanced detection performance. However, both the CTM and CSM cases involve *correlation* and thus some processing gain is anticipated.

For threshold detection, the maximum value of the processed matrix is chosen as the test statistic for subsequent comparison with the threshold. The threshold used in the detection process is determined by processing a series of matrices created using R noise realization inputs (with noise power set according to desired SNR) and generating a set of R test statistics. The threshold is then set to achieve the desired probability of false alarm, P_{FA}, using the R noise-only test statistics. Note that for all results presented in this work, P_{FA} is maintained constant as SNR is varied. This condition is referred to as constant false alarm rate (CFAR) detection [14]. Next, matrix data is regenerated using the same noise realizations with the signal of interest present. Test statistics from these results are compared to the threshold and P_D is determined as the number of times the threshold is exceeded divided by R total realizations. This process is repeated for each desired SNR value.

A similar detection process is used to calculate P_D for the radiometer, matched filter, and multi-aperture cross correlation receiver implementations, although the outputs of these receivers are either multi-valued one-dimensional signals (multi-aperture cross correlation receiver), in which case the test statistic is the maximum value, or single valued (radiometer and matched filter), in which case the test statistic is the output itself.

Figure 3.10 illustrates the process flow used for channelized receiver detection. Various parameters are changed to generate results for different detection scenarios, including:

- Received Signal-to-Noise Ratio (SNR) (measured at the output of the RF filter)
- Number of IFFT and FFT points used to form the TTM (CTM) and SSM (CSM), respectively
- Channelized receiver channel bandwidths
- Starting phases of downconversion mixers (downconverting channelized receiver only)

3.4 Summary

This chapter introduced four different channelized receiver processing techniques considered for this work, including the temporal-temporal matrix (TTM), the cross temporal matrix (CTM), the spectral-spectral matrix (SSM), and the cross spectral matrix (CSM). A method for determining probability of detection (P_D) using threshold detection under constant false alarm rate (CFAR) conditions was also introduced. Results for this detection process with each of the matrices generated are shown in Chapter 4.

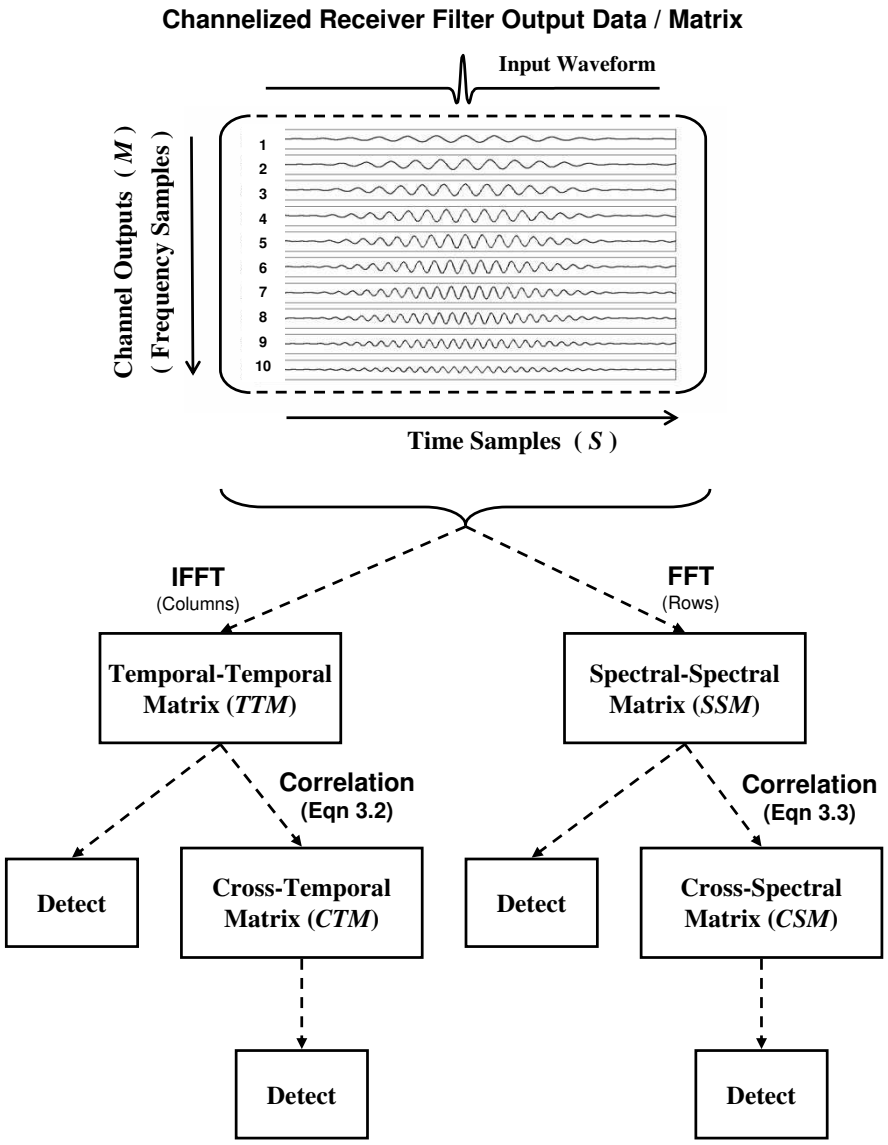

Figure 3.10 Detection Processing Flow

4. Detection Results and Analysis

4.1 Introduction

This chapter provides detection performance results for the receivers and processing techniques introduced in Chapters 2 and 3. First, Section 4.2 provides matched filter and radiometric detection performance results which bound the desired results for the proposed techniques. Next, Section 4.3 presents multi-aperture cross correlation receiver performance. Finally, Section 4.4 provides detection performance results using the matrix data and techniques introduced in Chapter 3 for both the channelized receiver and the downconverting channelized receiver.

4.2 Matched Filter and Radiometric Detection Performance

Matched filter and radiometric detection results are used as relative metrics for bounding the channelized receiver detection performance of the methods proposed in Chapter 3. The desired performance for any robust non-cooperative technique would be better than that of a radiometer, with somewhat poorer results expected when compared with matched filter detection (assuming AWGN channel conditions). Matched filter and radiometric probability of detection (P_D) results for $P_{FA} = 10^{-2}$ are shown in Fig. 4.1 where the received UWB signal is as shown previously in Fig. 3.1.

4.3 Multi-Aperture Cross Correlation Receiver Detection Performance

Multi-aperture cross correlation receiver results are presented for completeness as representing one means for performing non-cooperative detection [16]. Probability of detection results were calculated for $P_{FA} = 10^{-2}$ using the received UWB signal shown in Fig. 3.1. As shown in Fig. 4.2, the multi-aperture cross correlation receiver of Fig. 2.5 provides an improvement of approximately 1.5 dB over basic radiometric

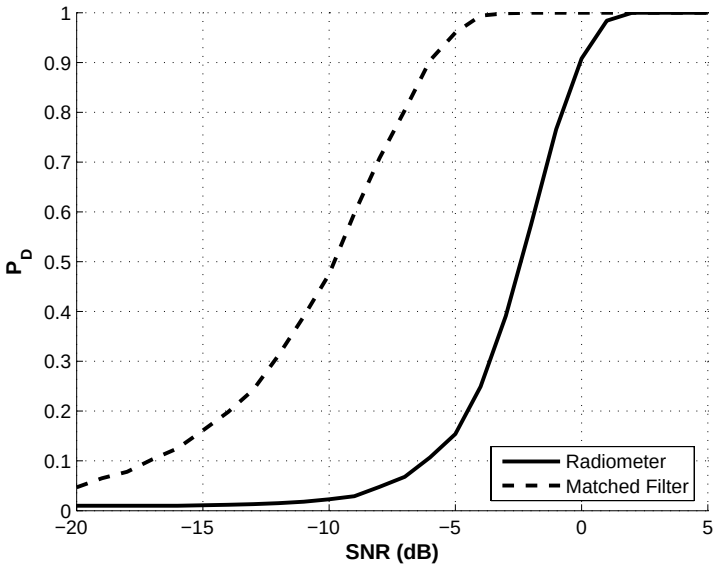

Figure 4.1 Matched Filter and Radiometric Detection Results for $P_{FA} = 10^{-2}$

detection at $P_D = 0.9$. These results are consistent with the theoretical performance improvement noted in [16].

4.4 Channelized Receiver Detection Performance

As stated in Chapter 3, channelized receiver detection is implemented by performing threshold detection on the processed channelized data matrices (TTM, CTM, SSM, and CSM) detailed in Section 3.2. The following sections provide detection results for each of these data matrices for $P_{FA} = 10^{-2}$ using the received UWB signal in Fig. 3.1.

4.4.1 Temporal-Temporal Matrix (TTM) Detection. Probability of detection (P_D) results are shown in Fig. 4.3 for a channelized receiver using $M = 20$, 250 MHz channels and a varying number of IFFT points (N_{ifft}) to form the TTM. As indicated in Fig. 4.3, detection performance improves as N_{ifft} increases until N_{ifft} becomes greater than the number of receiver channels. This conclusion is supported

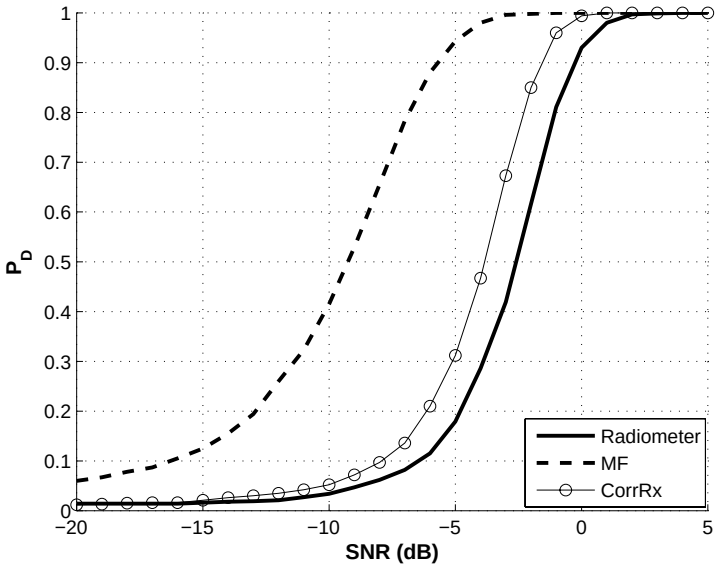

Figure 4.2 Cross Correlation Receiver (CorrRx) Detection Results Relative to Matched Filter and Radiometer for $P_{FA} = 10^{-2}$

by TTM detection results for channel bandwidths of 1.0 GHz, 500 MHz, and 100 MHz as included in Appendix A. For a channelized receiver employing 250 MHz channels, the best performance is achieved when $N_{ifft} \geq 32$, which corresponds to N_{ifft} values for which the IFFT no longer truncates the input data (note that $N_{ifft} = 32$ through $N_{ifft} = 256$ data is coincident in Fig. 4.3).

The effect of varying channel bandwidth is considered next. The number of IFFT points was selected so that channelized receivers employing different bandwidths all achieve the best performance. In this case, $N_{ifft} = 64$ was chosen since the smallest channel bandwidth considered is 100 MHz which requires $M = 50$ channels to span the 2.5 to 7.5 GHz frequency range. Probability of detection results for different receiver channel bandwidths and $N_{ifft} = 64$ are shown in Fig. 4.4. As indicated, the plots for all four channelized receiver bandwidths are perfectly coincident, indicating that detection performance is independent of channel bandwidth

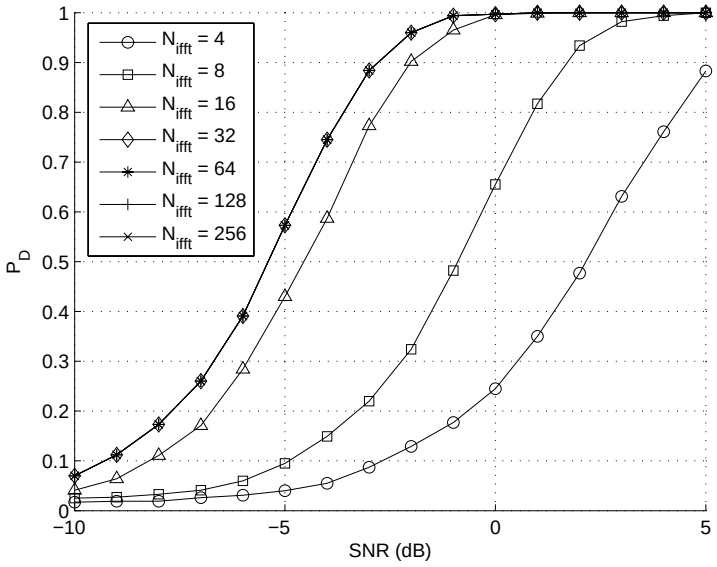

Figure 4.3 TTM Detection Performance for a *Channelized Receiver* with $M = 20$, 250 MHz Channels and Varying Number of IFFT Points

when N_{ifft} is properly chosen. The channelized receiver detection performance is approximately 2.5 dB better than the radiometer at $P_D = 0.9$.

4.4.2 Cross Temporal Matrix (CTM) Detection. Probability of detection (P_D) results are shown in Fig. 4.5 for a channelized receiver using $M = 20$, 250 MHz channels and a varying number of IFFT points (N_{ifft}) used to form the CTM from the corresponding TTM. As with TTM detection, CTM detection performance improves as N_{ifft} increases until N_{ifft} becomes greater than the number of channels. This conclusion is supported by the CTM results in Fig. 4.5, as well as, additional CTM detection results for channel bandwidths of 1.0 GHz, 500 MHz, and 100 MHz as included in Appendix A. Best performance is achieved when $N_{ifft} \geq 32$, which corresponds to N_{ifft} values for which the IFFT no longer truncates the input data (note that $N_{ifft} = 32$ through $N_{ifft} = 256$ data is coincident in Fig. 4.5).

Paralleling the TTM characterization proceess, the effect of varying channel bandwidth is considered next. The number of IFFT points was selected so that chan-

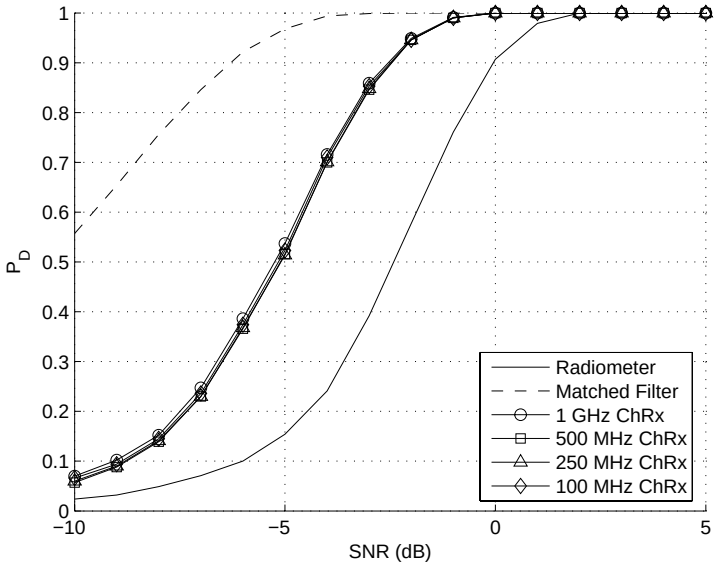

Figure 4.4 TTM Detection Performance for a *Channelized Receiver* Using $N_{ifft} = 64$ and Varying Channel Bandwidth

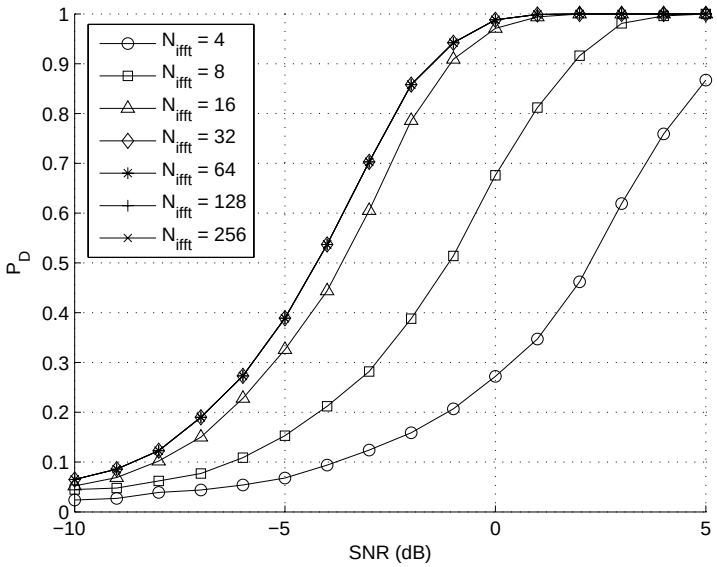

Figure 4.5 CTM Detection Performance for a *Channelized Receiver* with $M = 20$, 250 MHz Channels and Varying Number of IFFT Points

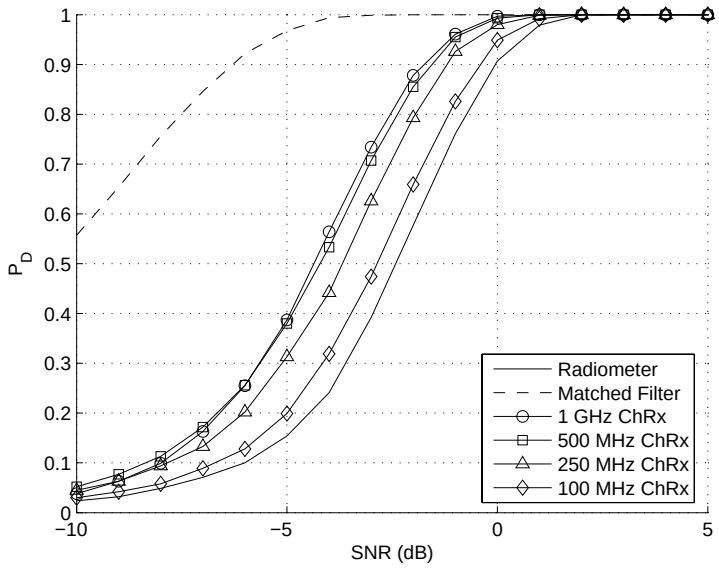

Figure 4.6 CTM Detection Performance for a *Channelized Receiver* Using $N_{ifft} = 64$ and Varying Channel Bandwidth

nelized receivers employing different bandwidths all achieve the best performance. Again, $N_{ifft} = 64$ was used since the smallest channel bandwidth considered is 100 MHz which requires $M = 50$ channels to span the 2.5 to 7.5 GHz frequency range. Probability of detection results for different channelized receiver channel bandwidths and $N_{ifft} = 64$ are shown in Fig. 4.6. These results indicate that increasing receiver channel bandwidth improves detection performance. The performance improvement over the radiometer varies from approximately 2.0 dB when using 1.0 GHz channels to approximately 0.25 dB when using 100 MHz channels at $P_D = 0.9$..

4.4.3 Spectral-Spectral Matrix (SSM) Detection. Probability of detection (P_D) results are shown in Fig. 4.7 for a channelized receiver with $M = 20$, 250 MHz channels and a varying number of FFT points (N_{fft}) used to form the SSM. Detection performance remains approximately the same for all N_{fft} values considered. This conclusion is supported by SSM results in Fig. 4.7, as well as,

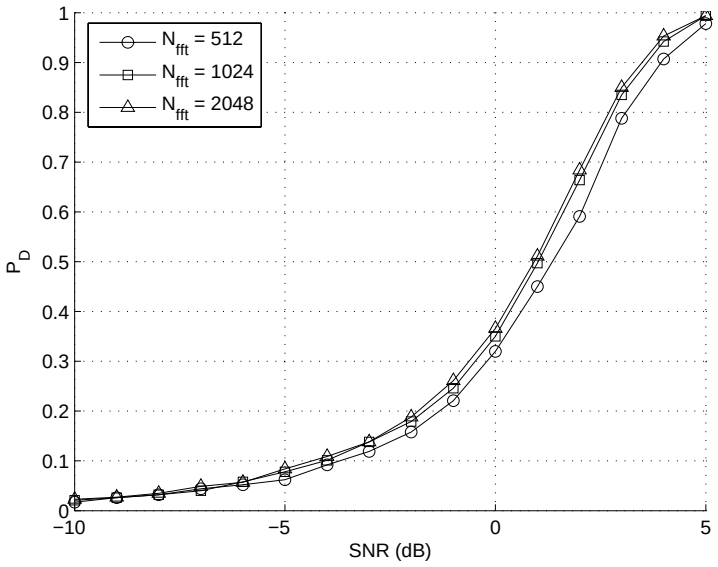

Figure 4.7 SSM Detection Performance for a *Channelized Receiver* with $M = 20$, 250 MHz Channels and Varying Number of FFT Points

additional SSM results for channel bandwidths of 1.0 GHz, 500 MHz, and 100 MHz as included in Appendix A.

The effect of varying the channel bandwidth is considered next. The number of FFT points was selected to provide both reliable detection performance and acceptable simulation run times. In this case, $N_{fft} = 512$ provided adequate results in terms of both performance and simulation run time and also ensured no time samples were discarded when performing the FFT. Probability of detection results for different channel bandwidths and $N_{fft} = 512$ are shown in Fig. 4.8. Detection performance varies slightly, but remains approximately the same over the range of channel bandwidths considered. Note also that SSM detection performance is consistently poorer than radiometric detection.

4.4.4 Cross Spectral Matrix (CSM) Detection. Probability of detection (P_D) results are shown in Fig. 4.9 for a channelized receiver using $M = 20$, 250 MHz channels and a varying number of FFT points (N_{fft}) used to form the

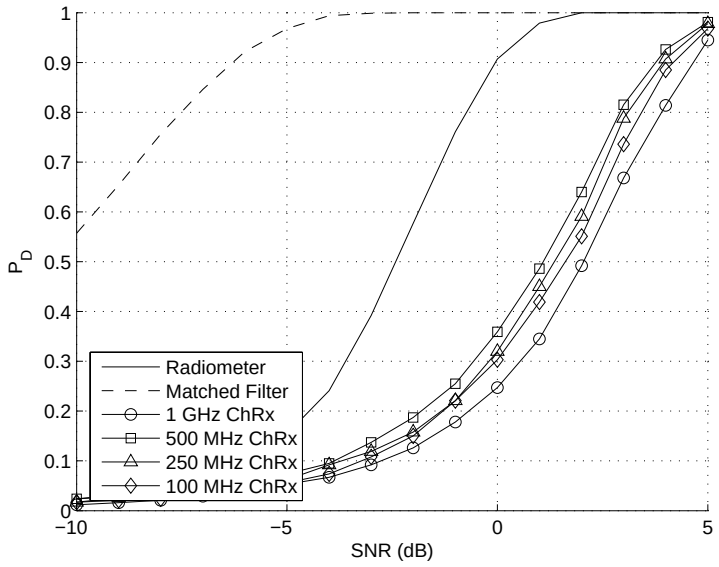

Figure 4.8 SSM Detection Performance for a *Channelized Receiver* Using $N_{fft} = 512$ and Varying Channel Bandwidth

CSM from the corresponding SSM. Detection performance remains approximately the same for all N_{fft} values considered. This conclusion is supported by the CSM results in Fig. 4.9, as well as, additional CSM results for channel bandwidths of 1.0 GHz, 500 MHz, and 100 MHz as included in Appendix A.

The effect of varying the channel bandwidth is considered next. The number of FFT points was selected to provide both reliable detection performance and acceptable simulation run times. In this case, $N_{fft} = 512$ provided adequate results in terms of both performance and simulation run time and also ensured no time samples were discarded when performing the FFT. Probability of detection results for different channel bandwidths and $N_{fft} = 512$ are shown in Fig. 4.10. Unlike CTM detection performance in Fig. 4.6 which shows improvement relative to the radiometer, CSM detection performance is consistently poorer than the radiomter; CSM performance varies slightly but remains approximately the same over the range of bandwidths considered.

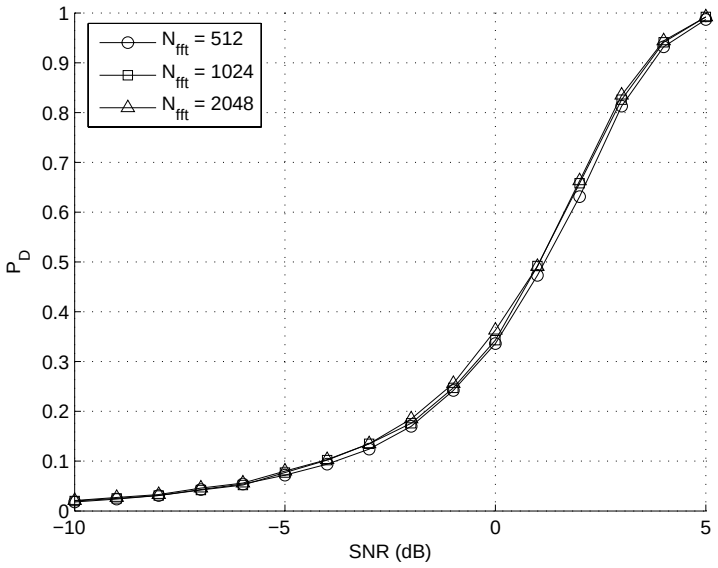

Figure 4.9 CSM Detection Performance for a *Channelized Receiver* with $M = 20$, 250 MHz Channels and Varying Number of FFT Points

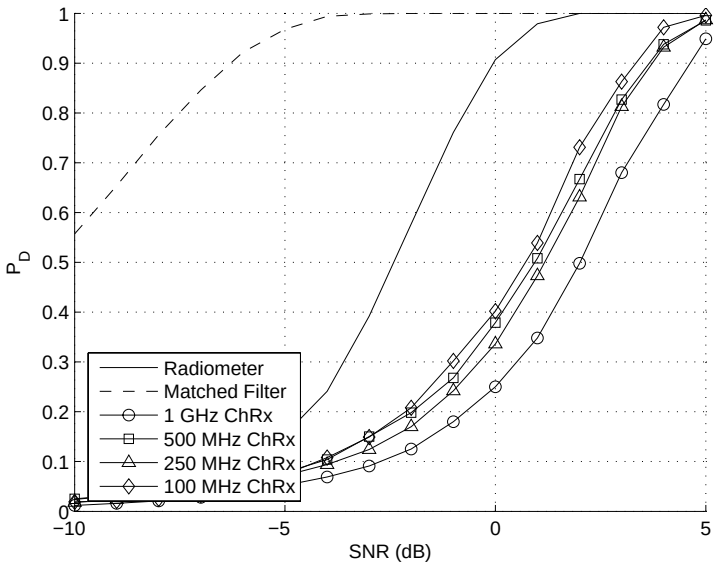

Figure 4.10 CSM Detection Performance for a *Channelized Receiver* Using $N_{fft} = 512$ and Varying Channel Bandwidth

4.5 Downconverting Channelized Receiver Detection Performance

As stated in Chapter 3, channelized receiver detection is implemented by performing threshold detection on the processed downconverting channelized receiver output matrices. Due to the variation in detection performance of the downconverting channelized receiver relative to the downconversion mixer phases, SNR vs. P_D results for the channelized receiver processing techniques are not compared with SNR vs. P_D results for the radiometer and the matched filter. Instead, the detection performance variation is plotted as a function of the initial phases on the downconversion mixers for a constant SNR and the performance of the proessing technique is compared to radiometric performance at that SNR. All detection performance results were calculated using $P_{FA} = 10^{-2}$.

4.5.1 Downconverting Temporal-Temporal Matrix (TTM) Detection. Probability of detection (P_D) results are shown in Fig. 4.11 for a downconverting channelized receiver with $M = 20$, 250 MHz channels and a varying number of IFFT points (N_{ifft}) used to form the TTM. Detection performance improves as N_{ifft} increases and appears to asymptotically approach a limit (i.e. at some point increasing N_{ifft} no longer improves performance). Considering the downcoverting TTM results in Fig. 4.11, along with additional TTM results for channel bandwidths of 1.0 GHz, 500 MHz, and 100 MHz as included in Appendix A, it appears that best performance is achieved when N_{ifft} becomes greater than twice the number of channelized receiver channels, or $N_{ifft} > 2M$. It is noted that performance for $N_{ifft} = 32$ is close to the performance for $N_{ifft} \geq 64$ and that $N_{ifft} \geq 32$ corresponds to N_{ifft} values for which the IFFT no longer truncates the input data.

Detection performance response due to variation in initial downconversion mixer phase value is considered next. The initial phase values of all mixers were set equal at the start of the observation interval and subsequently varied to generate results presented in Figs. 4.12 and 4.13. The signal-to-noise ratio (SNR) was held

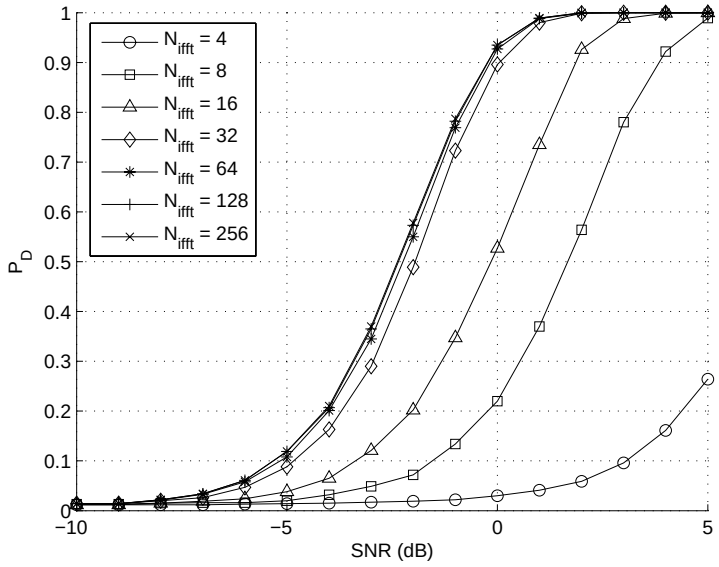

Figure 4.11 TTM Detection Performance for a *Downconverting Channelized Receiver* with $M = 20$, 250 MHz Channels and Varying Number of IFFT Points

constant at $SNR = 0$ dB for these results. As illustrated in Fig. 4.13, variation in detection performance resulting from initial phase variation decreases as the number of channels is increased (corresponding to a decrease in channelized receiver channel bandwidth).

Radiometric performance at $SNR = 0$ dB is approximately $P_D = 0.9$ (see Fig. 4.1). Thus, data in Fig. 4.13 suggests that detection using TTM data *can* outperform the radiometer when using 1.0 GHz and 500 MHz channel bandwidths. Detection performance varies minimally around radiometric performance ($P_D = 0.9$) for channel bandwidths of 250 MHz and 100 MHz.

4.5.2 Downconverting Cross Temporal Matrix (CTM) Detection.

Probability of detection (P_D) results are shown in Fig. 4.14 for a downconverting channelized receiver with $M = 20$, 250 MHz channels and a varying number of IFFT points (N_{ifft}) used to form the CTM from the corresponding TTM. Detection

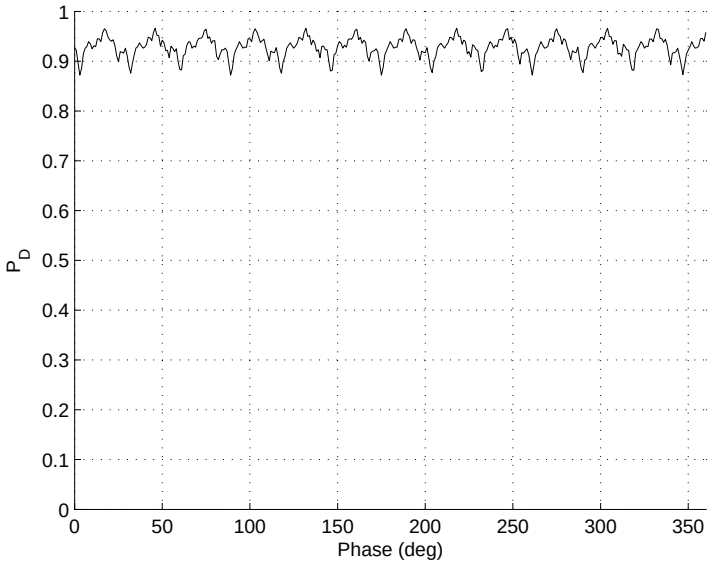

Figure 4.12 TTM Detection Performance Versus Mixer Phase for a *Downconverting Channelized Receiver* Using $SNR = 0$ dB with $M = 20$, 250 MHz Channels

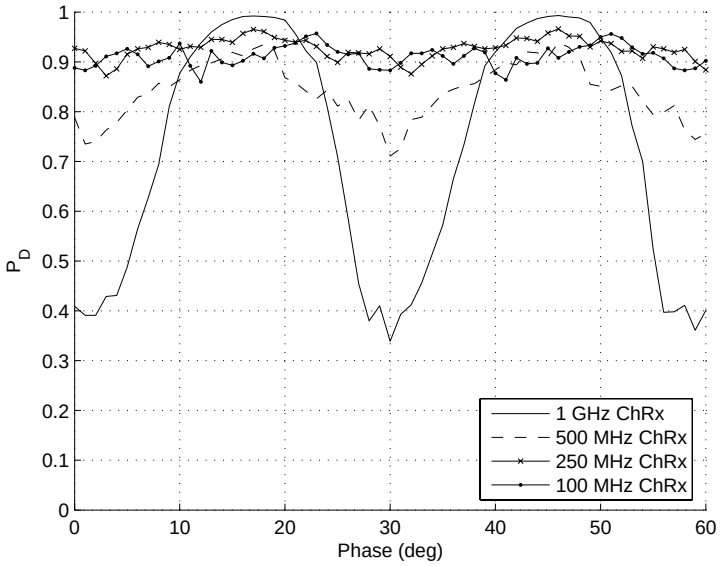

Figure 4.13 TTM Detection Performance Versus Mixer Phase for a *Downconverting Channelized Receiver* Using $SNR = 0$ dB with Varying Channel Bandwidth

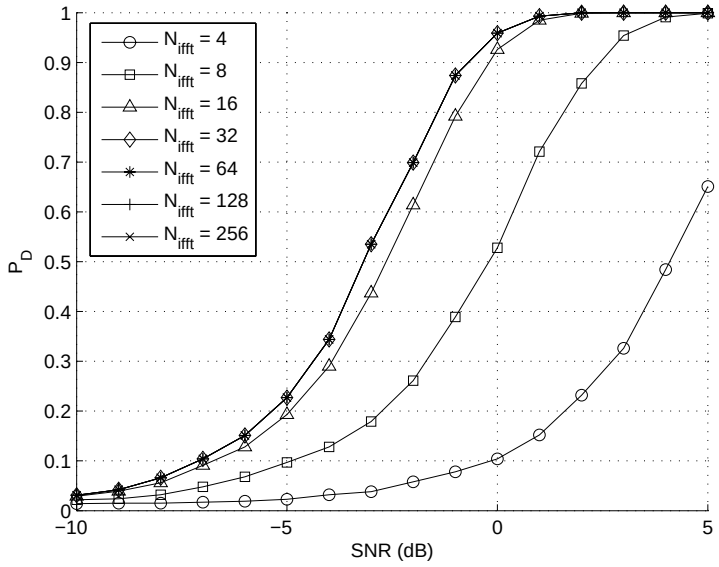

Figure 4.14 CTM Detection Performance for a *Downconverting Channelized Receiver* with $M = 20$, 250 MHz Channels and Varying Number of IFFT Points

performance improves as N_{ifft} increases until N_{ifft} becomes greater than the number of channels used in the channelized receiver. This conclusion is supported by the downconverting CTM results in Fig. 4.14, as well as, additional downconverting CTM results for channel bandwidths of 1.0 GHz, 500 MHz, and 100 MHz as included in Appendix A. Best performance is achieved when $N_{ifft} \geq 32$, which corresponds to N_{ifft} values for which the IFFT no longer truncates the input data (note that $N_{ifft} = 32$ through $N_{ifft} = 256$ data is coincident in the figure).

Detection performance response due to variation in initial downconversion mixer phase value is considered next. The initial phase values of all mixers were set equal at the start of the observation interval and subsequently varied to generate results presented in Figs. 4.15 and 4.16. The signal-to-noise ratio (SNR) was held constant at $SNR = 0$ dB for these results. Consistent with TTM results in Fig. 4.13, CTM results in Fig. 4.16 show that variation in detection performance re-

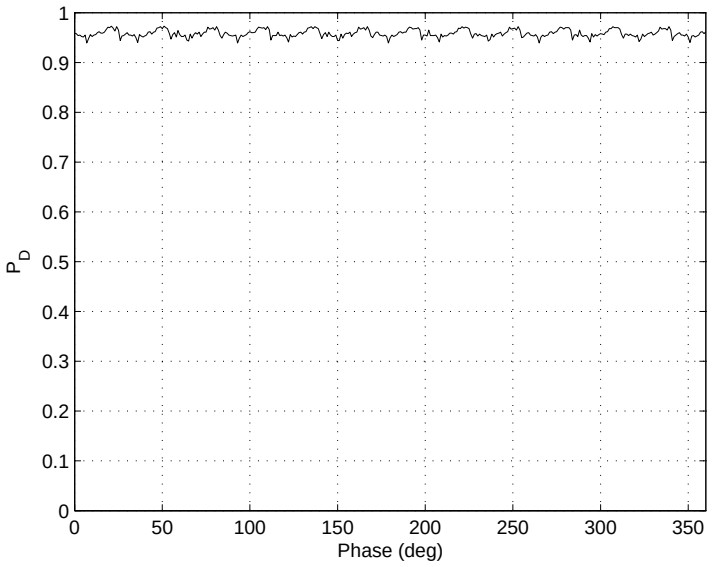

Figure 4.15 CTM Detection Performance Versus Mixer Phase for a *Downconverting Channelized Receiver* Using $SNR = 0$ dB with $M = 20$, 250 MHz Channels

sulting from initial phase variation decreases as the number of channels is increased (corresponding to a decrease in channelized receiver channel bandwidth).

Radiometric performance at $SNR = 0$ dB is approximately $P_D = 0.9$ (see Fig. 4.1). Thus, data in Fig. 4.16 suggests that detection using CTM data *can* outperform the radiometer when using a channel bandwidth of 1.0 GHz. Detection performance exceeds radiometric performance and shows very little variation due to phase for channel bandwidths of 500 MHz, 250 MHz, and 100 MHz.

4.5.3 Downconverting Spectral-Spectral Matrix (SSM) Detection.

Probability of detection (P_D) results are shown in Fig. 4.17 for a downconverting channelized receiver with $M = 20$, 250 MHz channels and a varying number of FFT points (N_{fft}) used to form the SSM. Detection performance remains approximately the same for all N_{fft} values considered. This conclusion is supported by the downconverting SSM results in Fig. 4.17, as well as, additional downconverting SSM

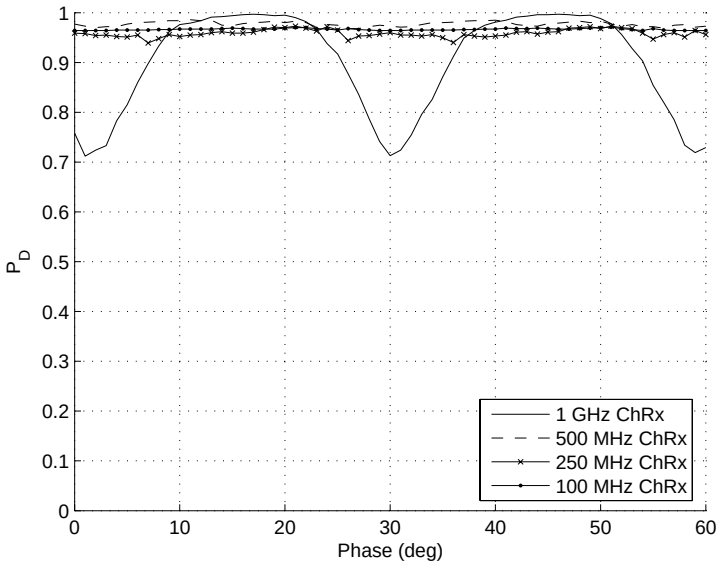

Figure 4.16 CTM Detection Performance Versus Mixer Phase for a *Downconverting Channelized Receiver* Using $SNR = 0$ dB with Varying Channel Bandwidth

results for channel bandwidths of 1.0 GHz, 500 MHz, and 100 MHz as included in Appendix A.

Detection performance response due to variation in initial downconversion mixer phase value is considered next. The initial phase values of all mixers were set equal at the start of the observation interval and subsequently varied to generate results presented in Figs. 4.18 and 4.19. The SNR was kept constant, at $SNR = 0$ dB and the number of FFT points was chosen to be $N_{fft} = 512$ (to ensure no time samples are discarded when performing the FFT). As illustrated in Fig. 4.19, variation in detection performance resulting from phase variations decreases slightly as the number of channels increases. However, the detection performance variation is not reduced to that exhibited in the downconverting TTM and CTM results of Fig. 4.11 and Fig. 4.14, respectively.

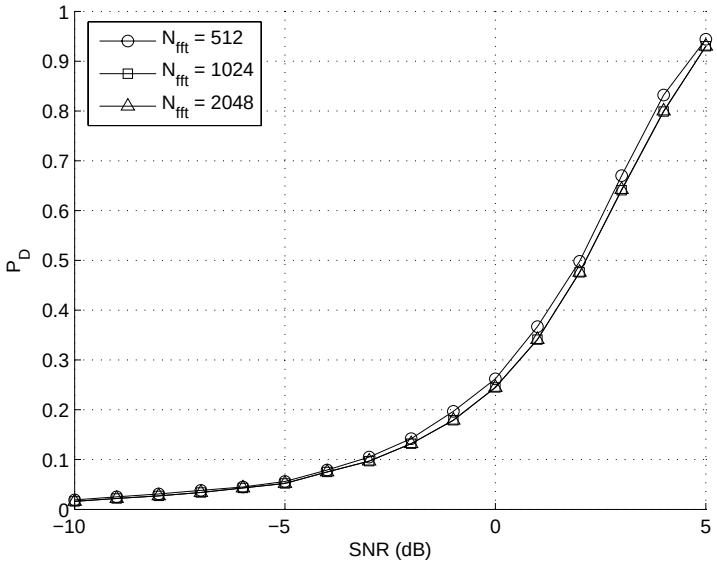

Figure 4.17 SSM Detection Performance for a *Downconverting Channelized Receiver* with $M = 20$, 250 MHz Channels and Varying Number of FFT Points

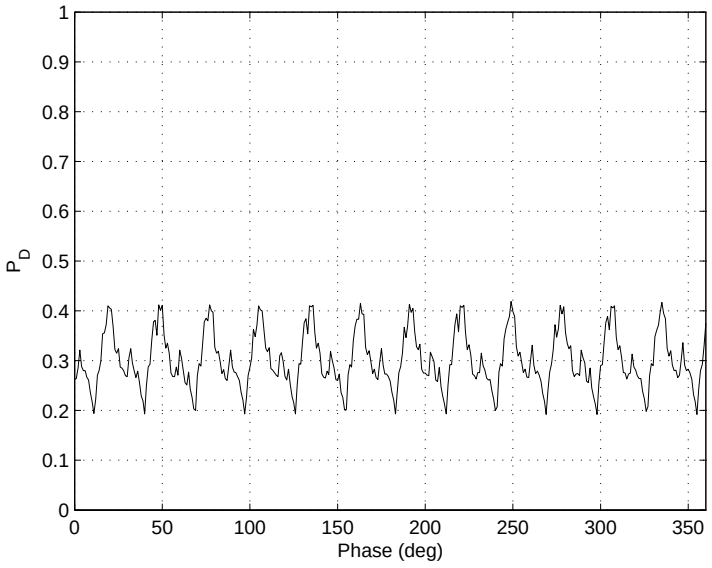

Figure 4.18 SSM Detection Performance Versus Mixer Phase for a *Downconverting Channelized Receiver* Using $SNR = 0$ dB with $M = 20$, 250 MHz Channels

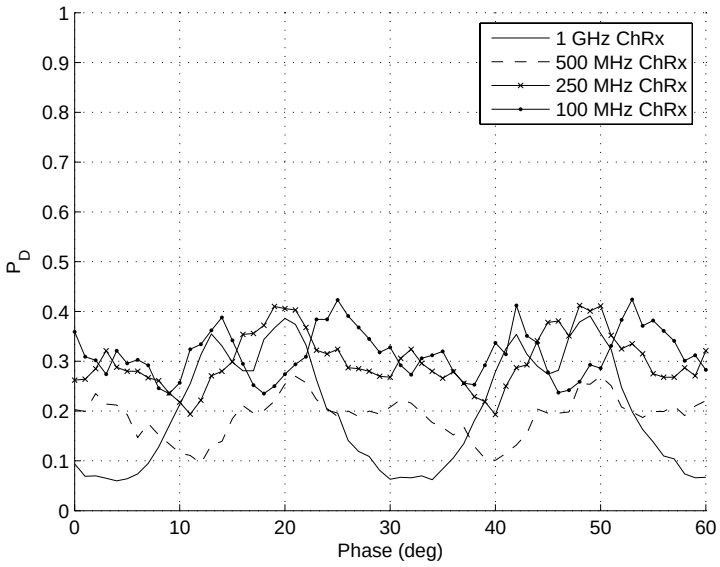

Figure 4.19 SSM Detection Performance Versus Mixer Phase for a *Downconverting Channelized Receiver* Using $SNR = 0$ dB with Varying Channel Bandwidth

Given radiometric performance at $SNR = 0$ dB is approximately $P_D = 0.9$, results in Fig. 4.19 clearly indicate that downconverting SSM detection performance is much poorer than the radiometer for all channel bandwidths considered.

4.5.4 Downconverting Cross Spectral Matrix (CSM) Detection.

Probability of detection (P_D) results are shown in Fig. 4.20 for a downconverting channelized receiver with $M = 20$, 250 MHz channels and a varying number of FFT points (N_{fft}) used to form the CSM from the corresponding SSM. Detection performance remains approximately the same for all N_{fft} values considered. This conclusion is supported by the downconverting CSM results in Fig. 4.20, as well as, additional downconverting CSM results for channel bandwidths of 1.0 GHz, 500 MHz, and 100 MHz as included in Appendix A.

Detection performance response due to variation in initial downconversion mixer phase value is considered next. The initial phase values of all mixers were set

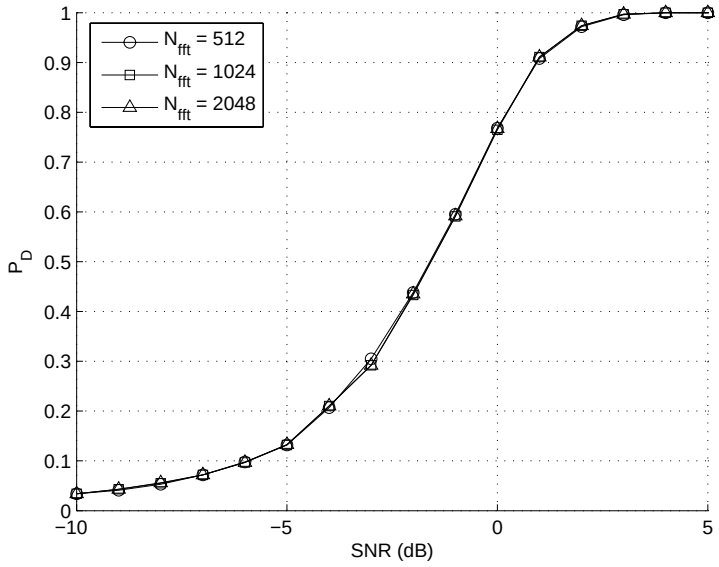

Figure 4.20 CSM Detection Performance for a *Downconverting Channelized Receiver* with $M = 20$, 250 MHz Channels and Varying Number of FFT Points

equal at the start of the observation interval and subsequently varied to generate results presented in Figs. 4.21 and 4.22. The SNR was kept constant, at $SNR = 0$ dB and the number of FFT points was chosen to be $N_{fft} = 512$ (to ensure no time samples are discarded when performing the FFT). As illustrated in Fig. 4.22, the variation in detection performance due to phase variations decreases as the number of channels is increased, and at the same time detection performance increases.

Given radiometric performance at $SNR = 0$ dB is approximately $P_D = 0.9$, data in Fig. 4.22 suggests that downconverting CSM detection outperforms the radiometer when using a receiver channel bandwidth of 100 MHz. Radiometric detection outperforms CSM detection for all other channel bandwidths considered (1.0 GHz, 500 MHz, and 250 MHz) with performance improving as channel bandwidth decreases (corresponding to an increase in the number of channels).

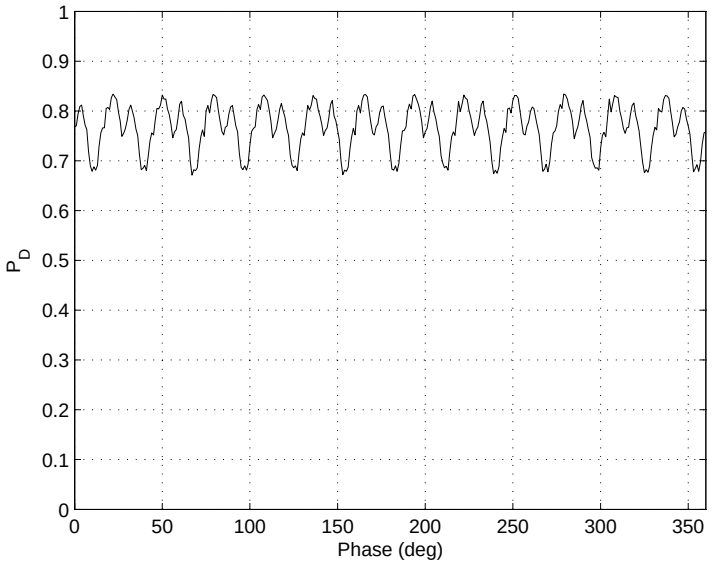

Figure 4.21 CSM Detection Performance Versus Mixer Phase for a *Downconverting Channelized Receiver* Using $SNR = 0$ dB with $M = 20$, 250 MHz Channels

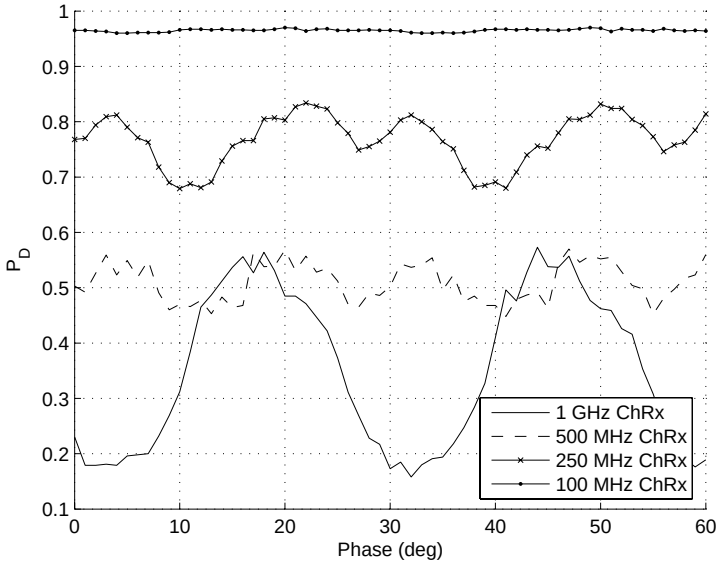

Figure 4.22 CSM Detection Performance Versus Mixer Phase for a *Downconverting Channelized Receiver* Using $SNR = 0$ dB with Varying Channel Bandwidth

4.6 Summary

Detection performance results were provided for each of the receivers and processing techniques introduced in Chapters 2 and 3. First, matched filter and radiometric detection performance results were introduced for the UWB waveform under consideration. These results effectively bound anticipated results for the proposed non-cooperative techniques. For completeness, detection performance of a multi-aperture cross correlation technique was introduced next as being representative of one specific non-cooperative detection technique. Finally, detection performance results using the matrix data (TTM, CTM, SSM and CSM) and techniques introduced in Chapter 3 were presented for both the channelized receiver and the downconverting channelized receiver.

5. Conclusions

5.1 Summary

The majority of this thesis has been devoted to introducing and analyzing channelized receiver processing techniques for use in detecting ultra wideband signals, specifically, a single UWB impulse in noise. The detection techniques considered operated on data contained in the temporal-temporal matrix (TTM), created by performing an IFFT on columns of the $M \times S$ *Channelized Data Matrix* (CDM); the cross temporal matrix (CTM), created by performing a correlation between all combinations of TTM columns; the spectral-spectral matrix (SSM), created by performing an FFT on the rows of the CDM; and the cross spectral matrix (CSM), created by performing a correlation between all combinations of SSM columns. Threshold detection was performed using each of these matrices and probability of detection results generated for varying parameters, including received SNR, the number of IFFT and FFT points used to form the TTM (CTM) and SSM (CSM), respectively, receiver channel bandwidth, and the initial phase value of downconversion mixers (downconverting channelized receiver only).

Three other receiver architectures were considered, including the matched filter, the radiometer, and the multi-aperture cross correlation receiver. Detection performance of the matched filter and radiometric receivers serve as performance bounds (upper and lower, respectively) for characterizing channelized receiver performance. Detection performance of the multi-aperture cross correlation receiver is provided by way of completeness in that its performance is representative of what can be achieved using non-cooperative (non-matched filter) techniques.

5.2 Conclusions

5.2.1 Channelized Receiver Detection Performance. Detection performance of the channelized receiver using the TTM (with an optimum number of

IFFT points as discussed in Chapter 4) provides approximately 2.5 dB improvement over the radiometer while performing approximately 3.5 dB poorer than the matched filter at $P_D = 0.9$. Likewise, detection performance using the CTM is better than radiometric performance (using the optimum number IFFT points) but not quite as good as that realized when using the TTM. It was also shown that CTM detection performance degrades as channel bandwidth decreases.

Detection performance using either of the spectral-based processing techniques (i.e. SSM or CSM) was poorer than that of the radiometer. The best performance achieved by either of these techniques was approximately 4.0 dB poorer than radiometric detection at $P_D = 0.9$. This result was expected since the power in a UWB signal is spread across an extremely wide bandwidth, as shown in Fig. 2.2, such that channel noise quickly overcomes the UWB signal in the spectral domain as the SNR decreases.

5.2.2 Downconverting Channelized Receiver Performance. Detection performance of the downconverting channelized receiver using any of the channelized receiver processing techniques varies relative to the downconversion mixer phases. For detection using the TTM, detection performance variation decreases as the number of channels increases (channel bandwidth decreases) and for channel bandwidths of 250 MHz and 100 MHz, detection performance approximately equals that of the radiometer. Detection performance using the CTM generated with 1.0 GHz channels provides detection ranging from approximately $P_D = 0.7$ to $P_D = 1$ as mixer phase varied from 0 to 360 degrees. For downconverting channelized receivers using 100 MHz, 250 MHz, or 500 MHz channels, detection performance surpasses that of the radiometer while remaining relatively constant for all phase values.

Variation in downconversion mixer phase resulted in SSM detection performance variation for all channel bandwidths, although the amount of variation in detection performance appeared to decrease as the number of channels was increased

(decreasing channel bandwidth). Detection performance using the SSM does not come close to radiometric performance. Using the CSM, detection performance variation as a function of mixer phase occurs which decreases as the number of channels increases. The CSM detection performance surpasses that of the radiometer for the downconverting channelized receiver using 100 MHz channels, in which case the performance variation as a function of mixer phase was minimal.

5.3 Recommendations for Future Research

5.3.1 Detection Performance in Coexistence Scenarios. This work only considered received signals consisting of a single UWB signal with and without additive white Gaussian channel noise. Unfortunately, real world environments can contain many different signals using many different modulation types. Performance of the channelized receiver processing techniques presented here could be analyzed in coexisting scenarios, i.e., consider received signals containing the UWB signal considered here along with other signals such as narrowband tones, M-ary phase shift keyed (MPSK), M-ary frequency shift keyed (MFSK), direct sequence spread spectrum (DSSS), and other modulation types encountered in communication, navigation, and radar applications.

5.3.2 Channel Assessment and Characterization. In some cases, it may be beneficial to identify the number, type, and nature of signals present in an environment at any given time (channel assessment). With narrowband (characterized relative to UWB) signals present in the environment, it may be difficult to reliably detect and/or characterize UWB signals. Visual inspection of the two dimensional TTM, CTM, SSM, and CSM plots in Chapter 3 suggest the possibility of employing pattern recognition techniques in conjunction with the channelized receiver processing techniques presented in this work to make this determination.

Appendix A.

A.1 Channelized Receiver Detection Performance

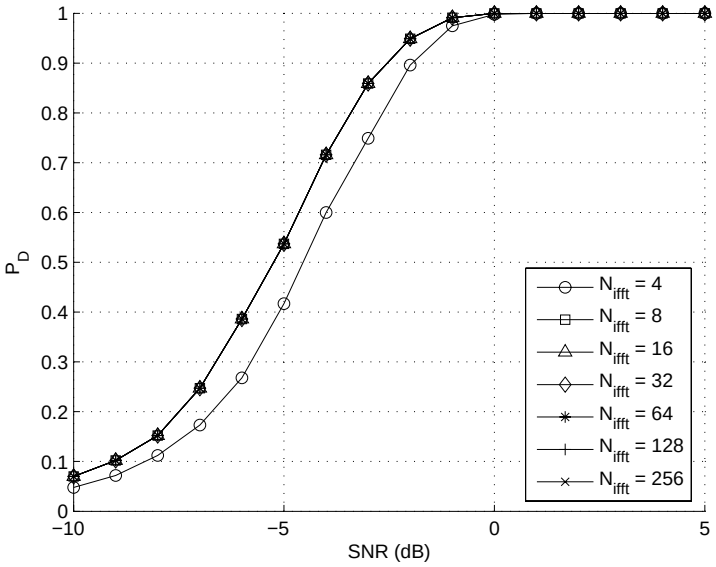

Figure A.1 TTM - 1 GHz ChRx (Varying Number of Points in IFFT)

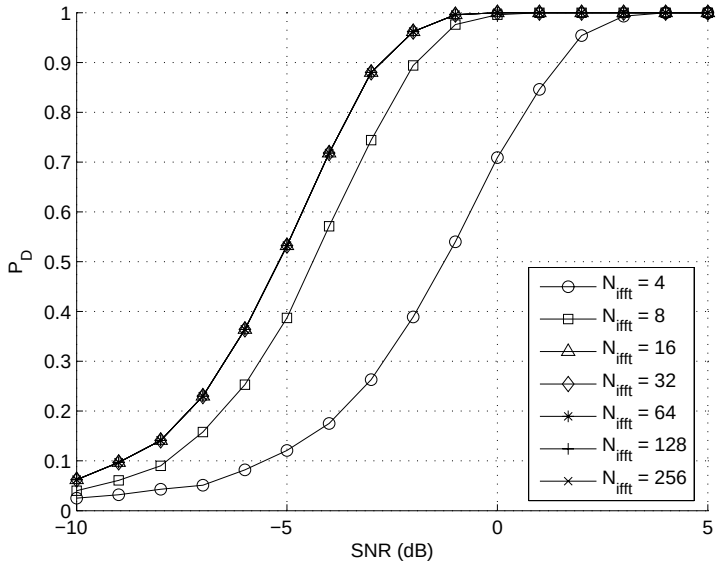

Figure A.2 TTM - 500 MHz ChRx (Varying Number of Points in IFFT)

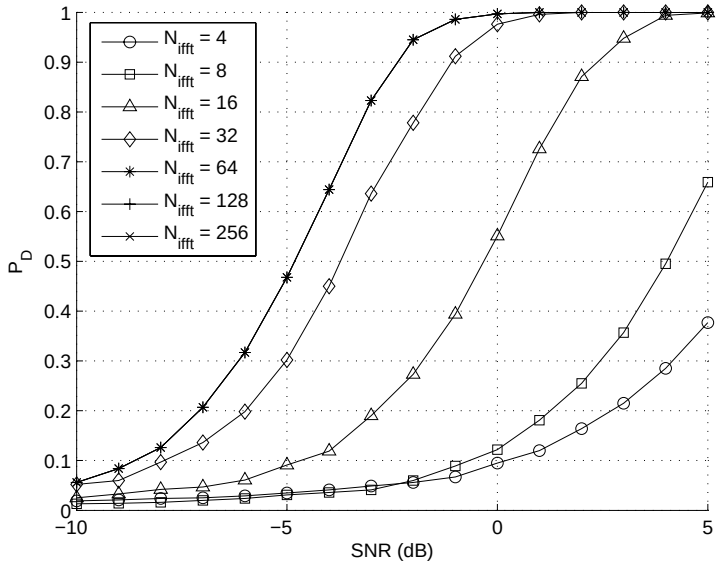

Figure A.3 TTM - 100 MHz ChRx (Varying Number of Points in IFFT)

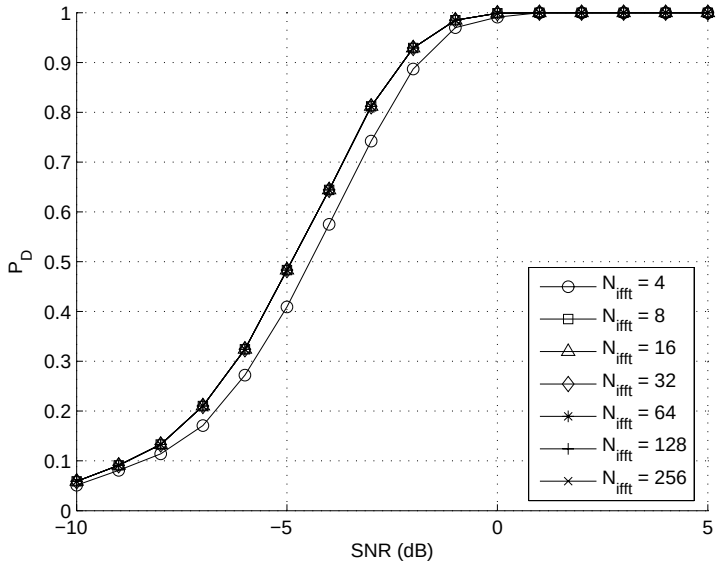

Figure A.4 CTM - 1 GHz ChRx (Varying Number of Points in IFFT)

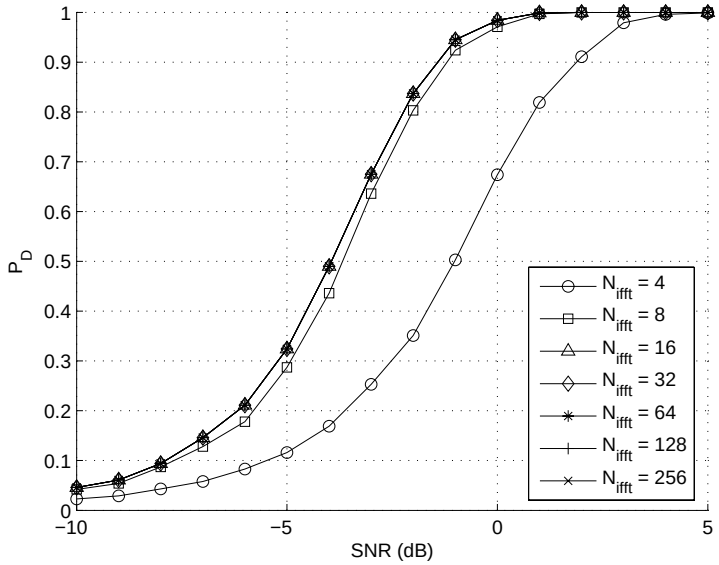

Figure A.5 CTM - 500 MHz ChRx (Varying Number of Points in IFFT)

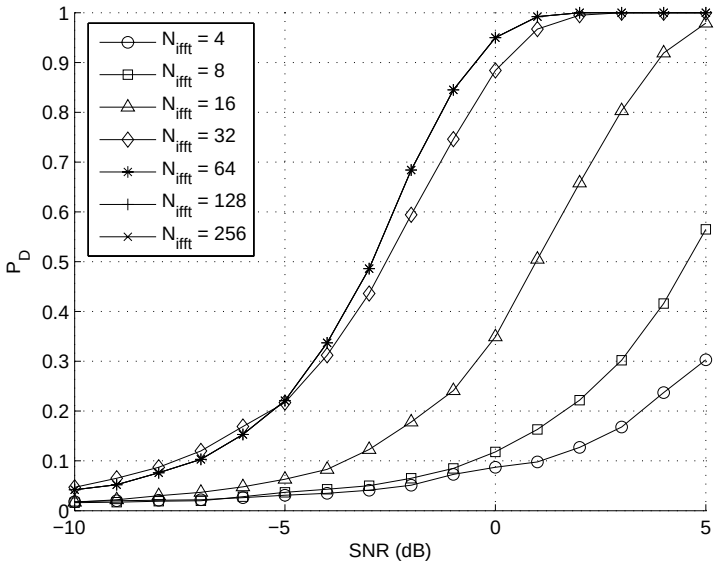

Figure A.6 CTM - 100 MHz ChRx (Varying Number of Points in IFFT)

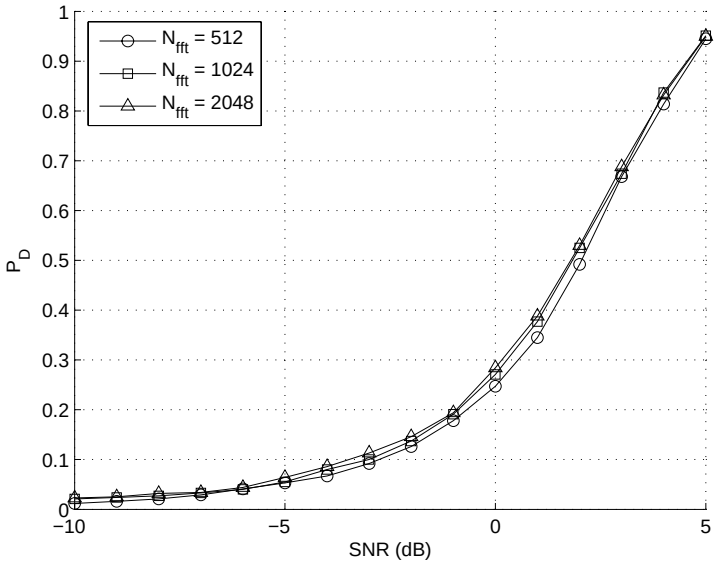

Figure A.7 SSM - 1 GHz ChRx (Varying Number of Points in FFT)

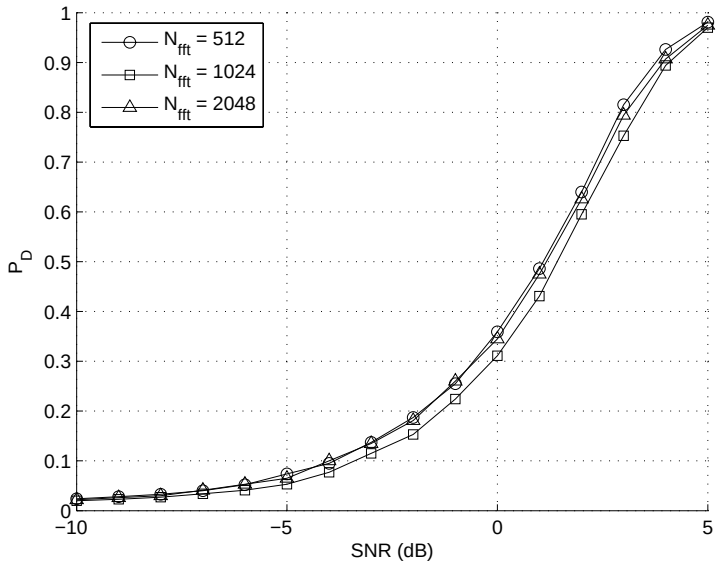

Figure A.8 SSM - 500 MHz ChRx (Varying Number of Points in FFT)

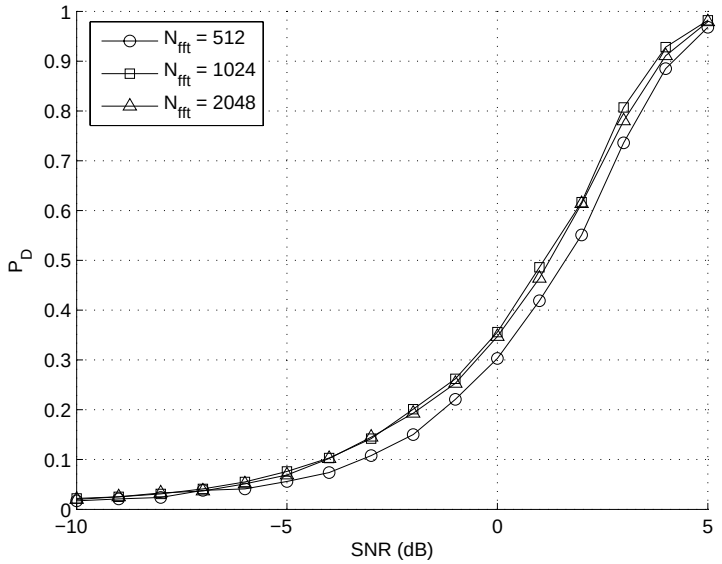

Figure A.9 SSM - 100 MHz ChRx (Varying Number of Points in FFT)

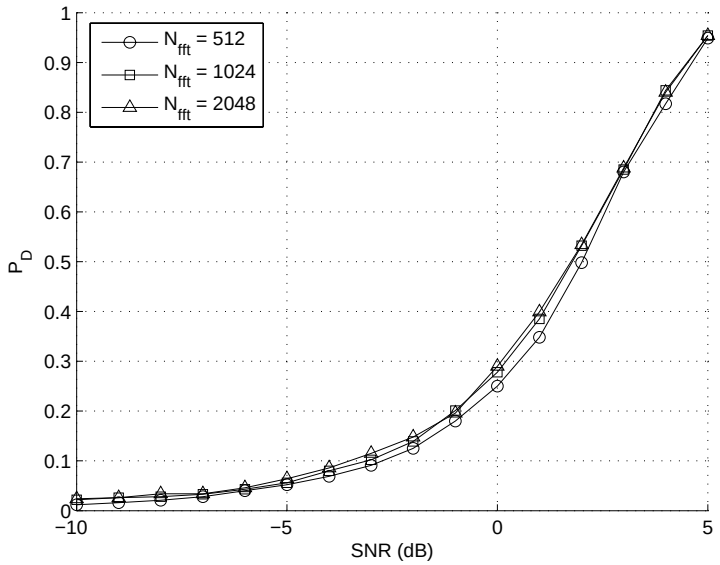

Figure A.10 CSM - 1 GHz ChRx (Varying Number of Points in FFT)

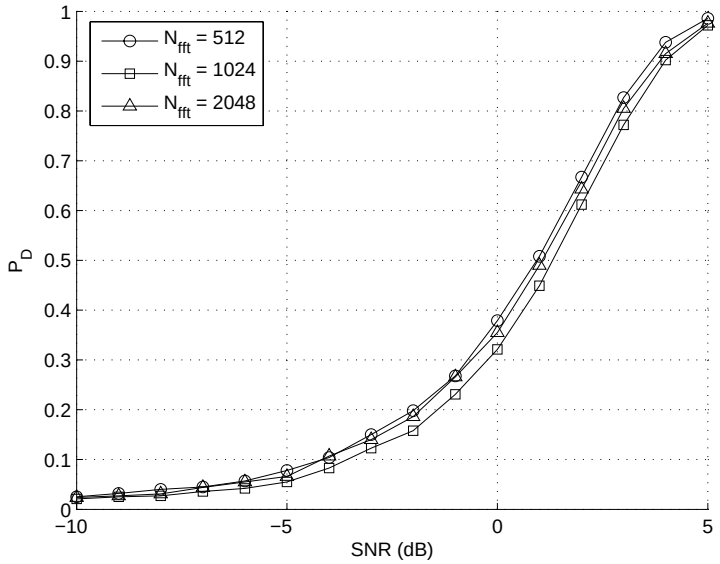

Figure A.11 CSM - 500 MHz ChRx (Varying Number of Points in FFT)

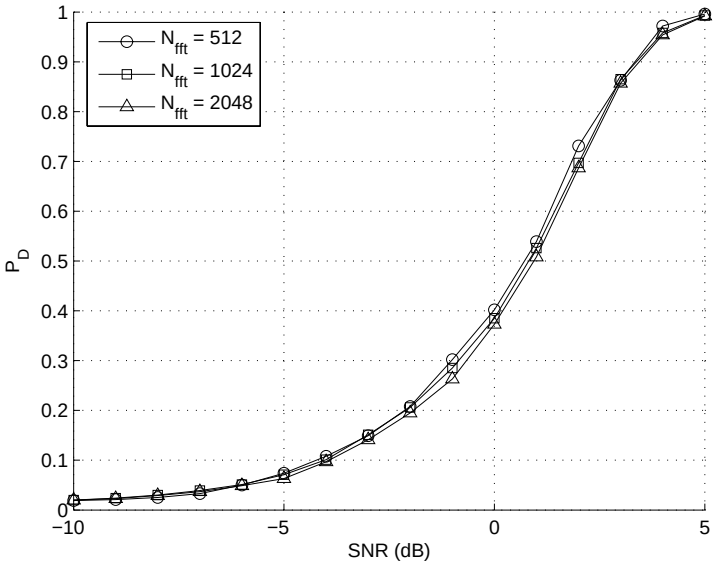

Figure A.12 CSM - 100 MHz ChRx (Varying Number of Points in FFT)

A.2 Down-Converting Channelized Receiver Detection Performance

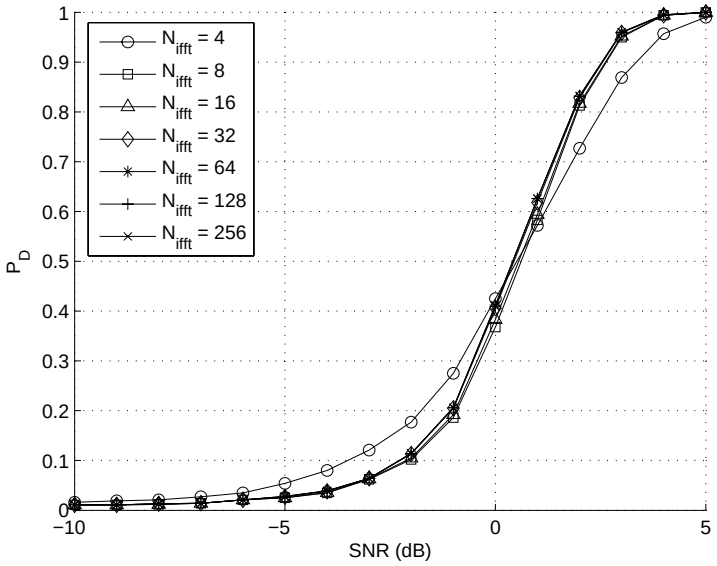

Figure A.13 TTM - 1 GHz DC ChRx (Varying Number of Points in IFFT)

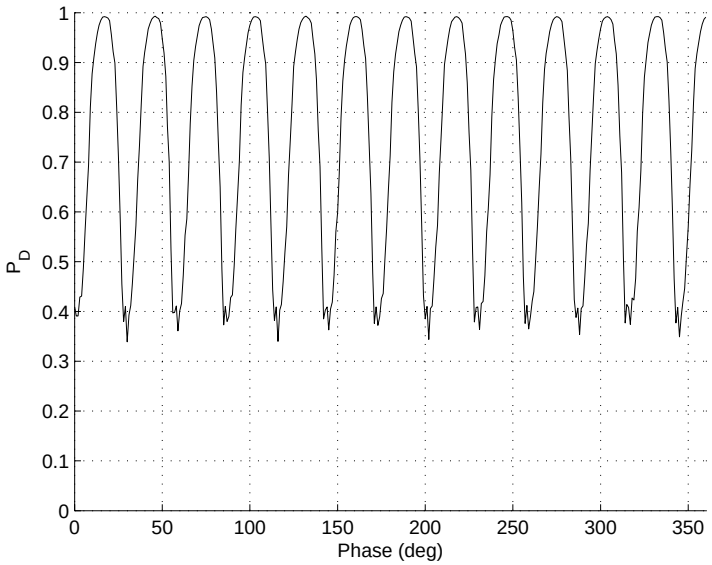

Figure A.14 TTM - 1 GHz DC ChRx, SNR = 0 dB (Varying Starting Phases)

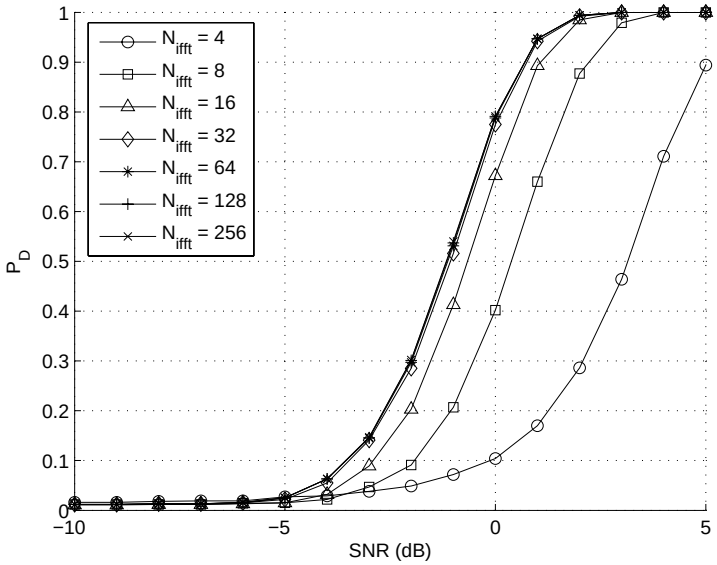

Figure A.15 TTM - 500 MHz DC ChRx (Varying Number of Points in IFFT)

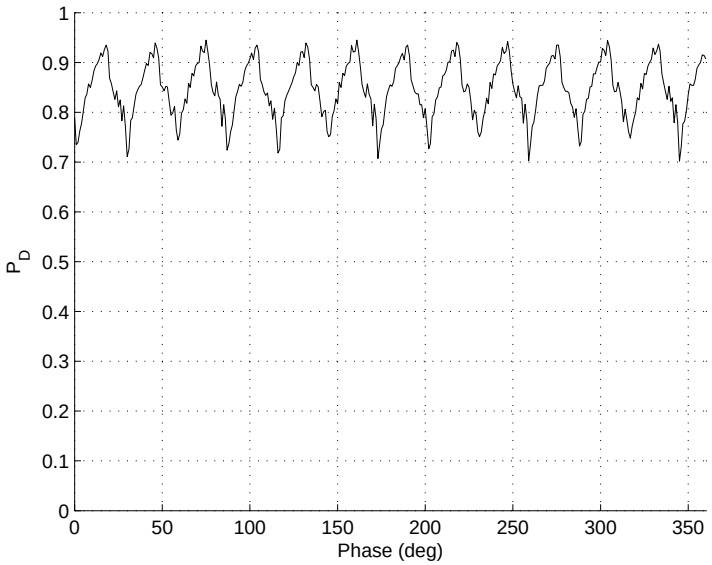

Figure A.16 TTM - 500 MHz DC ChRx, SNR = 0 dB (Varying Starting Phases)

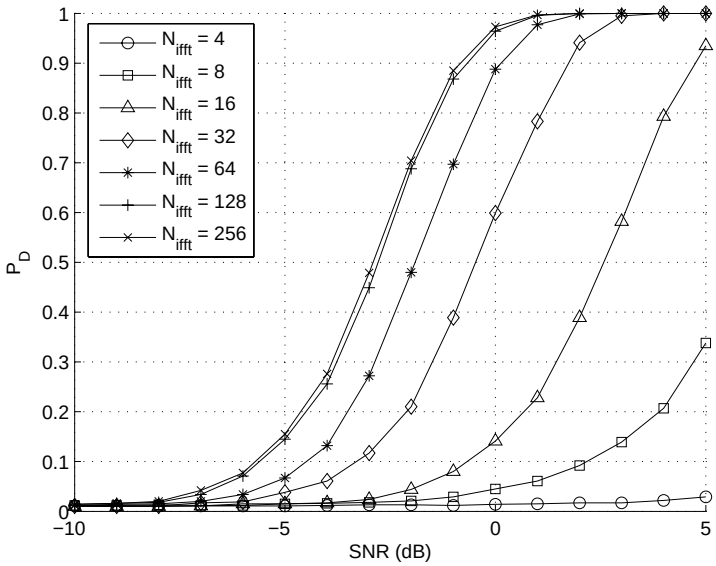

Figure A.17 TTM - 100 MHz DC ChRx (Varying Number of Points in IFFT)

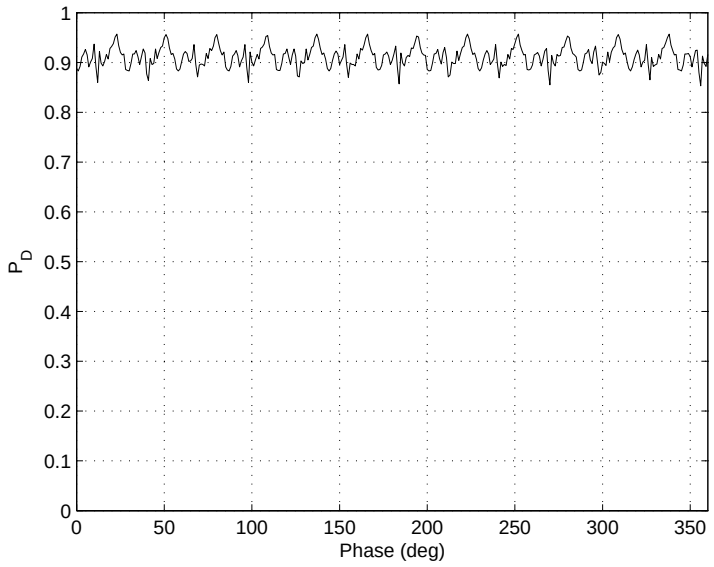

Figure A.18 TTM - 100 MHz DC ChRx, SNR = 0 dB (Varying Starting Phases)

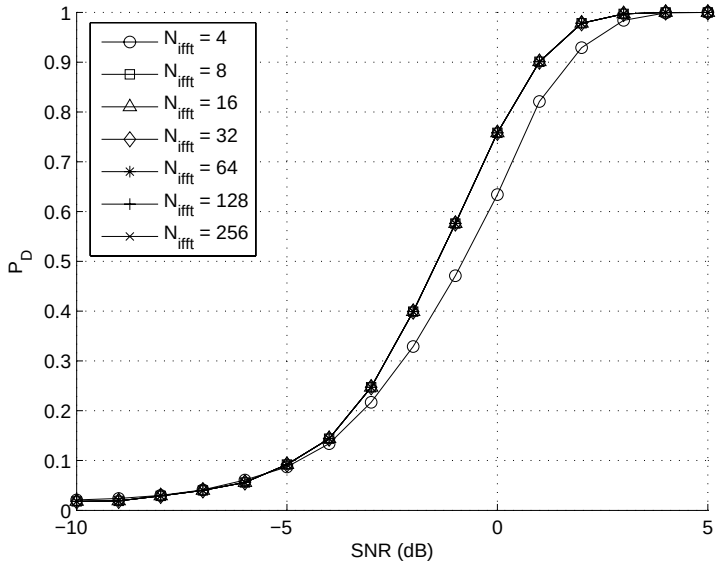

Figure A.19 CTM - 1 GHz DC ChRx (Varying Number of Points in IFFT)

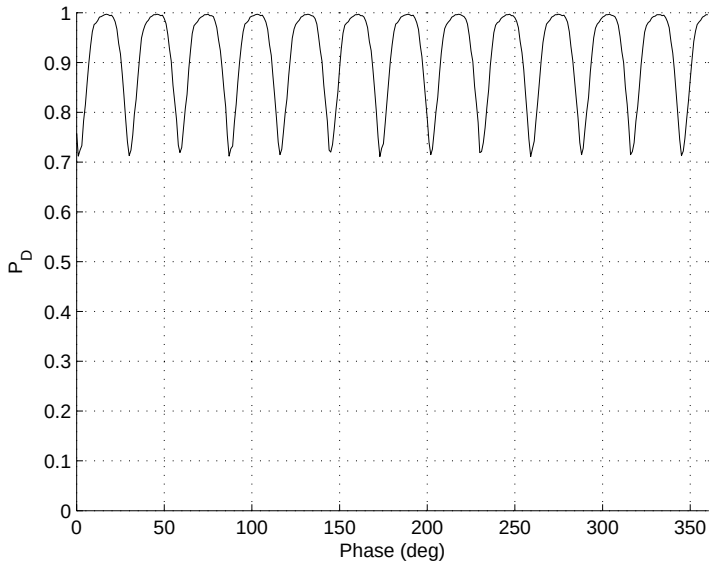

Figure A.20 CTM - 1 GHz DC ChRx, SNR = 0 dB (Varying Starting Phases)

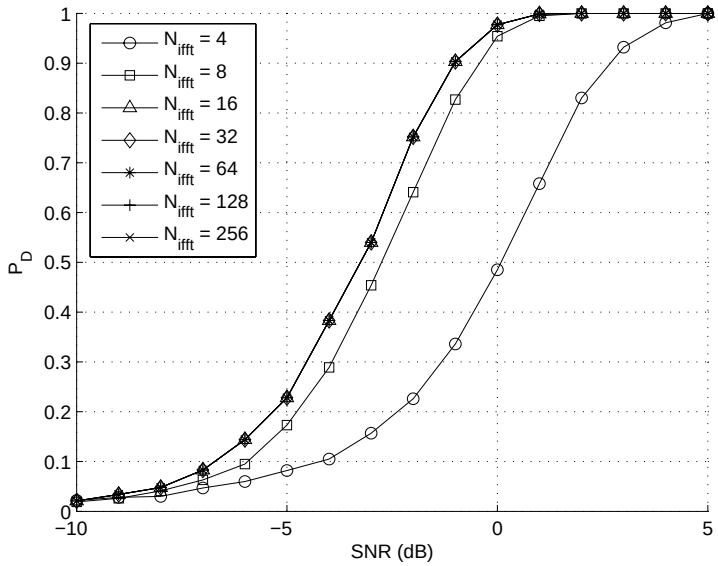

Figure A.21 CTM - 500 MHz DC ChRx (Varying Number of Points in IFFT)

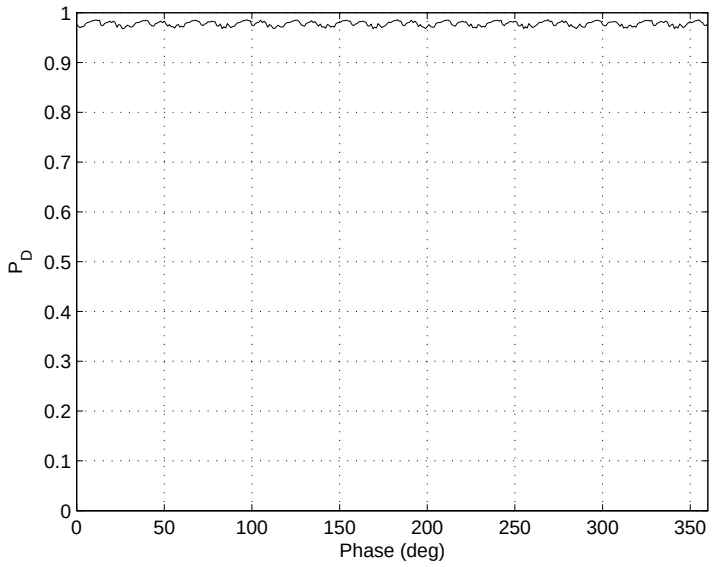

Figure A.22 CTM - 500 MHz DC ChRx, SNR = 0 dB (Varying Starting Phases)

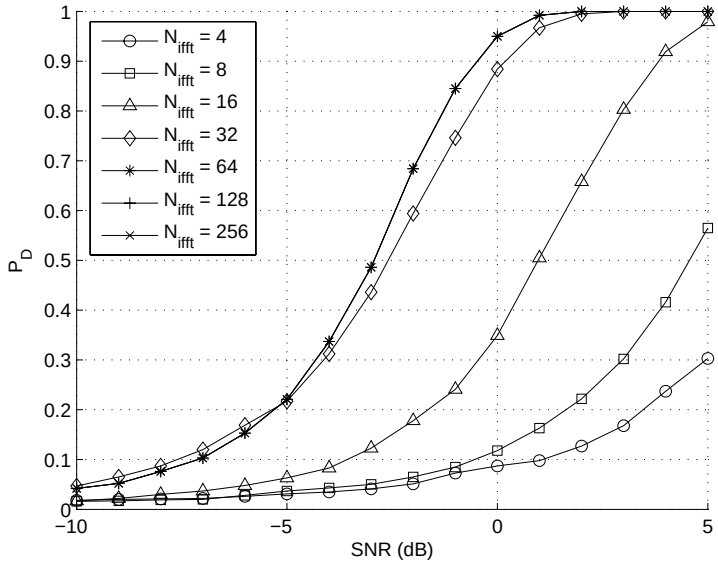

Figure A.23 CTM - 100 MHz DC ChRx (Varying Number of Points in IFFT)

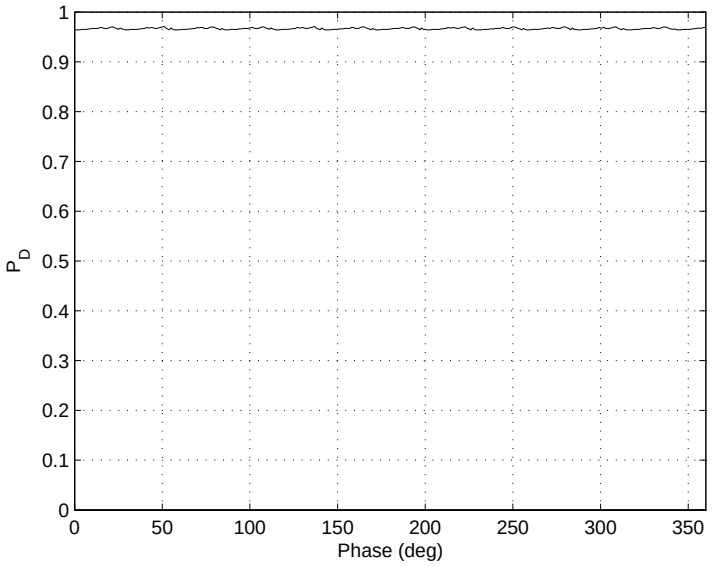

Figure A.24 CTM - 100 MHz DC ChRx, SNR = 0 dB (Varying Starting Phases)

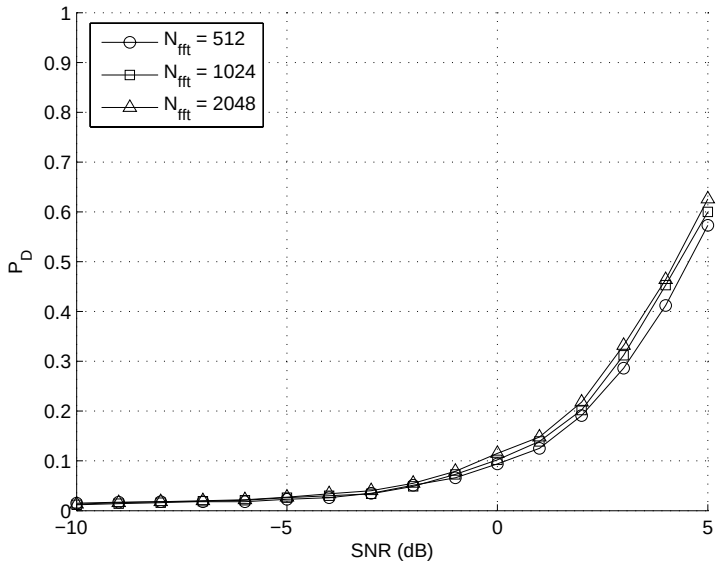

Figure A.25 SSM - 1 GHz DC ChRx (Varying Number of Points in FFT)

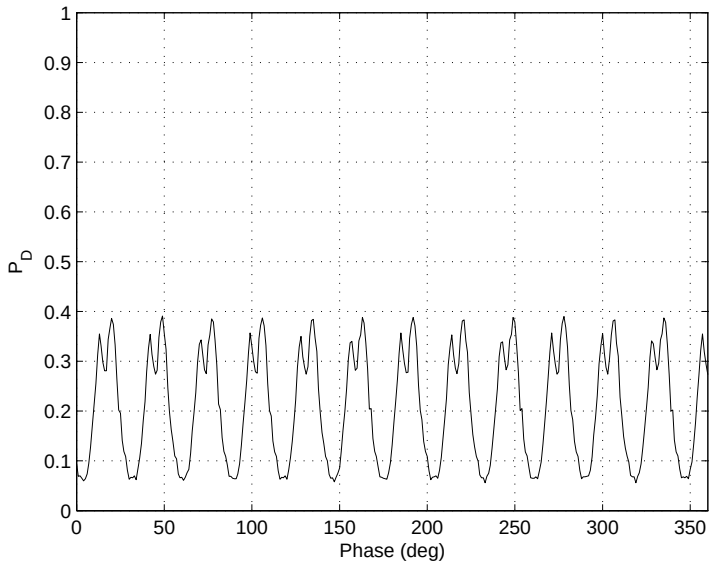

Figure A.26 SSM - 1 GHz DC ChRx, SNR = 0 dB (Varying Starting Phases)

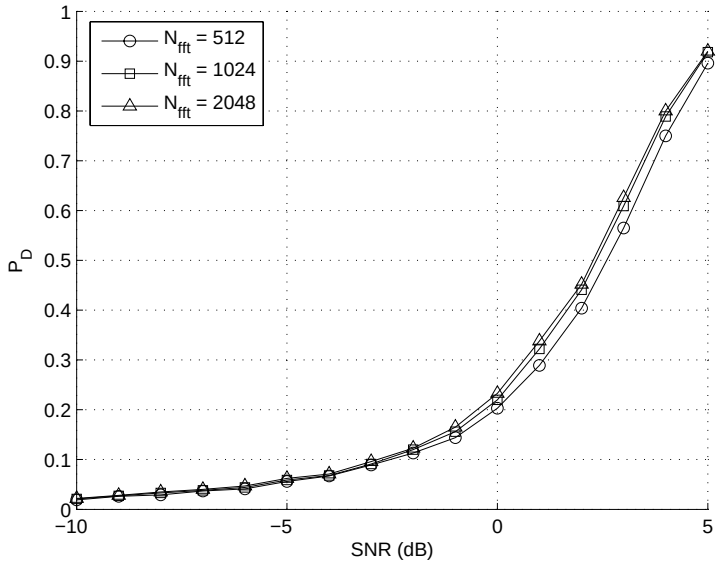

Figure A.27 SSM - 500 MHz DC ChRx (Varying Number of Points in FFT)

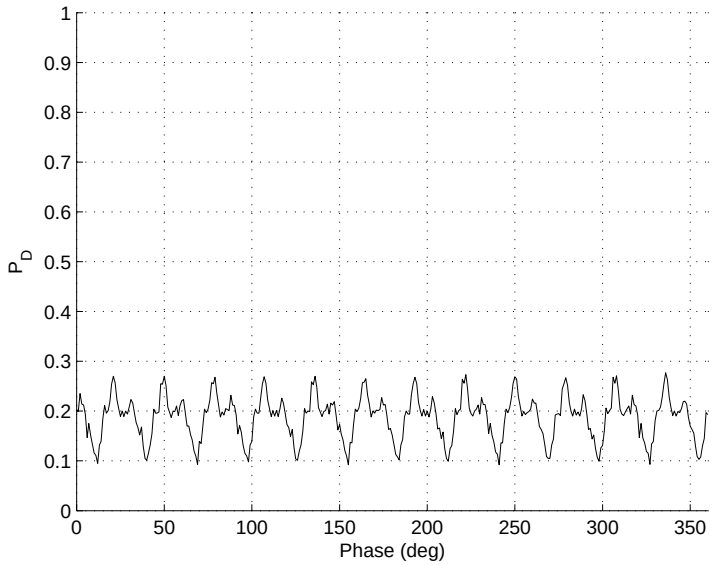

Figure A.28 SSM - 500 MHz DC ChRx, SNR = 0 dB (Varying Starting Phases)

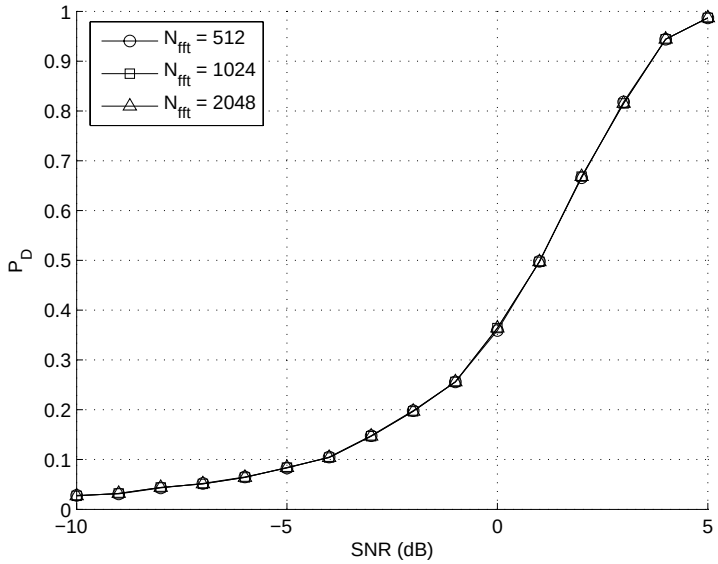

Figure A.29 SSM - 100 MHz DC ChRx (Varying Number of Points in FFT)

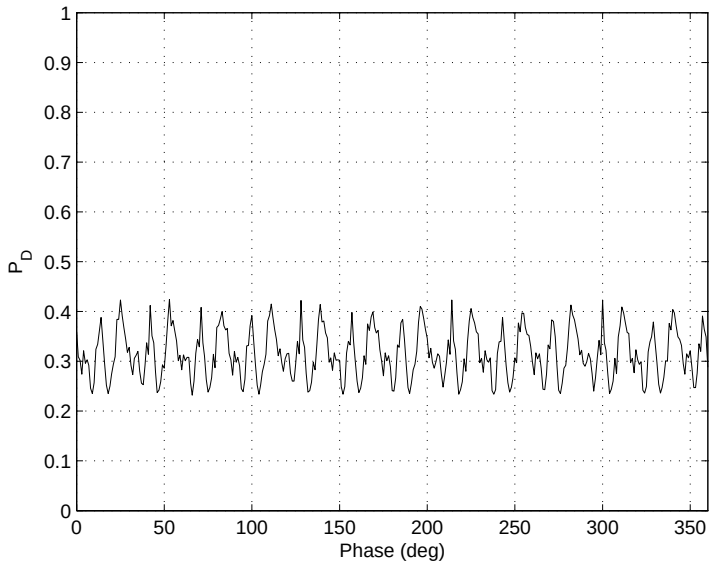

Figure A.30 SSM - 100 MHz DC ChRx, SNR = 0 dB (Varying Starting Phases)

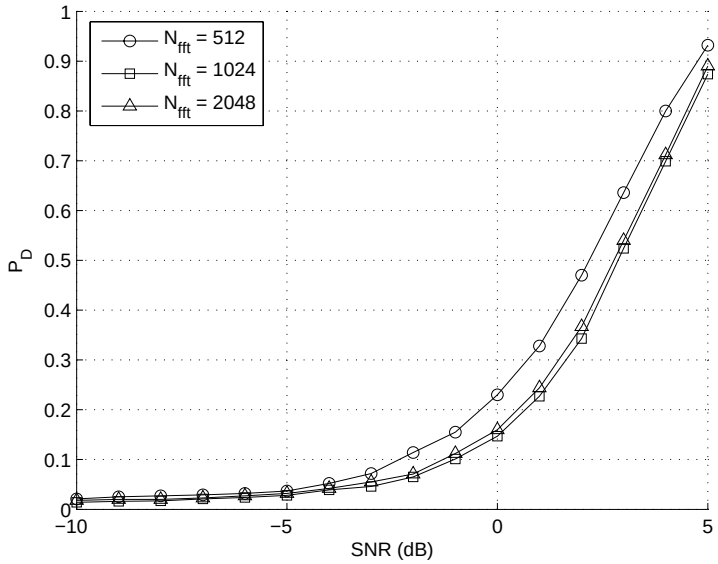

Figure A.31 CSM - 1 GHz DC ChRx (Varying Number of Points in FFT)

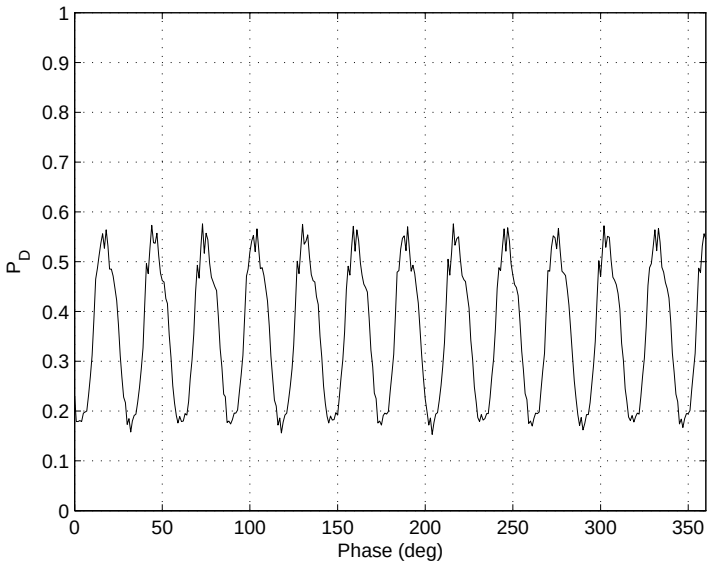

Figure A.32 CSM - 1 GHz DC ChRx, SNR = 0 dB (Varying Starting Phases)

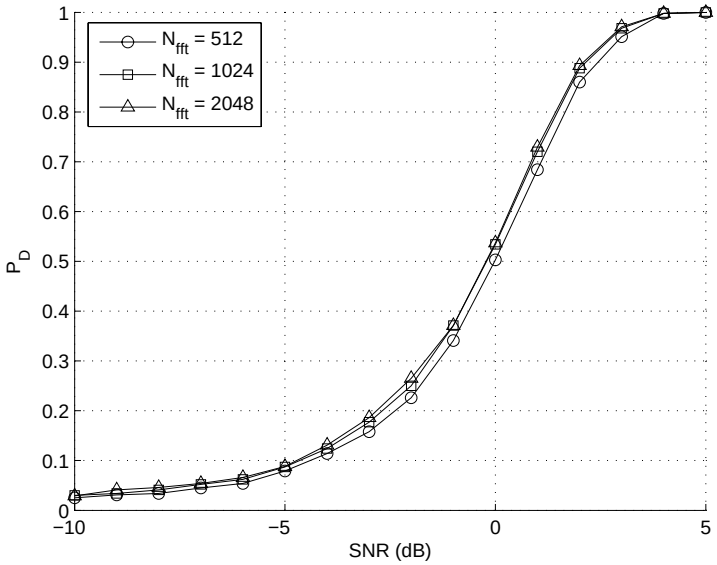

Figure A.33 CSM - 500 MHz DC ChRx (Varying Number of Points in FFT)

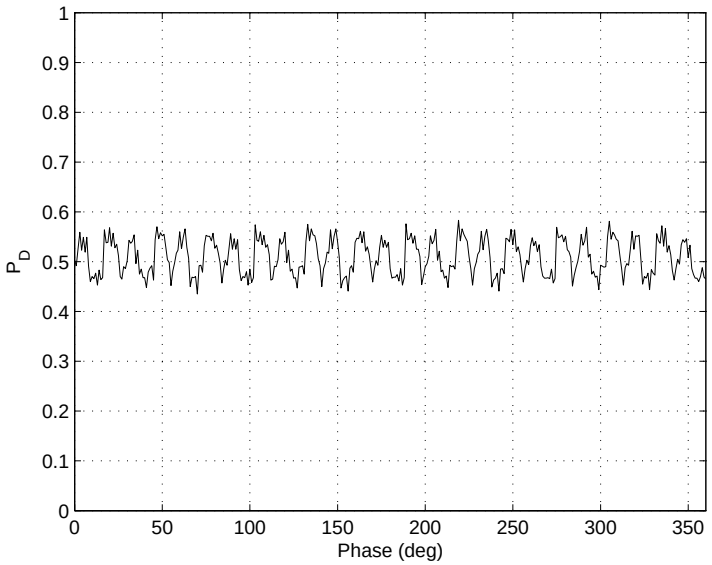

Figure A.34 CSM - 500 MHz DC ChRx, SNR = 0 dB (Varying Starting Phases)

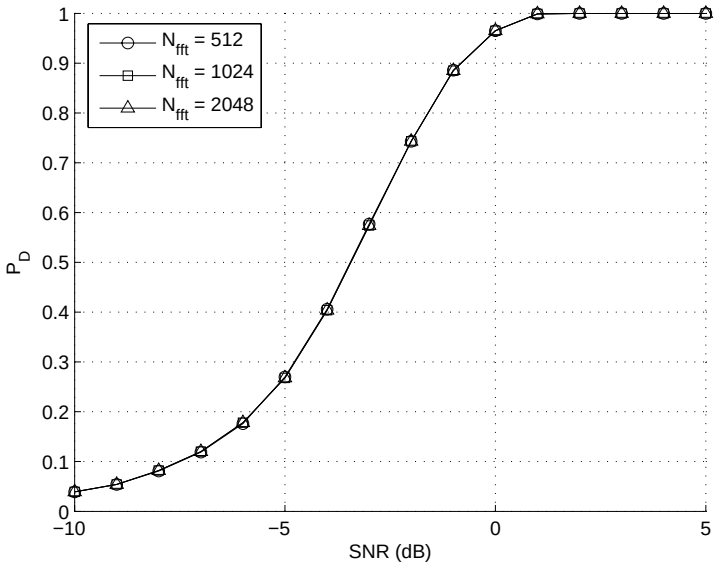

Figure A.35 CSM - 100 MHz DC ChRx (Varying Number of Points in FFT)

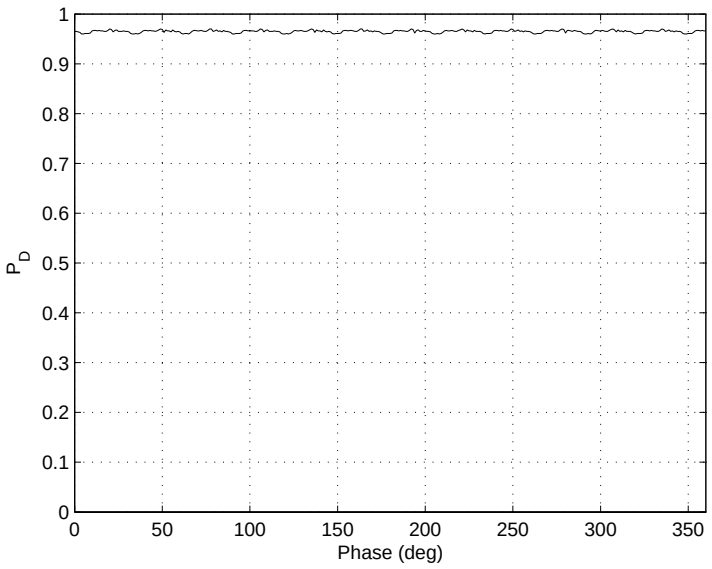

Figure A.36 CSM - 100 MHz DC ChRx, SNR = 0 dB (Varying Starting Phases)

Appendix B. Alternate UWB Pulse Offset

B.1 Input Signal and Processed Matrices

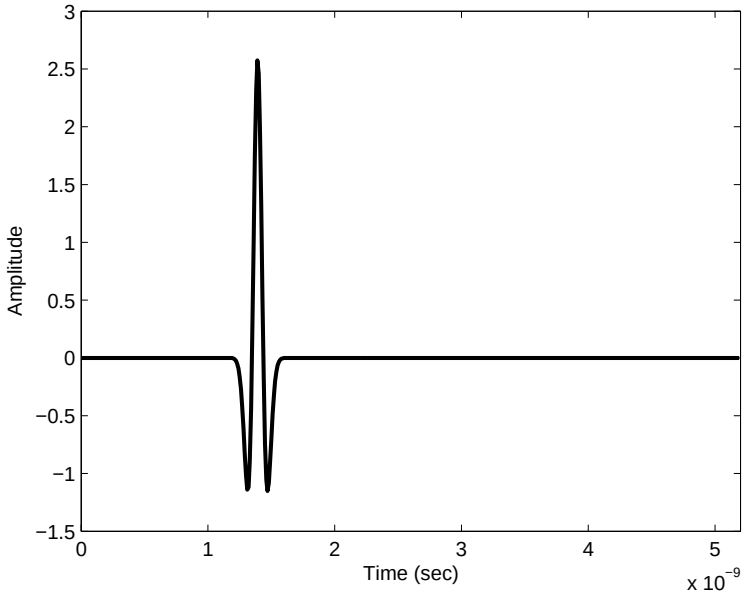

Figure B.1 UWB ChRx Input Signal

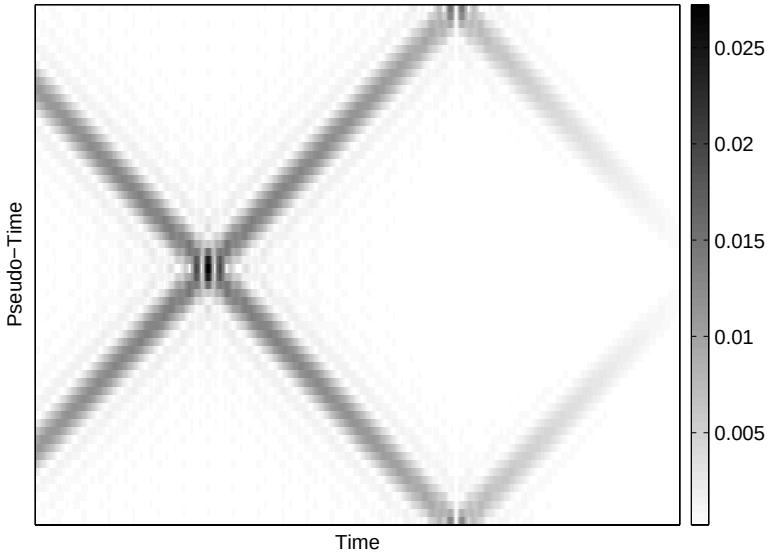

Figure B.2 Temporal-Temporal Matrix, No Noise Present

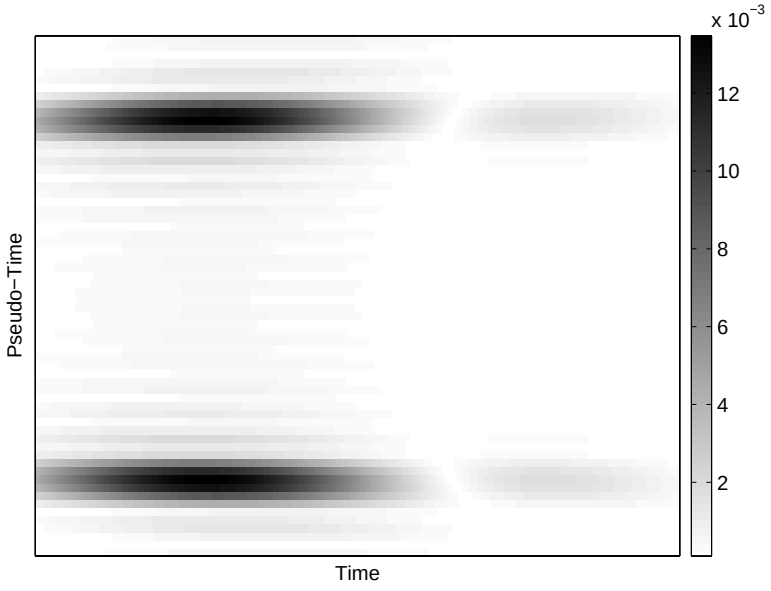

Figure B.3 Temporal-Temporal Matrix, Downconverting ChRx, No Noise Present

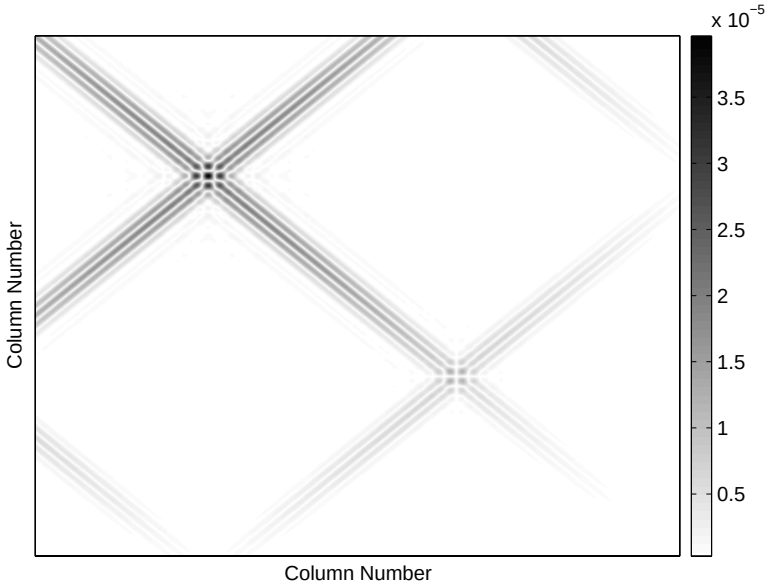

Figure B.4 Cross Temporal Matrix, No Noise Present

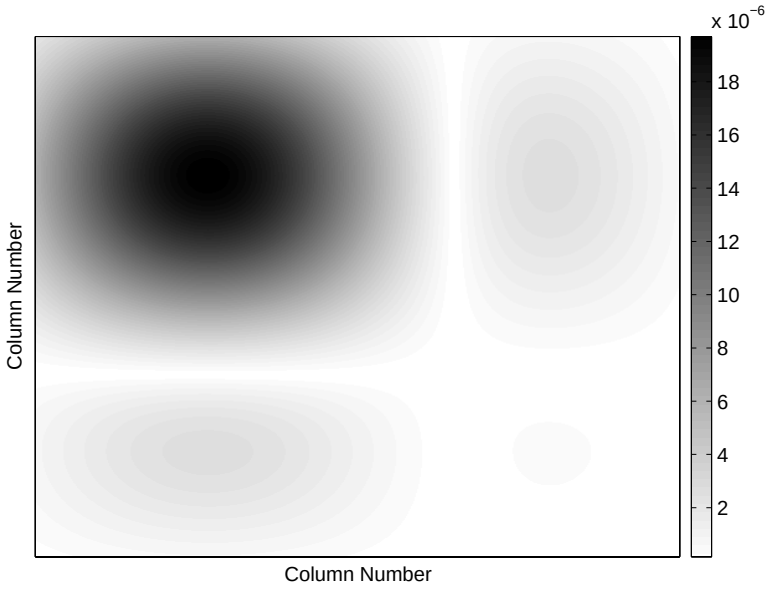

Figure B.5 Cross Temporal Matrix, Downconverting ChRx, No Noise Present

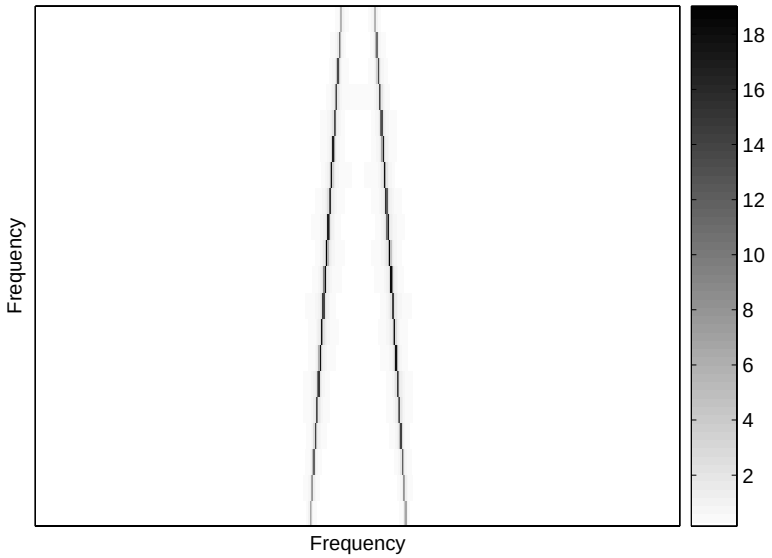

Figure B.6 Spectral-Spectral Matrix, No Noise Present

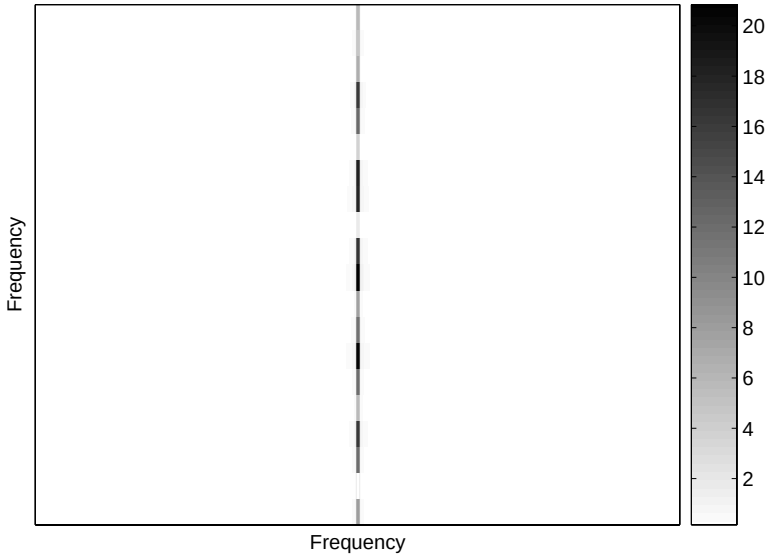

Figure B.7 Spectral-Spectral Matrix, Downconverting ChRx, No Noise Present

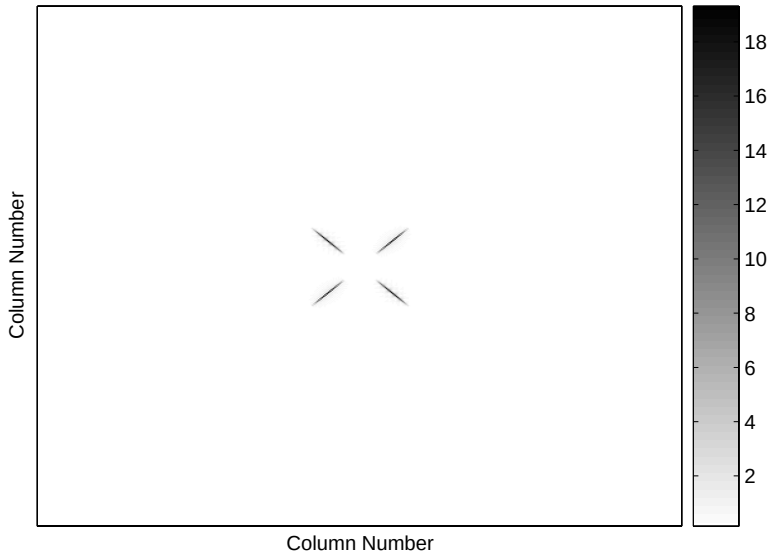

Figure B.8 Cross Spectral Matrix, No Noise Present

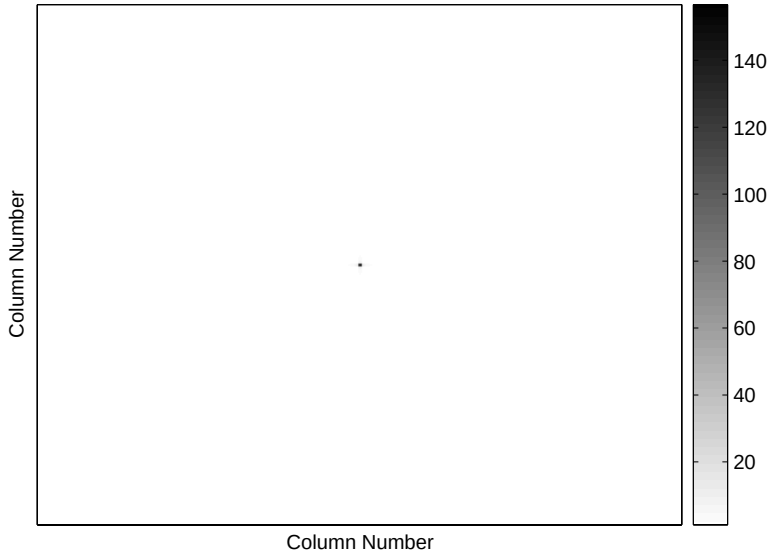

Figure B.9 Cross Spectral Matrix, Downconverting ChRx, No Noise Present

B.2 Channelized Receiver Detection Performance

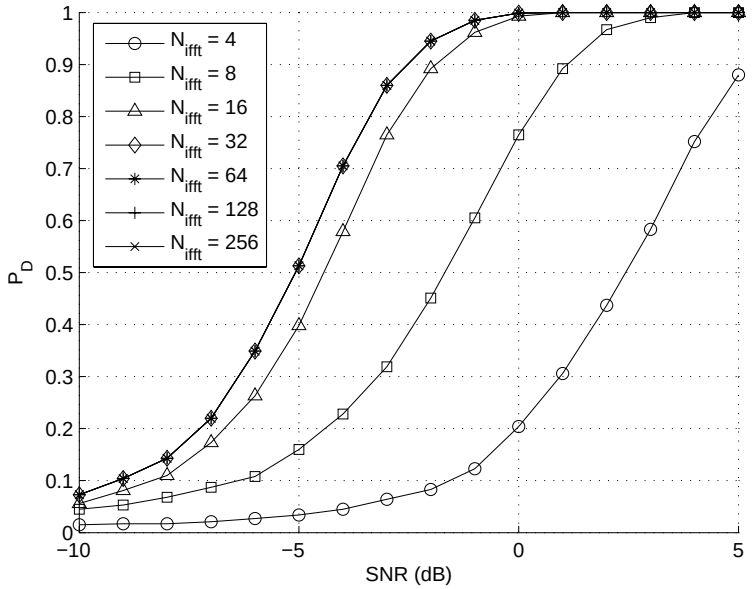

Figure B.10 TTM - 250 MHz ChRx (Varying Number of Points in IFFT)

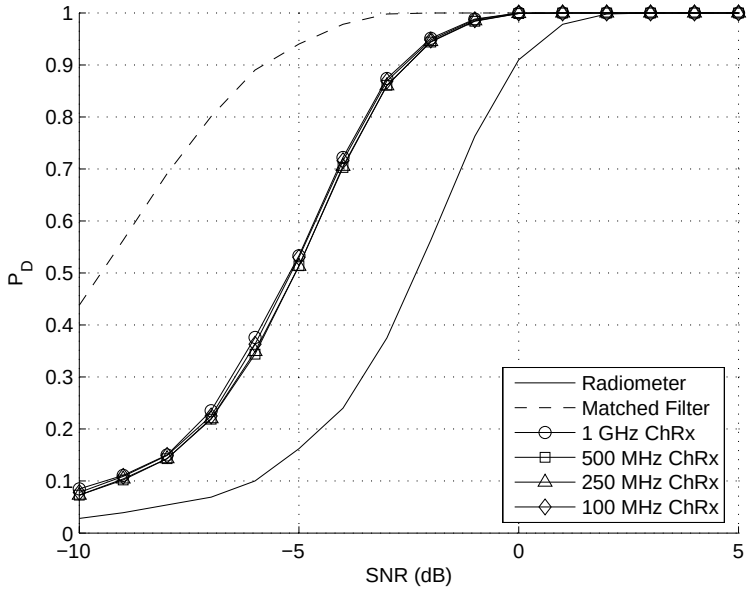

Figure B.11 TTM - $N_{ifft} = 64$

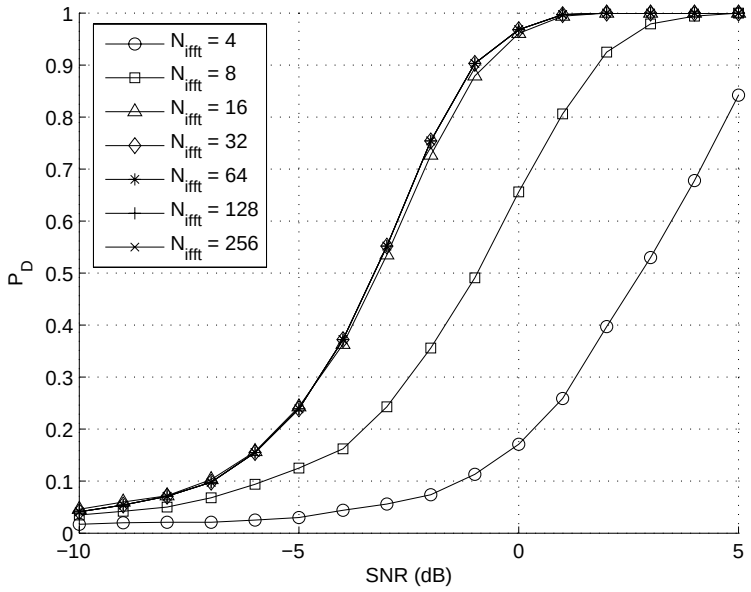

Figure B.12 CTM - 250 MHz ChRx (Varying Number of Points in IFFT)

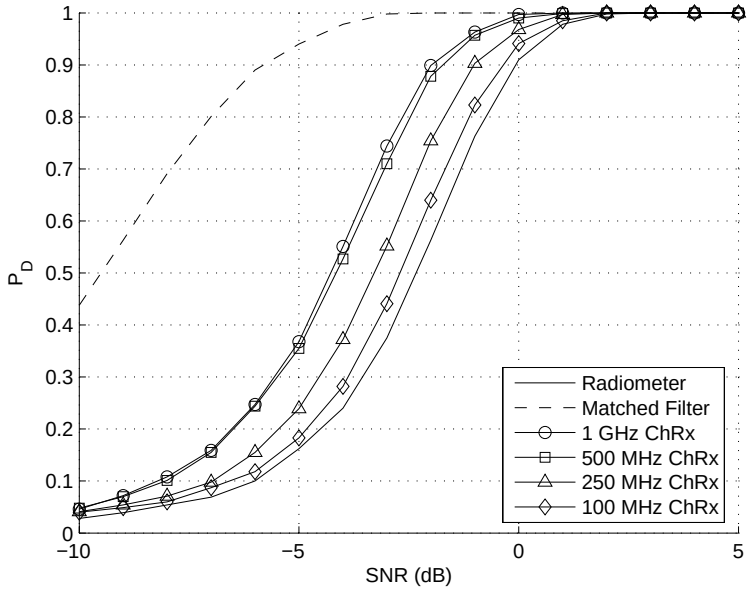

Figure B.13 CTM - $N_{ifft} = 64$

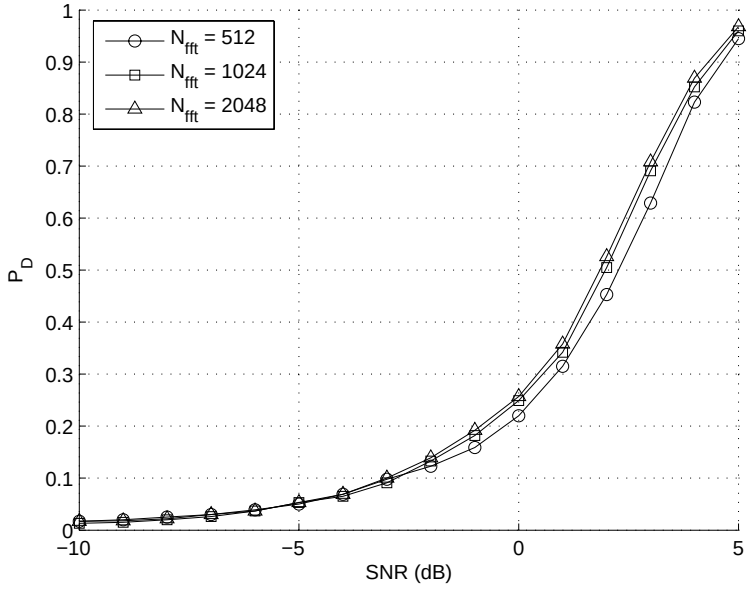

Figure B.14 SSM - 250 MHz ChRx (Varying Number of Points in IFFT)

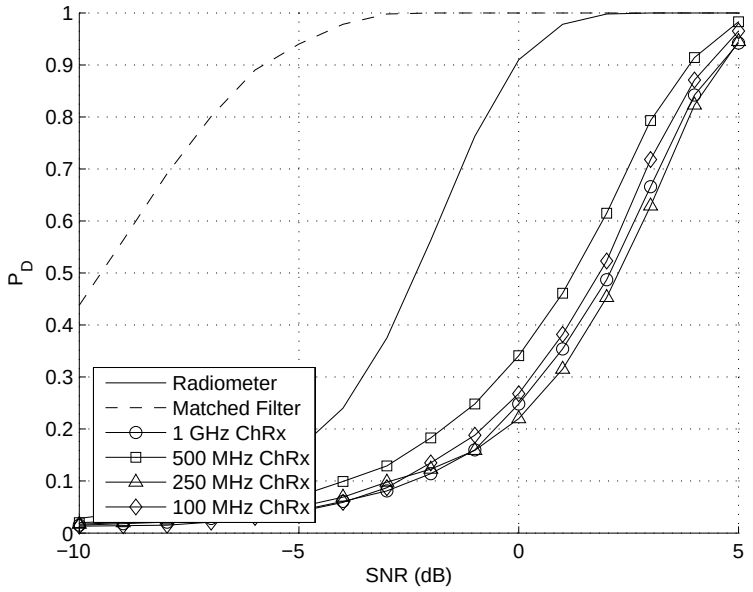

Figure B.15 SSM - $N_{fft} = 512$

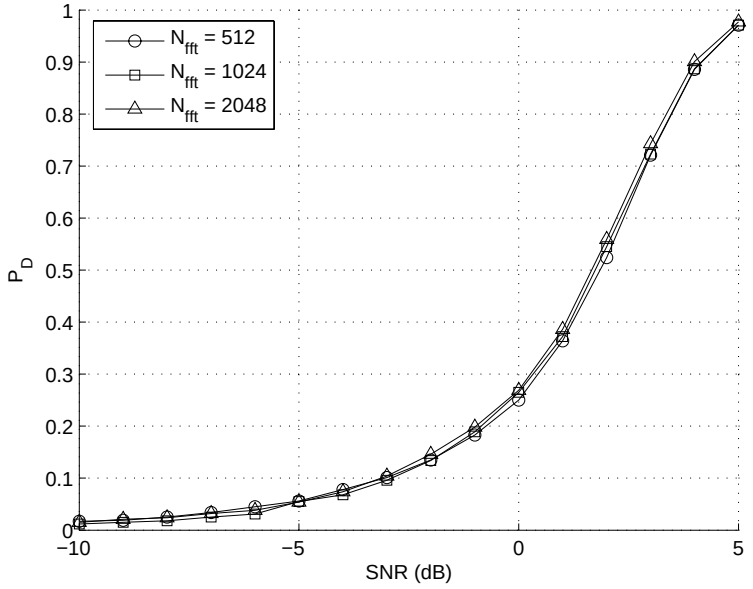

Figure B.16 CSM - 250 MHz ChRx (Varying Number of Points in IFFT)

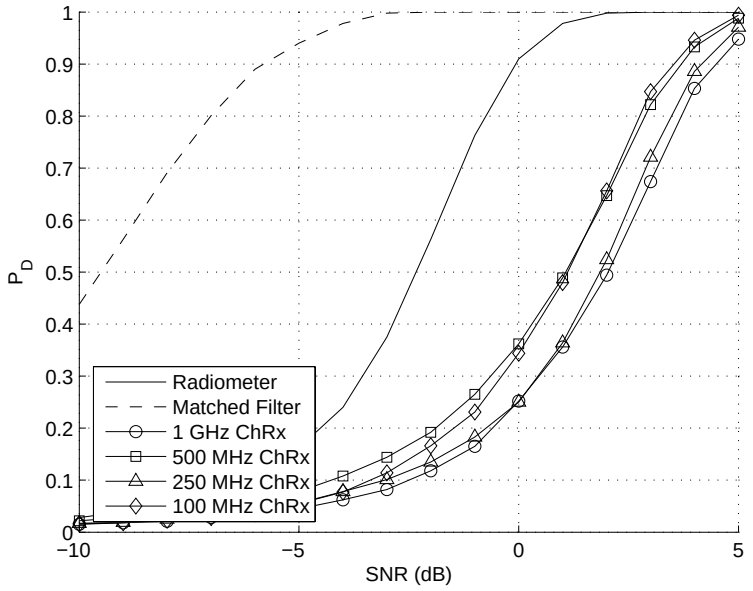

Figure B.17 CSM - $N_{fft} = 512$

B.3 Downconverting Channelized Receiver Detection Performance

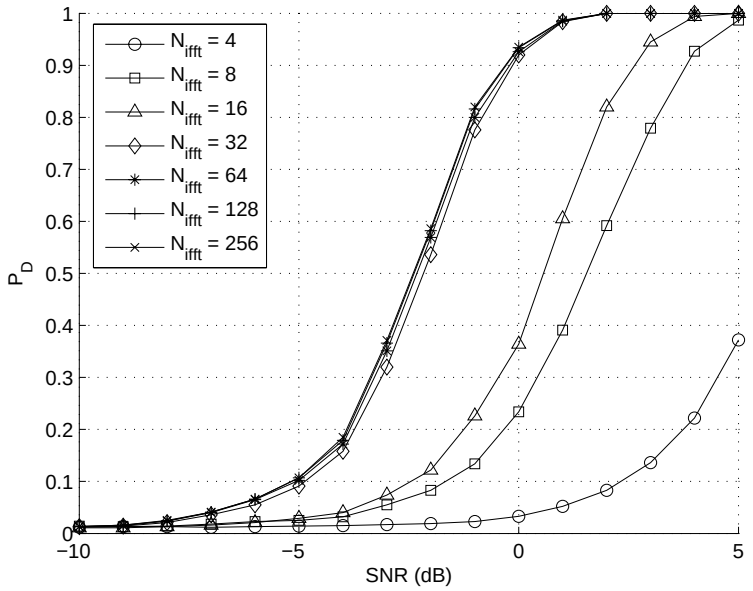

Figure B.18 TTM - 250 MHz DC ChRx (Varying Number of Points in IFFT)

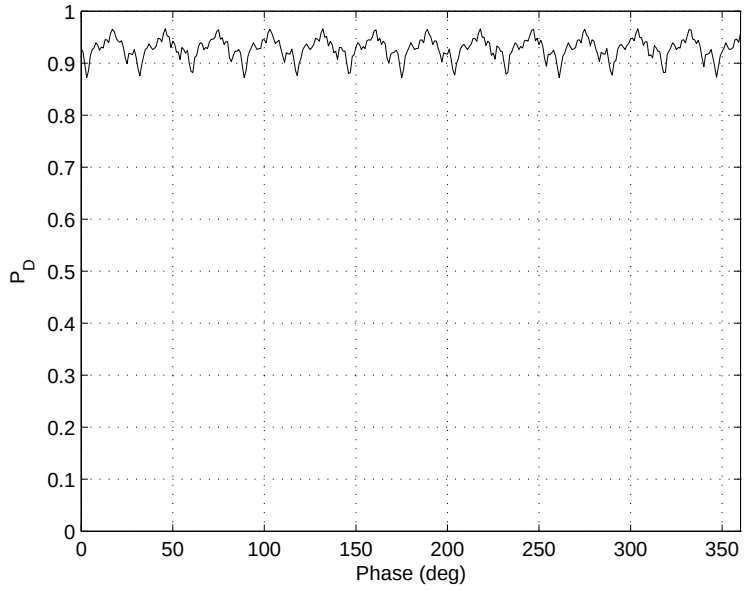

Figure B.19 TTM - 250 MHz DC ChRx, SNR = 0 dB (Varying Starting Phases)

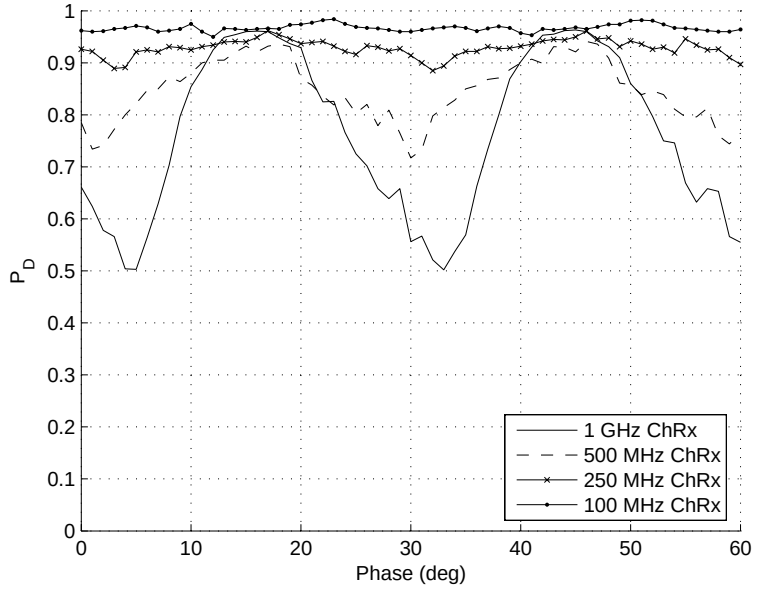

Figure B.20 TTM - DC ChRx, SNR = 0 dB (Varying Starting Phases)

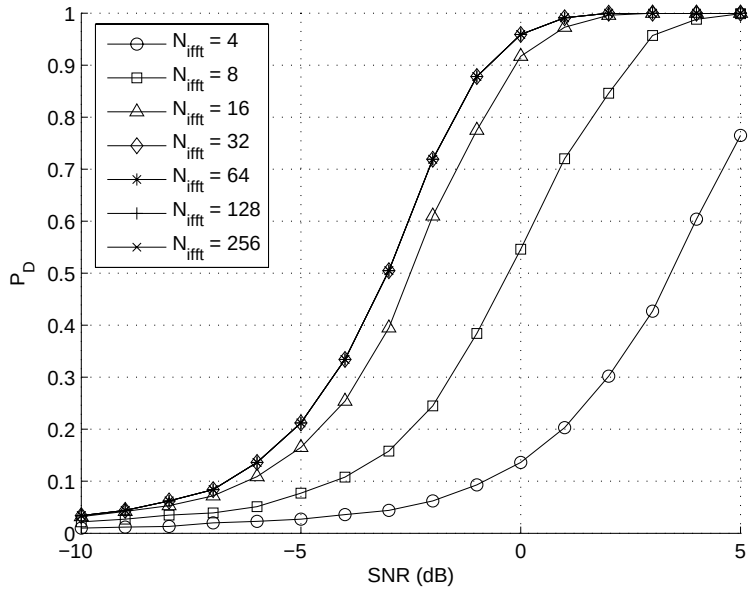

Figure B.21 CTM - 250 MHz DC ChRx (Varying Number of Points in IFFT)

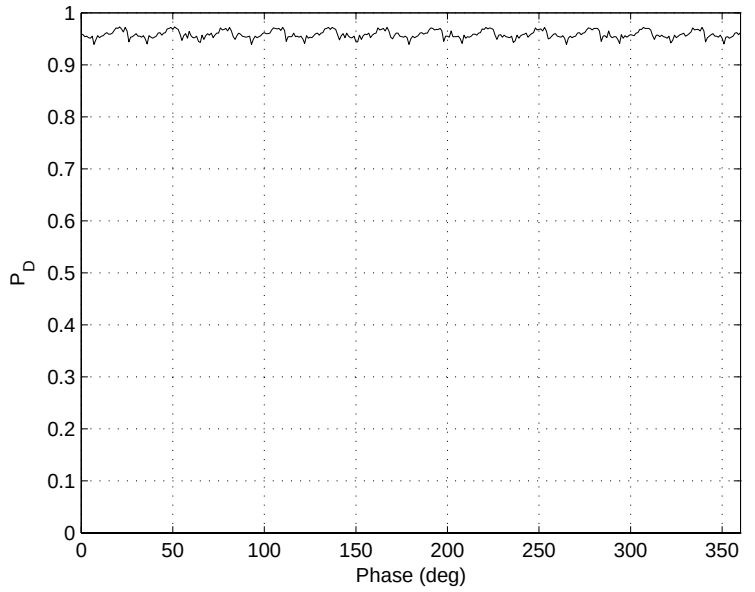

Figure B.22 CTM - 250 MHz DC ChRx, SNR = 0 dB (Varying Starting Phases)

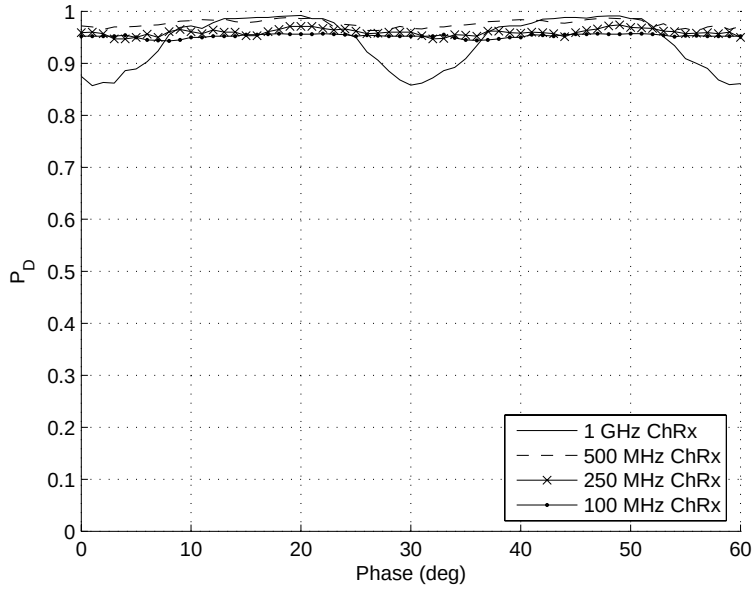

Figure B.23 CTM - DC ChRx, SNR = 0 dB (Varying Starting Phases)

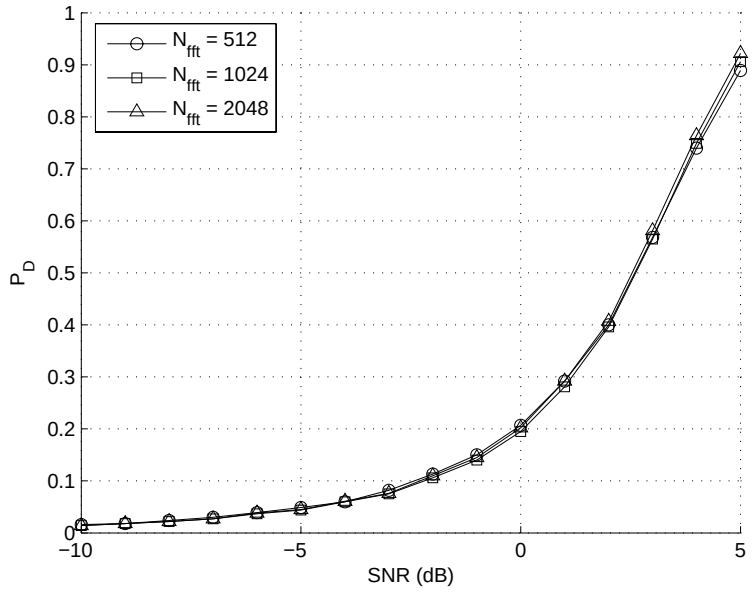

Figure B.24 SSM - 250 MHz DC ChRx (Varying Number of Points in IFFT)

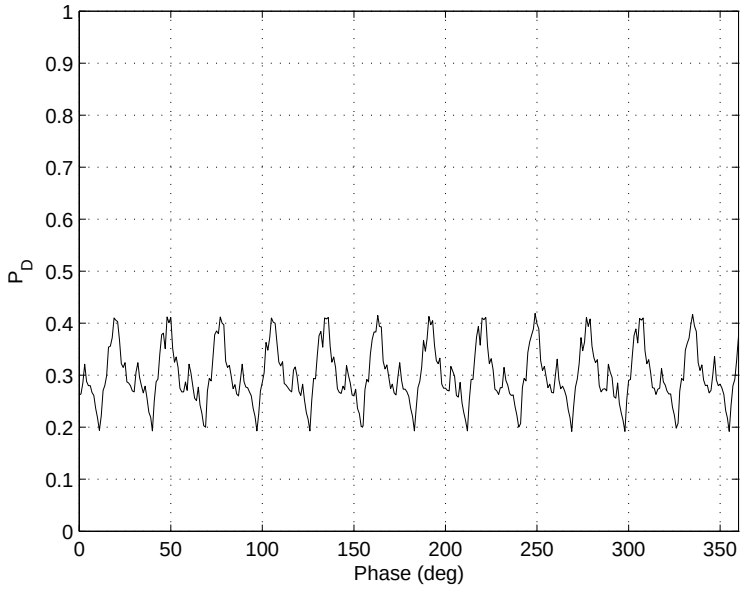

Figure B.25 SSM - 250 MHz DC ChRx, SNR = 0 dB (Varying Starting Phases)

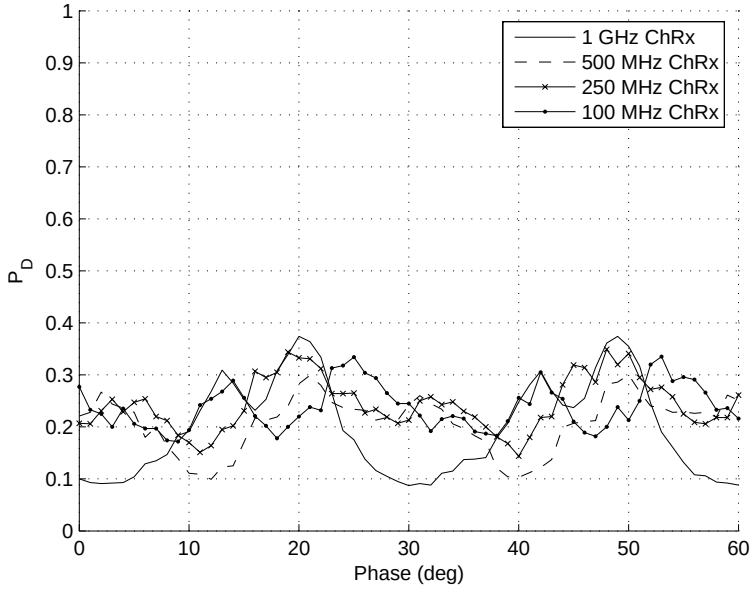

Figure B.26 SSM - DC ChRx, SNR = 0 dB (Varying Starting Phases)

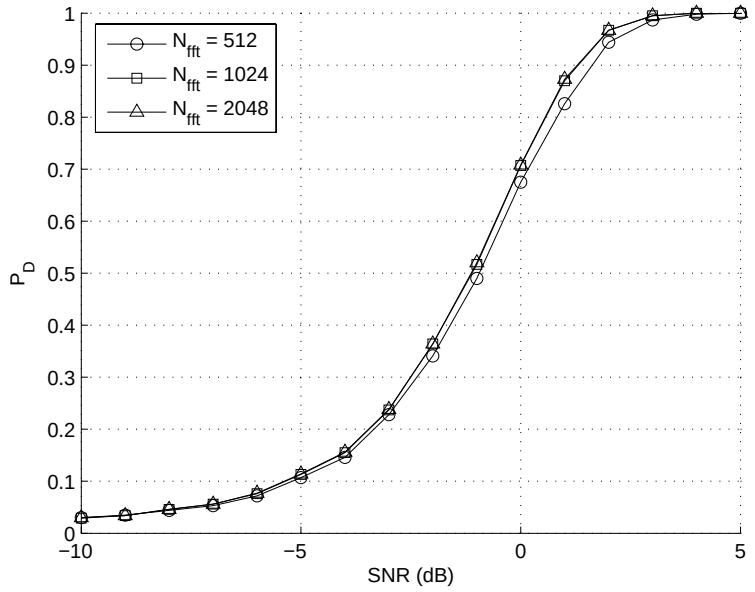

Figure B.27 CSM - 250 MHz DC ChRx (Varying Number of Points in IFFT)

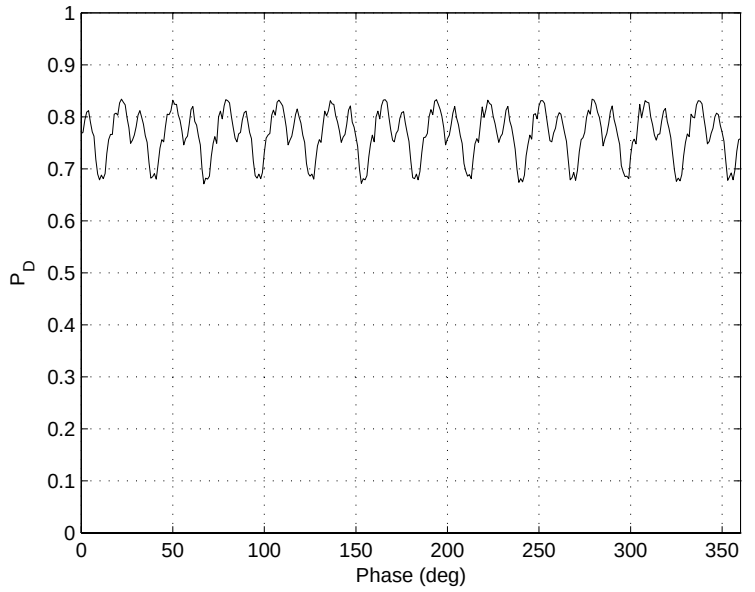

Figure B.28 CSM - 250 MHz DC ChRx, SNR = 0 dB (Varying Starting Phases)

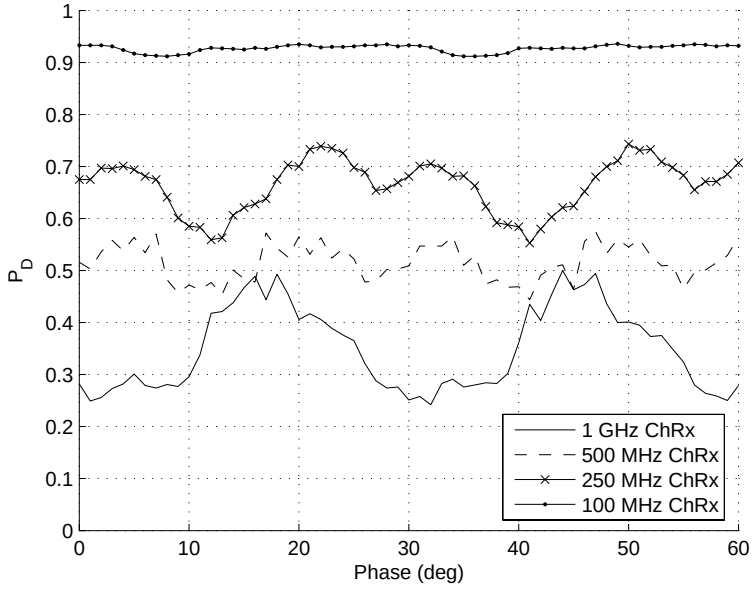

Figure B.29 CSM - DC ChRx, SNR = 0 dB (Varying Starting Phases)

Appendix C. MATLAB Code

```
% Brett D. Gronholz
% EENG 799 -- Summer/Fall 2004
% UWB Power Spectral Density
% -- Analytic
%%%%%%%%%%%%%%%%%%%%%%%%%%%%%%%%%%
clear all, close all, clc, format compact

%%%%%%%%%%%%%%%%%%%%%%%%%%
% UWB Signal Parameters
%%%%%%%%%%%%%%%%%%%%%%%%%%
fc = 5e9;       % center frequency
Tw = 2/fc;      % pulse duration
Tm = 0.4*Tw;    % pulse width parameter
Ts = 2*Tw;      % symbol duration
delta = Tw/2;   % position modulation offset

f = 0:1/(1000*Tw):40e9; % frequency vector

% FT of received UWB waveform
Wf = pi*Tm^3*f.^2/sqrt(2).*exp(-pi/2*Tm^2*f.^2);

%%%%%%%%%%%%%%%%%%%%%%%%%%%%
% Analytic PSD -- Uniform
%%%%%%%%%%%%%%%%%%%%%%%%%%%%
Suni_con = 1e-13*ones(1,length(f)); % continuous part
Suni_dis = 1/Ts^2*ones(1,length(f));% discrete part
n = find(mod(f,1/Ts) ~= 0);
for i = 1:length(n),
    Suni_dis(n(i)) = 1e-13;         % 'discretize' discrete part
end
Smod_uni = Suni_con + Suni_dis;     % sum continuous and discrete parts
Suni = Smod_uni .* (Wf.*conj(Wf));  % total signal PSD
Suni(1) = 1e-13;                    % avoid dB conversion warning
Suni_dB = 10*log10(abs(Suni));      % total signal PSD (dB)

figure(1)
plot(f,Suni_dB,'kx')
%axis([0 16e9 -160 -10]);
ylabel('Magnitude (dB)');
xlabel('Frequency (Hz)');
```

```
%%%%%%%%%%%%%%%%%%%%%%%%
% Analytic PSD -- PPM
%%%%%%%%%%%%%%%%%%%%%%%%
Sppm_con = (1/(2*Ts))*(1-cos(4*pi*f*delta));    % continuous part
Sppm_dis = (1/(2*Ts^2))*(1+cos(4*pi*f*delta));  % discrete part
n = find(mod(f,1/Ts) ~= 0);
for i = 1:length(n),
    Sppm_dis(n(i)) = 1e-13;         % 'discretize' discrete part
end
Smod_ppm = Sppm_con + Sppm_dis;     % sum continuous and discrete parts
Sppm = Smod_ppm .* (Wf.*conj(Wf));  % total signal PSD
Sppm(1) = 1e-13;                    % avoid dB conversion warning
Sppm_dB = 10*log10(abs(Sppm));      % total signal PSD (dB)

figure(1),hold on
plot(f,Sppm_dB,'k')
axis([0 18e9 -180 -10]);
ylabel('Magnitude (dB)');
xlabel('Frequency (Hz)');
grid

%%%%%%%%%%%%%%%%%%%%%%%%
% Analytic PSD -- PAM
%%%%%%%%%%%%%%%%%%%%%%%%
Spam_con = 2/Ts;                    % continuous part
Spam_dis = 0;                       % discrete part
Smod_pam = Spam_con + Spam_dis;     % sum continuous and discrete parts
Spam = Smod_pam .* (Wf.*conj(Wf));  % total signal PSD
Spam(1) = 1e-13;                    % avoid dB conversion warning
Spam_dB = 10*log10(abs(Spam));      % total signal PSD (dB)

figure(1)
plot(f,Spam_dB,'k--')
% axis([0 16e9 -160 -100]);
ylabel('Magnitude (dB)');
xlabel('Frequency (Hz)');

%%%%%%%%%%%%%%%%%%%%%%%%%
% Analytic PSD -- BPPM
%%%%%%%%%%%%%%%%%%%%%%%%%
Sbppm_con = 1/Ts;                   % continuous part
```

```
Sbppm_dis = 0;                      % discrete part
Smod_bppm = Sbppm_con + Sbppm_dis;  % sum continuous and discrete parts
Sbppm = Smod_bppm .* (Wf.*conj(Wf));% total signal PSD
Sbppm(1) = 1e-13;                   % avoid dB conversion warning
Sbppm_dB = 10*log10(abs(Sbppm));    % total signal PSD (dB)

figure(1)
plot(f,Sbppm_dB,'k:')
% axis([0 16e9 -160 -100]);
ylabel('Magnitude (dB)');
xlabel('Frequency (Hz)');

legend('Uniform','PPM','PAM','BPPM')
```

```
% Brett D. Gronholz
% EENG 799 -- Summer/Fall 2004
% UWB Power Spectral Density
% -- Simulated
%%%%%%%%%%%%%%%%%%%%%%%%%%%%%%%%
clear all, close all, clc, format compact

%%%%%%%%%%%%%%%%%%%%%%%%%%%
% UWB Signal Parameters
%%%%%%%%%%%%%%%%%%%%%%%%%%%
fc = 5e9;       % center frequency
Tw = 2/fc;      % pulse duration
Ts = 2*Tw;      % symbol duration
To = Ts;        % symbol repetition interval
delt = 0.04*Tw; % time resolution
Ns = 1000;      % number of symbols
P = 1;          % signal power
jtr = 0;        % jitter as percentage of Ts
dly = 0;        % first pulse delay

%%%%%%%%%%%%
% Uniform
%%%%%%%%%%%%
uni = uwb(Tw,To,delt,Ns,P,jtr,'uni',dly);   % uniform pulse train
% uni = awgn(uni,-10,'measured');             % add AWGN

%%%%%%%%%%%%%%%%%%%%%%%%%%%%%%%
% PSD of uniform pulse train
%%%%%%%%%%%%%%%%%%%%%%%%%%%%%%%
uni_tot = length(uni);              % length of signal
f = 1/delt*(0:uni_tot/2)/uni_tot;   % frequency vector
UNI = fft(uni);                     % FFT
Suni = (abs(UNI/uni_tot).^2)*Ns*To; % PSD
for i = 1:length(Suni),
    if Suni(i) == 0,
        Suni(i) = 1e-13;            % avoid dB conversion warning
    end
end
Suni_dB = 10*log10(Suni);           % PSD (dB)

figure(1)
plot(f,Suni_dB(1:uni_tot/2+1),'bx')
```

```
axis([0 20e9 -170 -40]);
ylabel('Magnitude (dB)');
xlabel('Frequency (Hz)');
grid

%%%%%%%%
% PPM
%%%%%%%%
ppm = uwb(Tw,To,delt,Ns,P,jtr,'ppm',dly);   % PPM pulse train
% ppm = awgn(ppm,-10,'measured');             % add AWGN

%%%%%%%%%%%%%%%%%%%%%%%%%%%%
% PSD of PPM Pulse Train
%%%%%%%%%%%%%%%%%%%%%%%%%%%%
ppm_tot = length(ppm);               % length of signal
f = 1/delt*(0:ppm_tot/2)/ppm_tot;    % frequency vector
PPM = fft(ppm);                      % FFT
Sppm = (abs(PPM/ppm_tot).^2)*Ns*To; % PSD
Sppm_dB = 10*log10(Sppm);            % PSD (dB)

figure(2)
plot(f,Sppm_dB(1:ppm_tot/2+1),'b')
axis([0 20e9 -170 -40]);
ylabel('Magnitude (dB)');
xlabel('Frequency (Hz)');
grid

%%%%%%%%
% PAM
%%%%%%%%
pam = uwb(Tw,To,delt,Ns,P,jtr,'pam',dly);   % PAM pulse train
% pam = awgn(pam,-10,'measured');             % add AWGN

%%%%%%%%%%%%%%%%%%%%%%%%%%%%
% PSD of PAM Pulse Train
%%%%%%%%%%%%%%%%%%%%%%%%%%%%
pam_tot = length(pam);                  % length of signal
f = 1/delt*(0:pam_tot/2)/pam_tot;       % frequency vector
PAM = fft(pam);                         % FFT
Spam = (abs(PAM/pam_tot).^2)*Ns*2*To;   % PSD
Spam_dB = 10*log10(Spam);               % PSD (dB)
```

```
figure(3)
plot(f,Spam_dB(1:pam_tot/2+1),'b')
axis([0 20e9 -170 -40]);
ylabel('Magnitude (dB)');
xlabel('Frequency (Hz)');
grid

%%%%%%%%%
% BPPM
%%%%%%%%%
bppm = uwb(Tw,To,delt,Ns,P,jtr,'bppm',dly); % BPPM pulse train
% bppm = awgn(bppm,-10,'measured');           % add AWGN

%%%%%%%%%%%%%%%%%%%%%%%%%%%%
% PSD of BPPM pulse train
%%%%%%%%%%%%%%%%%%%%%%%%%%%%
bppm_tot = length(bppm);                % length of signal
f = 1/delt*(0:bppm_tot/2)/bppm_tot;     % frequency vector
BPPM = fft(bppm);                       % FFT
Sbppm =(abs(BPPM/bppm_tot).^2)*Ns*To;   % PSD
Sbppm_dB = 10*log10(Sbppm);             % PSD (dB)

figure(4)
plot(f,Sbppm_dB(1:bppm_tot/2+1),'b')
axis([0 20e9 -170 -40]);
ylabel('Magnitude (dB)');
xlabel('Frequency (Hz)');
grid
```

```
% Brett D. Gronholz
% EENG 799 - Summer/Fall 2004
% Wideband Correlation Receiver
%  - UWB Signal Detection
%%%%%%%%%%%%%%%%%%%%%%%%%%%%%%%%%%%%%%%%%%%%%%%%%%%
clear all close all, clc, format compact

%%%%%%%%%%%%%%%%%%%%%%%%%%%
% Simulation Parameters
%%%%%%%%%%%%%%%%%%%%%%%%%%%
SNR = 0;                % input signal SNR in dB
fl = 2.5e9;             % lower BPF frequency
fh = 7.5e9;             % upper BPF frequency
Nz = 400;               % one-sided zero padding length for 'filtfilt'
N = 4;                  % filter order

%%%%%%%%%%%%%%%%%%%%%%%%%%%
% UWB Signal Parameters
%%%%%%%%%%%%%%%%%%%%%%%%%%%
fc = 5e9;       % center frequency
Tw = 2/fc;      % pulse duration
Ts = 2*Tw;      % symbol duration
To = 10*Ts;     % symbol repetition interval
delt = 0.01e-9; % time resolution
fs = 1/delt;    % sample frequency
Ns = 1;         % number of symbols
P = 1;          % signal power
jtr = 0;        % jitter as percentage of Ts
method = 'uni'; % modulation method
dly1 = 2e-9;    % first pulse delay, sig 1
dly2 = 4e-9;    % first pulse delay, sig 2

%%%%%%%%%%%%%%%%%%%%%%
% Generate Signals
%%%%%%%%%%%%%%%%%%%%%%
x1 = uwb(Tw,To,delt,Ns,P,jtr,method,dly1);  % UWB signal out of antenna 1
x2 = uwb(Tw,To,delt,Ns,P,jtr,method,dly2);  % UWB signal out of antenna 2
Px1 = sum(x1.^2)/length(x1);                % power in UWB sig 1
Px2 = sum(x2.^2)/length(x2);                % power in UWB sig 2
n1 = randn(1,length(x1));                   % noise realization 1
n2 = randn(1,length(x2));                   % noise realization 2
```

```
%%%%%%%%%%%%%%%%%%%%%%%%%
% Filter Input Signals
%%%%%%%%%%%%%%%%%%%%%%%%%
[b,a] = butter(N,[fl/(fs/2) fh/(fs/2)]);% filter coeffs

xf1 = [zeros(1,Nz) x1 zeros(1,Nz)];     % zero-pad
xf1 = real(filtfilt(b,a,xf1));          % filter
xf1 = xf1(Nz+1:end-Nz);                 % remove zeros
Pxf1 = sum(xf1.^2)/length(xf1);         % power in filtered UWB signal

xf2 = [zeros(1,Nz) x2 zeros(1,Nz)];     % zero-pad
xf2 = real(filtfilt(b,a,xf2));          % filter
xf2 = xf2(Nz+1:end-Nz);                 % remove zeros
Pxf2 = sum(xf2.^2)/length(xf2);         % power in filtered UWB signal

nf1 = [zeros(1,Nz) n1 zeros(1,Nz)];     % zero-pad
nf1 = filtfilt(b,a,nf1);                % filter
nf1 = nf1(Nz+1:end-Nz);                 % remove zeros
nf1 = nf1/sqrt(var(nf1));               % normalize noise power
nf1 = sqrt(Pxf1/10^(SNR/10))*nf1;       % noise at required SNR

nf2 = [zeros(1,Nz) n2 zeros(1,Nz)];     % zero-pad
nf2 = filtfilt(b,a,nf2);                % filter
nf2 = nf2(Nz+1:end-Nz);                 % remove zeros
nf2 = nf2/sqrt(var(nf2));               % normalize noise power
nf2 = sqrt(Pxf2/10^(SNR/10))*nf2;       % noise at required SNR

%%%%%%%%%%%%%%%%
% Correlation
%%%%%%%%%%%%%%%%
[xc,lags] = xcorr(xf1+nf1,xf2+nf2);
plot(lags,abs(xc))
```

```
% Brett D. Gronholz
% EENG 799 -- Summer/Fall 2004
% UWB Detection Probability (Pd)
%   - Cross-Correlation Receiver
%%%%%%%%%%%%%%%%%%%%%%%%%%%%%%%%%%%%%%%%%%%%%%%%%%%
clear all, close all, clc, format compact

%%%%%%%%%%%%%%%%%%%%%%%%%%%
% Simulation Parameters
%%%%%%%%%%%%%%%%%%%%%%%%%%%
Wc = [1e9];          % channel bandwidths to simulate
Nz = [500];          % zero-padding lengths for each 'Wc' (one-sided)
fl = 2.5e9;          % lower Hrf/ChRx frequency
fh = 7.5e9;          % upper Hrf/ChRx frequency
dc = 0;              % downconvert? (1=yes,0=no)
ph = 0;              % DC phases to simulate
meth = 1;            % processing method (1=TTM,2=SSM,3=CTM,4=CSM)
Nfft = 64;           % (I)FFT length
Pfa = 10^-2;         % probability of false alarm
R = 10/Pfa;          % number of realizations
SNR = [-10:1:5];     % SNRs to simulate

%%%%%%%%%%%%%%%%%%%%%%%%%%%
% UWB Signal Parameters
%%%%%%%%%%%%%%%%%%%%%%%%%%%
fc = 5e9;        % center frequency
Tw = 2/fc;       % pulse duration
Ts = 2*Tw;       % symbol duration
To = Ts/2;       % symbol repetition interval
delt = 0.01e-9; % time resolution
fs = 1/delt;     % sample frequency
Ns = 1;          % number of symbols
P = 1;           % signal power
jtr = 0;         % jitter as percentage of Ts
method = 'uni'; % modulation method
dly1 = 0;    % first pulse delay, sig 1
dly2 = 0;    % first pulse delay, sig 2

%%%%%%%%%%%%%%%%%%%%%%
% Generate Signals
%%%%%%%%%%%%%%%%%%%%%%
x1 = uwb(Tw,To,delt,Ns,P,jtr,method,dly1);  % UWB signal at output of antenna 1
```

```
x1 = [zeros(1,240) x1 zeros(1,240)];        % add zeros
x2 = uwb(Tw,To,delt,Ns,P,jtr,method,dly2);  % UWB signal at output of antenna 2
x2 = [zeros(1,100) x2 zeros(1,380)];        % add zeros
Px1 = sum(x1.^2)/length(x1);                % power in UWB sig 1
Px2 = sum(x2.^2)/length(x2);                % power in UWB sig 2
n1 = randn(R,length(x1));                   % generate noise 1
n2 = randn(R,length(x2));                   % generate noise 2

%%%%%%%%%%%%%%%%%%%%%%%%%
% Filter Input Signals
%%%%%%%%%%%%%%%%%%%%%%%%%
N = 4;              % order of Hrf BPF
NzRF = 200;         % one-sided zero padding length for 'filtfilt'
[b,a] = butter(N,[fl/(fs/2) fh/(fs/2)]);% filter coeffs

xf1 = [zeros(1,NzRF) x1 zeros(1,NzRF)]; % zero-pad
xf1 = real(filtfilt(b,a,xf1));          % filter
xf1 = xf1(NzRF+1:end-NzRF);             % remove zeros
Pxf1 = sum(xf1.^2)/length(xf1);         % power in filtered UWB sig

xf2 = [zeros(1,NzRF) x2 zeros(1,NzRF)]; % zero-pad
xf2 = real(filtfilt(b,a,xf2));          % filter
xf2 = xf2(NzRF+1:end-NzRF);             % remove zeros
Pxf2 = sum(xf2.^2)/length(xf2);         % power in filtered UWB sig

nt1 = [zeros(R,NzRF) n1 zeros(R,NzRF)]; % zero-pad
for i = 1:R,
    nt1(i,:) = filtfilt(b,a,nt1(i,:));  % filter
    nf1(i,:) = nt1(i,NzRF+1:end-NzRF);  % remove zeros
end
nf1 = nf1/sqrt(var(nf1(:)'));           % normalize noise power

nt2 = [zeros(R,NzRF) n2 zeros(R,NzRF)]; % zero-pad
for i = 1:R,
    nt2(i,:) = filtfilt(b,a,nt2(i,:));  % filter
    nf2(i,:) = nt2(i,NzRF+1:end-NzRF);  % remove zeros
end
nf2 = nf2/sqrt(var(nf2(:)'));           % normalize noise power

%%%%%%%%%%
% Inputs
%%%%%%%%%%
```

```
s1_in = xf1;                              % input signal 1
n1_in = nf1;                              % input noise 1
Ps1_in = sum(s1_in.^2)/length(s1_in);     % power in input signal 1
s2_in = xf2;                              % input signal 2
n2_in = nf2;                              % input noise 2
Ps2_in = sum(s2_in.^2)/length(s2_in);     % power in input signal 2

figure(1), hold on, grid
%%%%%%%%%%%%%%%%%%%%%%%%%%%%
% Radiometric Detection
%%%%%%%%%%%%%%%%%%%%%%%%%%%%
w = waitbar(0);
for i = 1:length(SNR),
    waitbar(i/length(SNR),w,['Radiometer Progress - ',...
        num2str(i),'/',num2str(length(SNR))]);
    nser = sqrt(Ps1_in/10^(SNR(i)/10))*n1_in;   % noise at required SNR
    Znr = sum(nser.^2,2);                       % noise test statistic
    Zsr = flipud(sort(Znr));                    % sort Zn (descending)
    Tr = Zsr(floor(Pfa*R)+1);                   % find/set threshold
    for k = 1:R,
        Zr(k) = sum((s1_in+nser(k,:)).^2);      % S+N test statistic
    end
    Pdr(i) = length(find(Zr > Tr))/R;           % probability of detection
end
figure(1), plot(SNR,Pdr,'k-'), xlabel('SNR (dB)'), ylabel('P_D')
close(w)

%%%%%%%%%%%%%%%%%%%%%%%%%%%%%%
% Matched Filter Detection
%%%%%%%%%%%%%%%%%%%%%%%%%%%%%%
w = waitbar(0);
for i = 1:length(SNR),
    waitbar(i/length(SNR),w,['Matched Filter Progress - ',...
        num2str(i),'/',num2str(length(SNR))]);
    nsem = sqrt(Ps1_in/10^(SNR(i)/10))*n1_in;   % noise at required SNR
    for k = 1:R,
        Znm(k) = sum(s1_in.*nsem(k,:));         % noise test statistic
    end
    Zsm = fliplr(sort(Znm));                    % sort Zn (descending)
    Tm = Zsm(floor(Pfa*R)+1);                   % find/set threshold
    Zxm = sum(s1_in.^2);                        % signal test statistic
    Zm = Zxm + Znm;                             % total test statistic
```

```
    Pdm(i) = length(find(Zm > Tm))/R;           % probability of detection
end
close(w)
figure(1), plot(SNR,Pdm,'k--'), xlabel('SNR (dB)'), ylabel('P_D')

%%%%%%%%%%%%%%%%%%%%%%%%%%%%%%%%
% Cross-Correlation Receiver
%%%%%%%%%%%%%%%%%%%%%%%%%%%%%%%%
w = waitbar(0);         % create progress bar
for q = 1:length(SNR),
    nse1 = sqrt(Ps1_in/10^(SNR(q)/10))*n1_in;   % noise at required SNR
    nse2 = sqrt(Ps2_in/10^(SNR(q)/10))*n2_in;   % noise at required SNR
    for k = 1:R,
        waitbar(q/length(SNR),w,['CorrRx 1 - ',num2str(q),...
            '/',num2str(length(SNR)),'; ',num2str(k),'/',num2str(R)]);
        inpn1 = nse1(k,:);              % input noise 1
        inps1 = s1_in + nse1(k,:);      % input signal 1 + noise 1
        inpn2 = nse2(k,:);              % input noise 2
        inps2 = s2_in + nse2(k,:);      % input signal 2 + noise 2
        outxn = xcorr(inpn1,inpn2);     % cross-correlation (noise)
        Zn(k) = max(abs(outxn(:)));     % max 'outxn' test statistic
        outxs = xcorr(inps1,inps2);     % cross-correlation (signal+noise)
        Z(k) = max(abs(outxs(:)));      % max 'outxs' test statistic
    end
    Zs = fliplr(sort(Zn));              % sort test statistics
    T = Zs(floor(Pfa*R)+1);             % find threshold
    Pd(q) = length(find(Z > T))/R;      % probability of detection
end
close(w)
figure(1), plot(SNR,Pd,'k-o'), xlabel('SNR (dB)'), ylabel('P_D')

save chxcorr_wc SNR Pdr Pdm Pd      % save required data to workspace
```

```
% Brett D. Gronholz
% EENG 799 -- Summer/Fall 2004
% Wideband Channelized Receiver
%  -- Processing
%%%%%%%%%%%%%%%%%%%%%%%%%%%%%%%%%%%%%%%%%%%%%%%%
clear all, close all, clc, format compact

%%%%%%%%%%%%%%%%%%%%%%%%%%
% Simulation Parameters
%%%%%%%%%%%%%%%%%%%%%%%%%%
Wc = 1e9;           % channel bandwidth
Nz = 200;           % one-sided zero padding length for 'filtfilt'
fl = 2.5e9;         % lower ChRx frequency
fh = 7.5e9;         % upper ChRx frequency
dc = 0;             % downconvert? (1 == yes,0 == no)
ph = 0;             % downconversion starting phase (in degrees)
meth = 1;           % processing method (1=TTM,2=SSM,3=CTM,4=CSM)
Nfft = 64;          % FFT length
SNR = 0;            % input signal SNR in dB
Nc = (fh-fl)/Wc;    % number of channels

%%%%%%%%%%%%%%%%%%%%%%%%%%
% UWB Signal Parameters
%%%%%%%%%%%%%%%%%%%%%%%%%%
fc = 5e9;       % center frequency
Tw = 2/fc;      % pulse duration
Ts = 2*Tw;      % symbol duration
To = Ts/2;      % symbol repetition interval
delt = 0.01e-9; % time resolution
fs = 1/delt;    % sample frequency
Ns = 1;         % number of symbols
P = 1;          % signal power
jtr = 0;        % jitter as percentage of Ts
method = 'uni'; % modulation method
dly = 0;        % first pulse delay

%%%%%%%%%%%%%%%%%%%%%%
% Generate Signals
%%%%%%%%%%%%%%%%%%%%%%
x = uwb(Tw,To,delt,Ns,P,jtr,method,dly);    % UWB signal
xs = length(x);                             % samples/pulse
x = [zeros(1,240) x zeros(1,240)];          % add zeros
```

```
Px = sum(x.^2)/length(x);                    % power in UWB signal
t = [0:delt:(length(x)*delt-delt)];          % time vector (length of 'x')
y = sqrt(2*Px)*cos(2*pi*5e9*t);              % NB signal (tone)
y = [zeros(1,240) y zeros(1,240)];           % add zeros
n = randn(1,length(x));                      % generate noise

%%%%%%%%%%%%%%%%%%%%%%%%%
% Filter Input Signals
%%%%%%%%%%%%%%%%%%%%%%%%%
N = 4;                                       % filter order
NzRF = 200;                                  % one-sided zero padding length
[b,a] = butter(N,[fl/(fs/2) fh/(fs/2)]);% filter coeffs

xf = [zeros(1,NzRF) x zeros(1,NzRF)];    % zero-pad
xf = real(filtfilt(b,a,xf));             % filter
xf = xf(NzRF+1:end-NzRF);                % remove zeros
Pxf = sum(xf.^2)/length(xf);             % power in filtered UWB signal

yf = [zeros(1,NzRF) y zeros(1,NzRF)];    % zero-pad
yf = real(filtfilt(b,a,yf));             % filter
yf = yf(NzRF+1:end-NzRF);                % remove zeros
yf = sqrt(Pxf/var(yf))*yf;               % scale

nf = [zeros(1,NzRF) n zeros(1,NzRF)];    % zero-pad
nf = filtfilt(b,a,nf);                   % filter
nf = nf(NzRF+1:end-NzRF);                % remove zeros
nf = nf/sqrt(var(nf));                   % normalize noise power
nf = sqrt(Pxf/10^(SNR/10))*nf;           % noise at required SNR

%%%%%%%%%%%%%%%%%%%%%%%%%
% Channelized Receiver
%%%%%%%%%%%%%%%%%%%%%%%%%
inp = xf;                                    % input sig
out = chrx(inp,fs,Wc,fl,fh,Nz,dc,ph);        % channelized receiver

%%%%%%%%%%%%%%%%%%%%%%%%%%%%%%%%%%%%
% Channelized Receiver Processing
%%%%%%%%%%%%%%%%%%%%%%%%%%%%%%%%%%%%
if meth == 1,
    outx = fftshift(ifft(out,Nfft,1),1);     % Temp-Temp Matrix
elseif meth == 2,
    outx = fftshift(fft(out,Nfft,2),2);      % Spec-Spec Matrix
```

```
elseif meth == 3,
    outx = ctm(out,Nfft,1,0);   % Cross-Temporal Matrix
elseif meth == 4,
    outx = csm(out,Nfft,1,0);   % Cross-Spectral Matrix
else
    error('Invalid value (meth)')
end
figure(1),pcolor(abs(outx)),shading('interp'),colormap(1-gray)

%%%%%%%%%%%%%%%%%%%%%%%%%%%%%%%%%%%%%%%%%%%%%%%%%%%%%%%%%%%
% Sum of Real/Imaginary Parts of Processed Matrix
%%%%%%%%%%%%%%%%%%%%%%%%%%%%%%%%%%%%%%%%%%%%%%%%%%%%%%%%%%%
figure(2)
subplot(2,2,1),plot(real(sum(outx,1)),'k'),title('Real - Sum of Rows')
axis([0 length(outx(1,:)) ...
    min(real(sum(outx,1)))-1e-4 max(real(sum(outx,1)))+1e-4])
subplot(2,2,2),plot(imag(sum(outx,1)),'k'),title('Imaginary - Sum of Rows')
axis([0 length(outx(1,:)) ...
    min(imag(sum(outx,1)))-1e-4 max(imag(sum(outx,1)))+1e-4])
subplot(2,2,3),plot(real(sum(outx,2)),'k'),title('Real - Sum of Columns')
axis([0 Nfft min(real(sum(outx,2)))-1e-4 max(real(sum(outx,2)))+1e-4])
subplot(2,2,4),plot(imag(sum(outx,2)),'k'),title('Imaginary - Sum of Columns')
axis([0 Nfft min(imag(sum(outx,2)))-1e-4 max(imag(sum(outx,2)))+1e-4])

%%%%%%%%%%%%%%%%%%%%%%%%%%%%%%%%%%%%%%%%%%%%%%%%%%%%%%%%%%%
% Plot Channelized Receiver Outputs
%%%%%%%%%%%%%%%%%%%%%%%%%%%%%%%%%%%%%%%%%%%%%%%%%%%%%%%%%%%
figure(3)
for i = 1:Nc,
   subplot(Nc,1,i),plot(out(i,:),'k')
   axis([0 length(out) min(out(:))-1e-1 max(out(:))+1e-1])
   ylabel(['Ch ',num2str(i)])
end
```

```
% Brett D. Gronholz
% EENG 799 -- Summer/Fall 2004
% UWB Detection Probability (Pd)
%   -- Varying Points in (I)FFT and SNR
%%%%%%%%%%%%%%%%%%%%%%%%%%%%%%%%%%%%%%%%%%%%%%%%
clear all, close all, clc, format compact

%%%%%%%%%%%%%%%%%%%%%%%%%%%%
% Simulation Parameters
%%%%%%%%%%%%%%%%%%%%%%%%%%%%
Wc = [1e9];         % channel bandwidth to simulate
Nz = [200];         % zero-padding length for 'Wc'
fl = 2.5e9;         % lower ChRx frequency
fh = 7.5e9;         % upper ChRx frequency
dc = 0;             % downconvert? (1=yes,0=no)
ph = 0;             % DC mixer starting phase
meth = 1;           % processing method (1=TTM,2=SSM,3=CTM,4=CSM)
Nfft = [4,8,16,32,64,128,256];      % FFT lengths to simulate (TTM/CTM)
% Nfft = [512,1024, 2048];    % FFT lengths to simulate (SSM/CSM)
SNR = [-10:1:5];    % SNR to simulate
Pfa = 10^-2;        % probability of false alarm
R = 10/Pfa;         % number of realizations

%%%%%%%%%%%%%%%%%%%%%%%%%%%%
% UWB Signal Parameters
%%%%%%%%%%%%%%%%%%%%%%%%%%%%
fc = 5e9;       % center frequency
Tw = 2/fc;      % pulse duration
Ts = 2*Tw;      % symbol duration
To = Ts/2;      % symbol repetition interval
delt = 0.01e-9; % time resolution
fs = 1/delt;    % sample frequency
Ns = 1;         % number of symbols
P = 1;          % signal power
jtr = 0;        % jitter as percentage of Ts
method = 'uni'; % modulation method
dly = 0;        % first pulse delay

%%%%%%%%%%%%%%%%%%%%%%
% Generate Signals
%%%%%%%%%%%%%%%%%%%%%%
x = uwb(Tw,To,delt,Ns,P,jtr,method,dly);    % UWB signal
```

```
x = [zeros(1,240) x zeros(1,240)];          % add zeros
Px = sum(x.^2)/length(x);                   % power in UWB signal
t = [0:delt:(length(x)*delt-delt)];         % time vector (length of 'x')
y = sqrt(2*Px)*cos(2*pi*5e9*t);             % NB signal (tone)
n = randn(R,length(x));                     % 'R' noise realizations

%%%%%%%%%%%%%%%%%%%%%%%%%%%%%%%
% Filter Input Signals (Hrf)
%%%%%%%%%%%%%%%%%%%%%%%%%%%%%%%
N = 4;              % order of Hrf BPF
NzRF = 200;         % one-sided zero padding length
[b,a] = butter(N,[fl/(fs/2) fh/(fs/2)]);% Hrf filter coeffs

xf = [zeros(1,NzRF) x zeros(1,NzRF)];   % zero-pad
xf = real(filtfilt(b,a,xf));            % filter
xf = xf(NzRF+1:end-NzRF);               % remove zeros
Pxf = sum(xf.^2)/length(xf);            % power in filtered UWB signal

yf = [zeros(1,NzRF) y zeros(1,NzRF)];   % zero-pad
yf = real(filtfilt(b,a,yf));            % filter
yf = yf(NzRF+1:end-NzRF);               % remove zeros
yf = sqrt(Pxf/var(yf))*yf;              % scale (power equal to 'Pxf')

nt = [zeros(R,NzRF) n zeros(R,NzRF)];   % zero-pad
for i = 1:R,
    nt(i,:) = filtfilt(b,a,nt(i,:));    % filter
    nf(i,:) = nt(i,NzRF+1:end-NzRF);    % remove zeros
end
nf = nf/sqrt(var(nf(:)'));              % normalize noise power

%%%%%%%%%%%%%%%%
% ChRx Inputs
%%%%%%%%%%%%%%%%
s_in = xf;      % input signal
n_in = nf;      % input noise
Ps_in = sum(s_in.^2)/length(s_in);  % power in input signal

figure(1), hold on, grid
for c = 1:length(Nfft),     % Nfft loop
%%%%%%%%%%%%%%%%%%%%%%%%%%
% Channelized Receiver
%%%%%%%%%%%%%%%%%%%%%%%%%%
```

```
w = waitbar(0);             % create progress bar
for q = 1:length(SNR),      % SNR loop
    nse = sqrt(Ps_in/10^(SNR(q)/10))*n_in;  % noise at required SNR
    for k = 1:R,            % realizations loop
        waitbar(q/length(SNR),w,['ChRx Progress - ',num2str(q),'/',...
            num2str(length(SNR)),'; ',num2str(k),'/',num2str(R)]);
        inpn = nse(k,:);                    % input N
        inps = s_in + nse(k,:);             % input S+N
        outn = chrx(inpn,fs,Wc,fl,fh,Nz,dc,ph); % output N
        outs = chrx(inps,fs,Wc,fl,fh,Nz,dc,ph); % output S+N
        if meth == 1,
            outxn = ifft(outn,Nfft(c),1);  % Temp-Temp Matrix, N
            outxs = ifft(outs,Nfft(c),1);  % Temp-Temp Matrix, S+N
        elseif meth == 2,
            outxn = fft(outn,Nfft(c),2);   % Spec-Spec Matrix, N
            outxs = fft(outs,Nfft(c),2);   % Spec-Spec Matrix, S+N
        elseif meth == 3,
            outxn = ctm(outn,Nfft(c),1,0); % Cross-Temporal Matrix, N
            outxs = ctm(outs,Nfft(c),1,0); % Cross-Temporal Matrix, S+N
        elseif meth == 4,
            outxn = csm(outn,Nfft(c),1,0); % Cross-Spectral Matrix, N
            outxs = csm(outs,Nfft(c),1,0); % Cross-Spectral Matrix, S+N
        else
            error('Invalid value (meth)')
        end
        Zn(k) = max(abs(outxn(:)));     % max 'outxn' test statistic
        Z(k) = max(abs(outxs(:)));      % max 'outxs' test statistic
    end
    Zs = fliplr(sort(Zn));              % sort 'outxn' test statistics
    T = Zs(floor(Pfa*R)+1);             % find/set threshold
    Pd(c,q) = length(find(Z > T))/R;    % probability of detection
end
close(w)

if c == 1,
    figure(1), plot(SNR,Pd(c,:),'k-o'), xlabel('SNR (dB)'), ylabel('P_D')
elseif c == 2,
    figure(1), plot(SNR,Pd(c,:),'k-s'), xlabel('SNR (dB)'), ylabel('P_D')
elseif c == 3,
    figure(1), plot(SNR,Pd(c,:),'k-^'), xlabel('SNR (dB)'), ylabel('P_D')
elseif c == 4,
    figure(1), plot(SNR,Pd(c,:),'k-d'), xlabel('SNR (dB)'), ylabel('P_D')
```

```
elseif c == 5,
    figure(1), plot(SNR,Pd(c,:),'k-*'), xlabel('SNR (dB)'), ylabel('P_D')
elseif c == 6,
    figure(1), plot(SNR,Pd(c,:),'k-+'), xlabel('SNR (dB)'), ylabel('P_D')
elseif c == 7,
    figure(1), plot(SNR,Pd(c,:),'k-x'), xlabel('SNR (dB)'), ylabel('P_D')
end

end

save ttm1_nfft SNR Pd       % save required data to workspace
```

```
% Brett D. Gronholz
% EENG 799 -- Summer/Fall 2004
% UWB Detection Probability (Pd)
%   -- Varying Channel Bandwidth and SNR
%%%%%%%%%%%%%%%%%%%%%%%%%%%%%%%%%%%%%%%%%%%%%%%%
clear all, close all, clc, format compact

%%%%%%%%%%%%%%%%%%%%%%%%%%%
% Simulation Parameters
%%%%%%%%%%%%%%%%%%%%%%%%%%%
Wc = [1e9,0.5e9,0.25e9,0.1e9];  % channel bandwidths to simulate
Nz = [200,400,800,2000];        % zero-padding lengths for each 'Wc'
fl = 2.5e9;          % lower Hrf/ChRx frequency
fh = 7.5e9;          % upper Hrf/ChRx frequency
dc = 0;              % downconvert? (1=yes,0=no)
ph = 0;              % DC phases to simulate
meth = 1;            % processing method (1=TTM,2=SSM,3=CTM,4=CSM)
Nfft = 64;           % (I)FFT length
SNR = [-10:1:5];     % SNRs to simulate
Pfa = 10^-2;         % probability of false alarm
R = 10/Pfa;          % number of realizations

%%%%%%%%%%%%%%%%%%%%%%%%%%%
% UWB Signal Parameters
%%%%%%%%%%%%%%%%%%%%%%%%%%%
fc = 5e9;       % center frequency
Tw = 2/fc;      % pulse duration
Ts = 2*Tw;      % symbol duration
To = Ts/2;      % symbol repetition interval
delt = 0.01e-9; % time resolution
fs = 1/delt;    % sample frequency
Ns = 1;         % number of symbols
P = 1;          % signal power
jtr = 0;        % jitter as percentage of Ts
method = 'uni'; % modulation method
dly = 0;        % first pulse delay

%%%%%%%%%%%%%%%%%%%%%%
% Generate Signals
%%%%%%%%%%%%%%%%%%%%%%
x = uwb(Tw,To,delt,Ns,P,jtr,method,dly);    % UWB signal
x = [zeros(1,240) x zeros(1,240)];          % add zeros
```

```
Px = sum(x.^2)/length(x);                    % power in UWB signal
t = [0:delt:(length(x)*delt-delt)];          % time vector (length of 'x')
y = sqrt(2*Px)*cos(2*pi*5e9*t);              % NB signal (tone)
n = randn(R,length(x));                      % 'R' noise realizations

%%%%%%%%%%%%%%%%%%%%%%%%%
% Filter Input Signals
%%%%%%%%%%%%%%%%%%%%%%%%%
N = 4;               % order of Hrf BPF
NzRF = 200;          % one-sided zero padding length
[b,a] = butter(N,[fl/(fs/2) fh/(fs/2)]);% Hrf filter coeffs

xf = [zeros(1,NzRF) x zeros(1,NzRF)];   % zero-pad
xf = real(filtfilt(b,a,xf));            % filter
xf = xf(NzRF+1:end-NzRF);               % remove zeros
Pxf = sum(xf.^2)/length(xf);            % power in filtered UWB signal

yf = [zeros(1,NzRF) y zeros(1,NzRF)];   % zero-pad
yf = real(filtfilt(b,a,yf));            % filter
yf = yf(NzRF+1:end-NzRF);               % remove zeros
yf = sqrt(Pxf/var(yf))*yf;              % scale

nt = [zeros(R,NzRF) n zeros(R,NzRF)];   % zero-pad
for i = 1:R,
    nt(i,:) = filtfilt(b,a,nt(i,:));    % filter
    nf(i,:) = nt(i,NzRF+1:end-NzRF);    % remove zeros
end
nf = nf/sqrt(var(nf(:)'));              % normalize noise power

%%%%%%%%%%%%%%%%
% ChRx Inputs
%%%%%%%%%%%%%%%%
s_in = xf;      % input signal
n_in = nf;      % input noise
Ps_in = sum(s_in.^2)/length(s_in);  % power in input signal

figure(1), hold on, grid
%%%%%%%%%%%%%%%%%%%%%%%%%%%
% Radiometric Detection
%%%%%%%%%%%%%%%%%%%%%%%%%%%
w = waitbar(0);         % create progress bar
for i = 1:length(SNR),  % SNR loop
```

```
    waitbar(i/length(SNR),w,['Radiometer Progress - ',...
        num2str(i),'/',num2str(length(SNR))]);
    nser = sqrt(Ps_in/10^(SNR(i)/10))*n_in; % noise at required SNR
    Znr = sum(nser.^2,2);                   % noise test statistic
    Zsr = flipud(sort(Znr));                % sort Zn (descending)
    Tr = Zsr(floor(Pfa*R)+1);               % find/set threshold
    for k = 1:R,
        Zr(k) = sum((s_in+nser(k,:)).^2);   % S+N test statistics
    end
    Pdr(i) = length(find(Zr > Tr))/R;       % probability of detection
end
close(w)
figure(1), plot(SNR,Pdr,'k-'), xlabel('SNR (dB)'), ylabel('P_D')

%%%%%%%%%%%%%%%%%%%%%%%%%%%%%
% Matched Filter Detection
%%%%%%%%%%%%%%%%%%%%%%%%%%%%%
w = waitbar(0);         % create progress bar
for i = 1:length(SNR),  % SNR loop
    waitbar(i/length(SNR),w,['Matched Filter Progress - ',...
        num2str(i),'/',num2str(length(SNR))]);
    nsem = sqrt(Ps_in/10^(SNR(i)/10))*n_in; % noise at required SNR
    for k = 1:R,
        Znm(k) = sum(s_in.*nsem(k,:));      % noise test statistic
    end
    Zsm = fliplr(sort(Znm));                % sort Znm (descending value)
    Tm = Zsm(floor(Pfa*R)+1);               % find threshold based on Pfa
    Zxm = sum(s_in.^2);                     % signal test statistic
    Zm = Zxm + Znm;                         % total test statistic
    Pdm(i) = length(find(Zm > Tm))/R;       % probability of detection
end
close(w)
figure(1), plot(SNR,Pdm,'k--'), xlabel('SNR (dB)'), ylabel('P_D')

for c = 1:length(Wc),       % ChBW loop
%%%%%%%%%%%%%%%%%%%%%%%%%%%
% Channelized Receiver
%%%%%%%%%%%%%%%%%%%%%%%%%%%
w = waitbar(0);         % create progress bar
for q = 1:length(SNR),  % SNR loop
    nse = sqrt(Ps_in/10^(SNR(q)/10))*n_in;  % noise at required SNR
    for k = 1:R,        % realizations loop
```

```
        waitbar(q/length(SNR),w,['ChRx Progress - ',num2str(q),'/',...
            num2str(length(SNR)),'; ',num2str(k),'/',num2str(R)]);
        inpn = nse(k,:);                % input N
        inps = s_in + nse(k,:);         % input S+N
        outn = chrx(inpn,fs,Wc(c),fl,fh,Nz(c),dc,ph);  % output N
        outs = chrx(inps,fs,Wc(c),fl,fh,Nz(c),dc,ph);  % output S+N
        if meth == 1,
            outxn = ifft(outn,Nfft,1);  % Temp-Temp Matrix, N
            outxs = ifft(outs,Nfft,1);  % Temp-Temp Matrix, S+N
        elseif meth == 2,
            outxn = fft(outn,Nfft,2);   % Spec-Spec Matrix, N
            outxs = fft(outs,Nfft,2);   % Spec-Spec Matrix, S+N
        elseif meth == 3,
            outxn = ctm(outn,Nfft,1,0); % Cross-Temporal Matrix, N
            outxs = ctm(outs,Nfft,1,0); % Cross-Temporal Matrix, S+N
        elseif meth == 4,
            outxn = csm(outn,Nfft,1,0); % Cross-Spectral Matrix, N
            outxs = csm(outs,Nfft,1,0); % Cross-Spectral Matrix, S+N
        else
            error('Invalid value (meth)')
        end
        Zn(k) = max(abs(outxn(:)));     % max 'outxn' test statistic
        Z(k) = max(abs(outxs(:)));      % max 'outxs' test statistic
    end
    Zs = fliplr(sort(Zn));              % sort 'outxn' test statistics
    T = Zs(floor(Pfa*R)+1);             % find/set threshold
    Pd(c,q) = length(find(Z > T))/R;    % probability of detection
end
close(w)
if c == 1,
    figure(1), plot(SNR,Pd(c,:),'k-o'), xlabel('SNR (dB)'), ylabel('P_D')
elseif c == 2,
    figure(1), plot(SNR,Pd(c,:),'k-s'), xlabel('SNR (dB)'), ylabel('P_D')
elseif c == 3,
    figure(1), plot(SNR,Pd(c,:),'k-^'), xlabel('SNR (dB)'), ylabel('P_D')
elseif c == 4,
    figure(1), plot(SNR,Pd(c,:),'k-d'), xlabel('SNR (dB)'), ylabel('P_D')
end

end

save ttm64_wc SNR Pdr Pdm Pd    % save required data to workspace
```

```
% Brett D. Gronholz
% EENG 799 -- Summer/Fall 2004
% UWB Detection Probability (Pd)
%   -- Varying Downconversion Mixer Phase and Channel Bandwidth
%       (fixed SNR)
%%%%%%%%%%%%%%%%%%%%%%%%%%%%%%%%%%%%%%%%%%%%%%%%%%%%%%%%%%%%%%%%%%%%%%%%%%%
clear all, close all, clc, format compact

%%%%%%%%%%%%%%%%%%%%%%%%%%%
% Simulation Parameters
%%%%%%%%%%%%%%%%%%%%%%%%%%%
Wc = [1e9];         % channel bandwidths to simulate
Nz = [200];         % zero-padding lengths for each 'Wc' (one-sided)
fl = 2.5e9;         % lower ChRx frequency
fh = 7.5e9;         % upper ChRx frequency
dc = 1;             % downconvert? (1=yes,0=no)
ph = [0:1:360];     % phases to simulate
meth = 1;           % processing method (1=TTM,2=SSM,3=CTM,4=CSM)
Nfft = 64;          % FFT length
SNR = 0;            % SNR to simulate
Pfa = 10^-2;        % probability of false alarm
R = 10/Pfa;         % number of realizations

%%%%%%%%%%%%%%%%%%%%%%%%%%%
% UWB Signal Parameters
%%%%%%%%%%%%%%%%%%%%%%%%%%%
fc = 5e9;       % center frequency
Tw = 2/fc;      % pulse duration
Ts = 2*Tw;      % symbol duration
To = Ts/2;      % symbol repetition interval
delt = 0.01e-9; % time resolution
fs = 1/delt;    % sample frequency
Ns = 1;         % number of symbols
P = 1;          % signal power
jtr = 0;        % jitter as percentage of Ts
method = 'uni'; % modulation method
dly = 0;        % first pulse delay

%%%%%%%%%%%%%%%%%%%%%%
% Generate Signals
%%%%%%%%%%%%%%%%%%%%%%
x = uwb(Tw,To,delt,Ns,P,jtr,method,dly);    % UWB signal
```

```
x = [zeros(1,240) x zeros(1,240)];          % add zeros
Px = sum(x.^2)/length(x);                   % power in UWB signal
t = [0:delt:(length(x)*delt-delt)];         % time vector (length of 'x')
y = sqrt(2*Px)*cos(2*pi*5e9*t);             % NB signal (tone)
n = randn(R,length(x));                     % 'R' noise realizations

%%%%%%%%%%%%%%%%%%%%%%%%%%%%%%%
% Filter Input Signals (Hrf)
%%%%%%%%%%%%%%%%%%%%%%%%%%%%%%%
N = 4;              % order of Hrf BPF
NzRF = 200;         % one-sided zero padding length for 'filtfilt'
[b,a] = butter(N,[fl/(fs/2) fh/(fs/2)]);% filter coeffs

xf = [zeros(1,NzRF) x zeros(1,NzRF)];   % zero-pad
xf = real(filtfilt(b,a,xf));            % filter
xf = xf(NzRF+1:end-NzRF);               % remove zeros
Pxf = sum(xf.^2)/length(xf);            % power in filtered UWB signal

yf = [zeros(1,NzRF) y zeros(1,NzRF)];   % zero-pad
yf = real(filtfilt(b,a,yf));            % filter
yf = yf(NzRF+1:end-NzRF);               % remove zeros
yf = sqrt(Pxf/var(yf))*yf;              % scale

nt = [zeros(R,NzRF) n zeros(R,NzRF)];   % zero-pad
for i = 1:R,
    nt(i,:) = filtfilt(b,a,nt(i,:));    % filter
    nf(i,:) = nt(i,NzRF+1:end-NzRF);    % remove zeros
end
nf = nf/sqrt(var(nf(:)'));              % normalize noise power

%%%%%%%%%%%%%%%%%
% ChRx Inputs
%%%%%%%%%%%%%%%%%
s_in = xf;      % input signal
n_in = nf;      % input noise
Ps_in = sum(s_in.^2)/length(s_in);  % power in input signal

figure(1), hold on, grid
for c = 1:length(Wc),       % ChBW loop
%%%%%%%%%%%%%%%%%%%%%%%%%%%
% Channelized Receiver
%%%%%%%%%%%%%%%%%%%%%%%%%%%
```

```
w = waitbar(0);             % create progress bar
nse = sqrt(Ps_in/10^(SNR/10))*n_in; % noise at required SNR
for q = 1:length(ph),       % phase loop
    for k = 1:R,            % realizations loop
        waitbar(q/length(ph),w,['ChRx 1 - ',num2str(q),'/',...
            num2str(length(ph)),'; ',num2str(k),'/',num2str(R)]);
        inpn = nse(k,:);                % input N
        inps = s_in + nse(k,:);         % input S+N
        outn = chrx(inpn,fs,Wc(c),fl,fh,Nz(c),dc,ph(q));  % output N
        outs = chrx(inps,fs,Wc(c),fl,fh,Nz(c),dc,ph(q));  % output S+N
        if meth == 1,
            outxn = ifft(outn,Nfft,1);  % Temp-Temp Matrix, N
            outxs = ifft(outs,Nfft,1);  % Temp-Temp Matrix, S+N
        elseif meth == 2,
            outxn = fft(outn,Nfft,2);   % Spec-Spec Matrix, N
            outxs = fft(outs,Nfft,2);   % Spec-Spec Matrix, S+N
        elseif meth == 3,
            outxn = ctm(outn,Nfft,1,0); % Cross-Temporal Matrix, N
            outxs = ctm(outs,Nfft,1,0); % Cross-Temporal Matrix, S+N
        elseif meth == 4,
            outxn = csm(outn,Nfft,1,0); % Cross-Spectral Matrix, N
            outxs = csm(outs,Nfft,1,0); % Cross-Spectral Matrix, S+N
        else
            error('Invalid value (meth)')
        end
        Zn(k) = max(abs(outxn(:)));     % max 'outxn' test statistic
        Z(k) = max(abs(outxs(:)));      % max 'outxs' test statistic
    end
    Zs = fliplr(sort(Zn));              % sort 'outxn' test statistics
    T = Zs(floor(Pfa*R)+1);             % find/set threshold
    Pd(c,q) = length(find(Z > T))/R;    % probability of detection
end
close(w)
if c == 1,
    figure(1), plot(ph,Pd(c,:),'k-o'), xlabel('Phase (deg)'), ylabel('P_D')
elseif c == 2,
    figure(1), plot(ph,Pd(c,:),'k-s'), xlabel('Phase (deg)'), ylabel('P_D')
elseif c == 3,
    figure(1), plot(ph,Pd(c,:),'k-^'), xlabel('Phase (deg)'), ylabel('P_D')
elseif c == 4,
    figure(1), plot(ph,Pd(c,:),'k-d'), xlabel('Phase (deg)'), ylabel('P_D')
end
```

```
end

save ttm1_ph ph Pd      % save required data to workspace
```

```
function sig = uwb(Tw,To,delt,Ns,P,jtr,method,dly);
%UWB  Ultra-Wideband Signal Generator
%   SIG = UWB(Tw,To,delt,Ns,P,jtr,method,dly)
%
%   INPUTS
%       Tw     - pulse duration
%       To     - symbol repetition interval
%       delt   - time resolution
%       Ns     - number of symbols
%       P      - signal power
%       jtr    - jitter as percentage of Ts = 2*Tw
%       method - 'uni', 'ppm', 'pam', or 'bppm'
%       dly    - first pulse delay
%
%   OUTPUT
%       sig    - UWB output signal
%

%
%   Brett D. Gronholz
%   EENG 799 -- Summer/Fall 2004
%

if nargin ~= 8,
    error('Not enough input arguments!')
end
if delt <= 0,
    error('Time resolution must be greater than 0!');
end
if Ns < 1,
    error('Number of symbols must be greater than zero!')
end
if P <= 0,
    error('Power must be greater than zero!')
end
if jtr > 1 | jtr < 0,
    error('Jitter percentage must be between 0 and 1.')
end
if dly < 0,
    error('First pulse delay time must be greater than or equal to 0.')
end
```

```
rand('state',sum(100*clock))

% Variables
Tm = 0.4*Tw;                    % pulse width parameter
t = 0:delt:(2*Tw-delt);         % time vector for UWB pulse generation
Nc = length(t);                 % number of samples/symbol
Nr = length(0:delt:To-delt);    % number of samples/repetition interval

% Generate UWB pulse (2nd derivative of Gaussian pulse)
w = (1-4*pi*((t-1.2*Tm)/Tm).^2).*exp(-2*pi*((t-1.2*Tm)/Tm).^2); % UWB pulse
Pw = (1/To)*sum(w.^2)*delt;         % power in w
s = sqrt(P/Pw)*w;                   % received UWB waveform

if strcmpi(method,'uni'),
    sig = zeros(1,Ns*Nr);
    r = round(2*(rand(1,Ns)-0.5)*jtr*Nc/2);
    r(1) = 0;
    for i = 1:Ns,
        sig(Nr*(i-1)+1+r(i):Nr*(i-1)+Nc/2+r(i)) = s(1:Nc/2);
    end

elseif strcmpi(method,'ppm'),
    ppm1 = s;
    ppm0 = fliplr(ppm1);
    sig = zeros(1,Ns*Nr);
    r = round(2*(rand(1,Ns)-0.5)*jtr*Nc);
    r(1) = 0;
    bits = randint(1,Ns);
    for i = 1:Ns,
        if bits(i) == 0,
            sig(Nr*(i-1)+1+r(i):Nr*(i-1)+Nc+r(i)) = ppm0;
        else
            sig(Nr*(i-1)+1+r(i):Nr*(i-1)+Nc+r(i)) = ppm1;
        end
    end

elseif strcmpi(method,'pam'),
    pam1 = sqrt(0.5)*s(1:Nc/2);
    pam0 = -pam1;
    sig = zeros(1,Ns*Nr);
    r = round(2*(rand(1,Ns)-0.5)*jtr*Nc/2);
    r(1) = 0;
```

```
    bits = randint(1,Ns);
    for i = 1:Ns,
        if bits(i) == 0,
            sig(Nr*(i-1)+1+r(i):Nr*(i-1)+Nc/2+r(i)) = pam0;
        else
            sig(Nr*(i-1)+1+r(i):Nr*(i-1)+Nc/2+r(i)) = pam1;
        end
    end

elseif strcmpi(method,'bppm'),
    bppm10 = s;
    bppm01 = -s;
    bppm00 = fliplr(bppm01);
    bppm11 = fliplr(bppm10);
    sig = zeros(1,Ns*Nr);
    r = round(2*(rand(1,Ns)-0.5)*jtr*Nc);
    r(1) = 0;
    bits = randint(1,2*Ns);
    for i = 1:Ns,
        switch bi2de([bits(2*i-1) bits(2*i)])
            case [0]
                sig(Nr*(i-1)+1+r(i):Nr*(i-1)+Nc+r(i)) = bppm00;
            case [1]
                sig(Nr*(i-1)+1+r(i):Nr*(i-1)+Nc+r(i)) = bppm01;
            case [2]
                sig(Nr*(i-1)+1+r(i):Nr*(i-1)+Nc+r(i)) = bppm10;
            case [3]
                sig(Nr*(i-1)+1+r(i):Nr*(i-1)+Nc+r(i)) = bppm11;
        end
    end

else
    error('Modulation type error.');
end

sig = [zeros(1,round(dly/delt)) sig];
```

```
function out = chrx(inp,fs,Wc,fl,fh,Nz,dc,ph)
% CHRX Channelized Receiver
%   out = chrx(inp,fs,Wc,fl,fh,Nz,dc,ph)
%
%   INPUTS
%       inp - input signal
%       fs  - sample frequency of input signal
%       Wc  - channel bandwidth
%       fl  - lower ChRx frequency
%       fh  - upper ChRx frequency
%       Nz  - one-sided zero padding length (for 'filtfilt')
%       dc  - downconvert? (1==yes,0==no)
%       ph  - downconversion starting phase
%
%   OUTPUT
%       out - channelized receiver output matrix
%

%
%   Brett D. Gronholz
%   EENG 799 -- Summer/Fall 2004
%

if nargin ~= 8,
    error('Not enough input arguments!')
end
if fs <= 0,
    error('Sample frequency (fs) must be positive and non-zero.')
end
if Wc <= 0,
    error('Channel bandwidth (Wc) must be positive and non-zero.')
end
if fl <= 0,
    error('Lower frequency (fl) must be positive and non-zero.')
end
if fh <= 0,
    error('Upper frequency (fh) must be positive and non-zero.')
end
if mod((fh-fl)/Wc,1) ~= 0,
    error('"fh-fl" must be an integer multiple of "Wc"')
end
if Nz < 0,
```

```
    error('Zero padding length (Nz) must be positive or zero.')
end
if (dc ~= 1 & dc ~= 0),
    error('Invalid parameter (dc)')
end

N = 4;              % filter order
Nc = (fh-fl)/Wc;    % number of channels
delt = 1/fs;        % delta t

inp = [zeros(1,Nz) inp zeros(1,Nz)];    % zero-pad
tdc = [0:delt:(length(inp)*delt-delt)]; % time vector for downconversion
for i = 1:Nc,
    if dc == 1, % downconvert
        [b,a] = butter(N,Wc/(fs/2));    % LPF coeffs
        inpx = real(inp.*exp(-j*2*pi*((fl+(i-1)*Wc)*tdc+pi/180*ph)));
    elseif dc == 0, % don't downconvert
        [b,a] = butter(N,[(fl+(i-1)*Wc)/(fs/2) (fl+i*Wc)/(fs/2)]);  % BPF coeffs
        inpx = inp;
    end
    outt(i,:) = real(filtfilt(b,a,inpx));   % filter input sig
    out(i,:) = outt(i,Nz+1:end-Nz);         % remove zeros
end
```

```
function Cout = csm(x,Nfft,dim,clr)
% CSM   Cross-Spectral Matrix
%   Cout = csm(x,Nfft,dim,clr)
%
%   INPUTS
%       x    - input matrix
%       Nfft - # of points in FFT (to form SSM)
%       dim  - dimension (1==col-by-col, 2==row-by-row)
%       clr  - set autocorrelation terms to zero if 1, normal if 0
%
%   OUTPUTS
%       Cout - Cross-Spectral Matrix (CSM)
%

%
%   Brett D. Gronholz
%   EENG 799 -- Summer/Fall 2004
%

if nargin ~= 4,
    error('Not enough input arguments!')
end
if Nfft < 1;
    error('Nfft must be a positive, non-zero integer.')
end
if (dim ~= 1 & dim ~= 0),
    error('Invalid parameter (dim)')
end
if (clr ~= 1 & clr ~= 0),
    error('Invalid parameter (clr)')
end

X = fft(x,Nfft,2);          % FFT of rows of input matrix

ndim = size(X,mod(dim,2)+1);% input matrix length along specified dimension
noth = size(X,dim);         % input matrix length along other dimension

clear Cout

if dim == 1,
    % Column-by-Column Correlation
    Cout = zeros(ndim,ndim);    % initialize matrix
```

```
    Cout = X'*X/noth;           % C-by-C correlation
elseif dim == 2,
    % Row-by-Row Correlation
    Cout = zeros(ndim,ndim);    % initialize matrix
    Cout = X*X'/noth;           % R-by-R correlation
end

if clr == 1,
    % Set Diagonal (Autocorrelation) Elements to Zero
    for i = 1:ndim,
        Cout(i,i) = 0;
    end
end
```

```
function Cout = ctm(x,Nfft,dim,clr)
% CTM   Cross-Temporal Matrix
%   Cout = ctm(x,Nfft,dim,clr)
%
%   INPUTS
%       x    - input matrix
%       Nfft - # of points in IFFT (to form TTM)
%       dim  - dimension (1==col-by-col, 2==row-by-row)
%       clr  - set autocorrelation terms to zero if 1, normal if 0
%
%   OUTPUTS
%       Cout - Cross-Temporal Matrix (CTM)
%

%
%   Brett D. Gronholz
%   EENG 799 -- Summer/Fall 2004
%

if nargin ~= 4,
    error('Not enough input arguments!')
end
if Nfft < 1;
    error('Nfft must be a positive, non-zero integer.')
end
if (dim ~= 1 & dim ~= 0),
    error('Invalid parameter (dim)')
end
if (clr ~= 1 & clr ~= 0),
    error('Invalid parameter (clr)')
end

X = ifft(x,Nfft,1);         % IFFT of columns of input matrix

ndim = size(X,mod(dim,2)+1);% input matrix length along specified dimension
noth = size(X,dim);         % input matrix length along other dimension

clear Cout

if dim == 1,
    % Column-by-Column Correlation
    Cout = zeros(ndim,ndim);    % initialize matrix
```

```
    Cout = X'*X/noth;           % C-by-C correlation
elseif dim == 2,
    % Row-by-Row Correlation
    Cout = zeros(ndim,ndim);    % initialize matrix
    Cout = X*X'/noth;           % R-by-R correlation
end

if clr == 1,
    % Set Diagonal (Autocorrelation) Elements to Zero
    for i = 1:ndim,
        Cout(i,i) = 0;
    end
end
```

Bibliography

[1] "First report and order: Revision of part 15 of the commission's rules regarding ultra-wideband transmission systems," No. ET Docket 98-153, (Washington), Federal Communications Commission, Government Printing Office, April 2002.

[2] M. A. Temple, R. Backscheider, D. E. Wruck, and T. B. Hale, "Characterization of radar detection performance in the presence of modern signal interference," in *First International Conference on Waveform Diversity and Design*, November 2004.

[3] A. H. Light, "Netex task 1: Measured effects of ultra wideband (uwb) emitters on existing narrowband military receivers," in *IEEE Conference on Ultra Wideband Systems and Technologies (UWBST) 2003*, November 2003.

[4] J. Lopez, "Analysis of electromagnetic interference of ultra wideband and 802.11a wlan employing orthogonal frequency division multiplexing," Master's thesis, Air Force Institute of Technology, 2004.

[5] D. K. Borah, R. Jana, and A. Stamoulis, "Performance evaluation of ieee 802.11a wireless lans in the presence of ultra wideband interference," in *Wireless Communications and Networking, 2003 (WCNC 2003)*, March 2003.

[6] A. Soltanian and L. E. Miller, "Coexistence of ultra-wideband systems and ieee 802.11a wlan, Wireless Communication Technologies Group, National Institute of Standards and Technology," October 2003.

[7] M. Hamalainen, V. Hovinen, A. E. Spezio, R. Test, H. J. Iinatti, and M. Latva-aho, "On the uwb system coexistence with gsm900, umts/wcdma, and gps," *IEEE Journal on Slected Areas in Communications*, vol. 20, no. 9, pp. 1712–1721, 2002.

[8] C. M. Canadeo, "Ultra wideband multiple access performance using th-ppm and ds-bspk modulations," Master's thesis, Air Force Institute of Technology, 2003.

[9] N. Lehmann and A. M. Haimovich, "New approach to control the power spectral density of a time hopping uwb signal," in *Proceedings of the Conference on Information Sciences and Systems, CISS*, March 2003.

[10] ——, "The power spectral density of a time hopping uwb signal: A survey," in *IEEE Conference on UWB Systems and Technologies (UWBST 2003)*, November 2003.

[11] J. Romme and L. Piazzo, "On the power spectral density of time hopping impulse radio," in *IEEE Conference on UWB Systems and Technologies (UWBST 2002)*, 2002.

[12] B. Sklar, *Digital Communications: Fundamentals and Applications.* New Jersey: Prentice Hall, 2001.

[13] H. L. Van Trees, *Detection, Estimation, and Modulation Theory (Part 1).* New York, NY: John Wiley and Sons, 2001.

[14] M. I. Skolnik, *Introduction to Radar Systems.* New York, NY: McGraw-Hill, 2002.

[15] R. F. Mills and G. E. Prescott, "A comparison of various radiometer detection models," *IEEE Transactions on Aerospace and Electronic Systems*, vol. 32, no. 1, pp. 467–473, 1996.

[16] D. J. Torrieri, *Principles of Secure Communication Systems.* Dedham, MA: Artech House, 1985.

[17] J. Tsui, *Digital Techniques for Wideband Receivers.* Norwood, MA: Artech House, 2001.

[18] W. Namgoong, "Channelized digital receivers for impulse radio," in *IEEE International Conference on Communications, 2003. (ICC '03)*, May 2003.

REPORT DOCUMENTATION PAGE

Form Approved
OMB No. 0704-0188

PLEASE DO NOT RETURN YOUR FORM TO THE ABOVE ADDRESS.

1. REPORT DATE *(DD-MM-YYYY)*	2. REPORT TYPE	3. DATES COVERED *(From - To)*
06-12-2004	Master's Thesis	Jan 2004 -- Dec 2004

4. TITLE AND SUBTITLE

NON-COOPERATIVE DETECTION OF ULTRA WIDEBAND SIGNALS

5a. CONTRACT NUMBER

5b. GRANT NUMBER

5c. PROGRAM ELEMENT NUMBER

6. AUTHOR(S)

Gronholz, Brett D.

5d. PROJECT NUMBER

5e. TASK NUMBER

5f. WORK UNIT NUMBER

7. PERFORMING ORGANIZATION NAME(S) AND ADDRESS(ES)

Air Force Institute of Technology
Graduate School of Engineering and Management (AFIT/EN)
2950 P Street, Building 641
WPAFB, OH 45433-7765

8. PERFORMING ORGANIZATION REPORT NUMBER

AFIT/GE/ENG/04-29

9. SPONSORING/MONITORING AGENCY NAME(S) AND ADDRESS(ES)

Mr. Tom D. Niedzwiecki
AFRL/SNRP
2241 Avionics Circle
WPAFB, OH 45433-4318
(937) 255-6127 x3727

10. SPONSOR/MONITOR'S ACRONYM(S)

11. SPONSOR/MONITOR'S REPORT NUMBER(S)

12. DISTRIBUTION/AVAILABILITY STATEMENT

APPROVED FOR PUBLIC RELEASE; DISTRIBUTION UNLIMITED.

13. SUPPLEMENTARY NOTES

14. ABSTRACT

Techniques for the non-cooperative (non-matched filter) detection of impulse-like ultra wideband signals using channelized receiver architectures are developed and evaluated. Each technique considered is modeled and simulations conducted to characterize detection performance, the results of which are compared with the detection performance of three receivers: the matched filter receiver, which provides optimum detection performance in AWGN; the radiometer, or energy detector; and the multi-aperture cross correlation receiver. It is shown that a channelized receiver (with no downconversion) can provide approximately 2.5 dB improvement over the radiometer when performing detection using the temporal-temporal matrix (TTM). The TTM processing technique provides the best performance of all the proposed channelized receiver techniques. Detection with a downconverting channelized receiver is shown dependent on mixer phase value with performance variation generally minimized as the number of channels increases (channel bandwidth decreases).

15. SUBJECT TERMS

Ultra Wideband, UWB, Detection

16. SECURITY CLASSIFICATION OF:			17. LIMITATION OF ABSTRACT	18. NUMBER OF PAGES	19a. NAME OF RESPONSIBLE PERSON
a. REPORT	b. ABSTRACT	c. THIS PAGE			Michael A. Temple, AFIT/ENG
U	U	U	UU	140	19b. TELEPHONE NUMBER *(Include area code)* (937) 255-3636 x4703; michael.temple@afit.edu